THE FERRIC LEACHING OF PYRITE

by

NOELENE MAY

BSc (Hons) (Chemistry)

University of Natal, Pietermaritzburg

Dissertation Presented for the Degree of

MASTER OF APPLIED SCIENCE

UNIVERSITY OF CAPE TOWN

APRIL 1997

SUMMARY

The bioleaching of pyrite has been found to occur via an indirect mechansim. Ferric iron leaches the pyrite, and is reduced to ferrous iron. Bacteria such as *Thiobacillus ferrooxidans* oxidise the ferrous iron to ferric iron, thus maintaining a high redox potential. In this thesis, the effect of the redox potential on the ferric leach rate was investigated by examining previously published data and by developing an experimental technique where dynamic redox potential measurements were used to study the kinetics of the sub-process.

The ferric leach rate of pyrite was found to be of the order of 5×10^{-7} moles pyrite per mole pyrite per second, which is of the same order of magnitude as rates reported for the bioleaching of pyrite over similar ranges of redox potential. The rate decreased as the redox potential decreased, in what appeared to be a Butler-Volmer-like manner. This, along with the observation that there was no significant effect of the total iron concentration, suggested the likelihood of an electrochemical mechanism being operative, with charge transfer at the pyrite surface being rate limiting.

ACKNOWLEDGEMENTS

I would like to express my thanks to the following people:

Professor G. S. Hansford for his enthusiastic supervision;

Dr. D. E. Ralph for his help with the experimental work and interpretation of results;

Mr. E. W. Randall for the design of the data logging system and assistance with electronics;

Mrs. S. Vasic for her contribution to the analytical work;

Mr. B. Cohen and Mrs. A. MacDonald for SEM photographs;

The staff of the main laboratory, the electronic workshop and the main workshop for their assistance;

The staff and postgraduate students of the Chemical Engineering Department, especially the 'Bio Group', for their assistance and for making the department a very pleasant environment in which to work.

TABLE OF CONTENTS

LIST OF FIGURES

LIST OF TABLES

NOMENCLATURE

α	transfer coefficient	
A	surface area	m^2
ADC	analogue to digital converter	
d	particle diameter	m
Δt	change in time	s
eV	electron volt	
E	redox potential	mV
E(0)	initial redox potential	mV
E_a	activation energy	$kJ.mol^{-1}$
E^o	standard redox potential	mV
F	Faraday constant	96485 $C.mol^{-1}$
$[Fe^{2+}]$	ferrous concentration	M
$[Fe^{2+}]_{initial}$	initial ferrous concentration	M
$[Fe^{2+}]_t$	threshold ferrous concentration	M
$[Fe^{3+}]$	ferric concentration	M
$[Fe^{3+}]_{initial}$	initial ferric concentration	M
$[Fe^{tot}]$	total iron concentration	M
$[Fe^{tot}]_{initial}$	initial total iron concentration	M
η	overpotential	mV
i	current density	$A.m^{-2}$
i_o	exchange current density	$A.m^{-2}$
k, K	rate constants	
K_i	inhibition constant	mol $Fe^{3+}.\ell^{-1}$
K_s	Monod constant	mol $Fe^{2+}.\ell^{-1}$
n	stoichiometric coefficient	
PC	personal computer	

q_{O_2}	bacterial specific oxygen utilisation rate	$molO_2.C\text{-}mol^{-1}.s^{-1}$
$q_{O_2}^{max}$	maximum specific oxygen consumption rate	$molO_2.C\text{-}mol^{-1}.s^{-1}$
$r_{Fe^{2+}}$	rate of ferrous production	$mol.\ell^{-1}.s^{-1}$
r_{FeS_2}	rate of pyrite production	$mol.\ell^{-1}.s^{-1}$
rpm	revolutions per minute	
R	universal gas constant	$8.314\ J.K^{-1}.mol^{-1}$
R^2	correlation coefficient	
SCE	saturated calomel electrode	
SEM	scanning electron microscopy	
SHE	standard hydrogen electrode	
t	time	s
T	temperature	K
V	volume	m^3
XRD	x-ray diffraction	
z	number of electrons transferred	

1. INTRODUCTION

Bioleaching is recognised as a suitable process for the pretreatment of refractory gold ores. It is advantageous over other processing techniques such as pressure leaching, roasting, nitric acid digestion and chlorination because it is suitable for the processing of low and complex grade ores, involves low capital investment and is environmentally acceptable. Besides the treatment of refractory gold bearing ores, bioleaching is also used for copper and uranium extraction, and is now being extended to the extraction of other metals like nickel, cobalt and cadmium (Torma, 1993). Bioleaching is also associated with acid mine drainage resulting from sulfide waste heaps which leads to ground water contamination from mining and minerals processing operations.

Recent research (Boon *et al.*, 1995) has shown that the bioleaching of sulfide minerals such as pyrite occurs via an indirect mechanism. Ferric iron leaches the mineral, producing ferrous iron, and the ferrous iron is oxidised to ferric iron by bacteria such as *Thiobacillus ferrooxidans* and *Leptospirillum ferrooxidans*. By regenerating ferric iron, the bacteria are able to maintain a high redox potential in bioleaching systems. The following two equations describe the bioleaching of pyrite:

Chemical ferric leach

$$FeS_2 + 8H_2O + 14Fe^{3+} \rightarrow 15Fe^{2+} + 2SO_4^{2-} + 16H^+ \qquad [1.1]$$

Bacterial oxidation of ferrous iron regenerating ferric iron

$$4Fe^{2+} + O_2 + 4H^+ \rightarrow 4Fe^{3+} + 2H_2O \qquad [1.2]$$

The existence of an indirect mechanism implies that the bacterial and chemical subprocesses can be characterised separately, allowing for the independent optimisation of bacterial growth and metabolism and mineral oxidation kinetics.

The bacterial oxidation of ferrous iron has been found to be a function of the ferric/ferrous ratio (Boon, 1996). In this thesis, it is postulated that the ferric leaching of pyrite is also a function of the ferric/ferrous ratio. Although considerable research has been done on the ferric leaching of pyrite, the reaction conditions have not been the same as those encountered in bioleaching. In particular, the redox potentials were much lower than those maintained by bacteria in bioleaching, so the chemical leaching data in the literature cannot be compared with bioleaching data. It is necessary to determine the chemical leach rate of pyrite at potentials similar to those of bioleaching to conclude that the bacteria do not directly cause an increase in the leach rate, but that the rates are a function of the redox potential, which the bacteria maintain.

This project is based on the two-step indirect hypothesis and has the specific objective of measuring the ferric leach kinetics of pyrite by following the redox potential of a pyrite slurry.

In this thesis, the reaction between pyrite and ferric iron in sulfuric acid was investigated by monitoring the redox potential of an acidic ferric sulfate solution when pyrite particles were added to it. The potential is related to the ferric/ferrous ratio by the Nernst Equation, Equation 1.3.

$$E = E^{\circ} + \frac{RT}{zF} \ln \frac{[Fe^{3+}]}{[Fe^{2+}]} \qquad [1.3]$$

The potential was found to drop during the course of the reaction, which is expected considering the Nernst Equation and the reaction stoichiometry of Equation 1.1.

The initial behaviour of such a system, and the effects of changing the total iron concentration and the mass of ore were investigated. The form of the dependence of the reaction rate on the ferric/ferrous ratio or the potential was compared with literature data, although previously published data had been obtained at lower potentials.

A number of possible mechanistic descriptions of the kinetics were discussed, including the applicability of the Butler-Volmer Equation, Equation 1.4 to relate the rate to the potential. On this basis, the likelihood of an electrochemical mechanism being operative was assumed.

$$i = i_o\left(\exp\left(\frac{(1-\alpha)F\eta}{RT}\right) - \exp\left(\frac{-\alpha F\eta}{RT}\right)\right) \qquad [1.4]$$

In summary, the emphasis of this work was to study the chemical ferric leach sub-process within the context of the indirect mechanism hypothesis by reconciling previously published data and investigating experimental techniques to obtain relevant data.

2. LITERATURE REVIEW

2.1 Oxidation of Sulfide Minerals

2.1.1 General oxidation processes

The oxidation of sulfide minerals is important both commercially and environmentally. Sulfide minerals must be oxidised to release metal value forming part of the sulfide ore (as in the production of copper (e.g. Torma, 1993)). Often sulfides form part of the gangue in an ore body and must be oxidised to release metals enclosed (as in the pretreatment of refractory gold ores, the sulfide must first be oxidised before leaching of the gold is possible (Brierley, 1994; Dew, 1995)). The natural oxidation of sulfides, especially in minerals processing waste dumps, leads to the production of acid mine drainage which has major environmental consequences. Understanding the fundamentals of sulfide mineral oxidation is thus important.

Metal sulfides have widely varying physical and chemical properties. Solid state properties influence the electrochemical and chemical surface reactions, causing the range of metal sulfides to have a very large range in reactivities and reaction mechanisms (Tributsch and Bennett, 1981).

Sulfide minerals can be degraded in either oxidative or non-oxidative processes. In non-oxidative processes, such as treatment with non-oxidising strong acids (Peters and Doyle, 1989), the sulfur moiety retains its oxidation state, usually forming H_2S as a product. In oxidative processes, such as occurs in bioleaching systems in the presence of bacteria, like *Thiobacillus ferrooxidans*, the sulfide is oxidised, forming a number of products, depending on the mineral and process conditions. All oxidative leaching reactions are exothermic (Ahonen and Tuovinen, 1989).

Pressure oxidation involves heating the mineral (typically to 80 - 250 °C) (Peters and Doyle, 1989) under conditions of high air or oxygen pressure. These harsh conditions often lead to the formation of SO_2 which is not usually a desired industrial product.

Hydrometallurgical treatments generally make use of milder conditions. Unlike most base metal oxides, the sulfides do not dissolve easily in mineral acids but require an oxidising agent (Dutrizac and MacDonald, 1974). Oxidants such as ferric iron, dissolved oxygen, ozone, nitric acid, hydrogen peroxide, chlorate salts, hypochlorites and cupric ions can be used, with the differences in kinetics usually attributed to the level of the oxidation potential (Peters and Doyle, 1989). The addition of oxidising agents modifies the solution and the surface properties of the mineral and the oxidation is controlled by both equilibrium and kinetic reactions at the mineral/solution interface (Fornasiero *et al.*, 1992). For an oxidant to leach a mineral, its potential must be higher than the electrochemical potential of the mineral (Riekkola-Vanhanen and Heimala, 1993). The greater the difference in potential between the two, the greater will be the driving force for the reaction (Wadsworth, 1987).

The extent to which sulfide minerals oxidise when simply exposed to air varies depending on the mineral and the length of time of exposure. Buckley and Woods (1984) exposed the freshly fractured surfaces of a selection of sulfide minerals to air. Galena that was exposed for less than a minute was only negligibly oxidised, but with longer periods of exposure lead-oxyhydroxide and later basic lead sulfate were formed. Bornite (Cu_5FeS_4) exposed to air formed iron oxide while the copper remained as a sulfide species, as did chalcopyrite ($CuFeS_2$), but at a much slower rate. Pyrrhotite reacted very quickly to form iron-oxyhydroxide after only a few seconds exposure.

Dissolved oxygen oxidation of sulfides is generally kinetically less important than oxidation by ferric iron (Wadsworth, 1987). If leaching occurs at elevated pressure, however, it may become the dominant oxidant, but oxygen transport could become rate limiting (Wadsworth, 1987). McKibben and Barnes (1986) found that sulfate ions were the major sulfur reaction product during the aqueous oxidation of pyrite with dissolved oxygen. The equation for the reaction between pyrite and oxygen is as follows:

$$2FeS_2 + 7O_2 + 2H_2O \rightarrow 2Fe^{2+} + 4SO_4^{2-} + 4H^+ \qquad [2.1]$$

Isotopic studies have shown that the sulfate oxygen in Equation 2.1 comes from water, and that the dissolved oxygen only acts as an electron acceptor (Taylor *et al.*, 1976). Both McKibben and Barnes (1986) and Williamson and Rimstidt (1994) found the reaction order for dissolved oxygen in the oxidation of pyrite to be 0.5. The latter authors found that the

reaction could not be modelled adequately using a simple, ideal Langmuir adsorption isotherm, but that a Freundlich isotherm was more suitable. This is consistent with the non-uniform attack of the pyrite surface by aqueous oxidants at sites of high excess surface energy.

Ferric iron is commercially a very important oxidising agent since it can be produced *in situ* (Wadsworth, 1987) (for example by bacteria or using oxygen). In an extensive review on the ferric leaching of sulfide minerals, Dutrizac and MacDonald (1974) reported that ferric iron had been observed to be a much more effective oxidising agent than gaseous oxygen, provided the leaching solution was sufficiently acidic to keep the iron in solution. This observation was also made by McKibben and Barnes (1986) who showed that the partial pressure of oxygen had very little effect on the rate of pyrite oxidation. Moses *et al.* (1987) also claimed that ferric iron is the direct oxidant of pyrite in both aerobic and anaerobic systems. To support this experimental evidence, they discussed that the probability of a direct reaction between molecular oxygen and pyrite is low, since pyrite is diamagnetic and oxygen is paramagnetic. This reasoning can also be applied to other minerals. Ferric leaching generally produces elemental sulfur as a product, although sulfate is thermodynamically more stable. Williamson and Rimstidt (1994) list several reports that the rate of oxidation of sulfide minerals by ferric iron is larger in chloride than sulfate medium. This could be because sulfate ions inhibit the rate determining step or chloride ions catalyse it, but this has not been proven. Crundwell (1988) showed passivation of sphalerite in ferric sulfate solutions but not ferric chloride solutions. The difference in kinetics in the presence of chloride or sulfate ions is likely to be due to complex formation.

The use of hydrogen peroxide as an oxidant is limited by its rapid anodic decomposition to hydrogen ions and oxygen (Wadsworth, 1987). This reaction is catalysed by ferrous iron and metallic surfaces, even under alkaline conditions. McKibben and Barnes (1986) found that H_2O_2 was consumed by catalytic decomposition almost as fast as by pyrite oxidation. In the reaction with pyrite, only sulfate ions were detected as the sulfur reaction product.

Chloride or hypochlorite leaching can be applied to sulfides of mercury, molybdenum, antimony, copper, zinc, lead and silver. These generally result in a solution of chloro-complexes and the production of sulfate (Koch, 1975). Although not common, cupric ions

can be used in suitable solvents. Cupric ions have been used to leach covellite and chalcocite (Koch, 1975).

As many sulfides are good electrical conductors, it is not surprising that their leaching has an electrochemical nature. Leach kinetics can be related to the potential of the solid mineral in contact with an aqueous electrolyte (Wadsworth, 1987). If the resistance of the mineral is low, the solid essentially assumes a uniform potential throughout and assumes a mixed potential determined by associated anodic and cathodic processes. This potential will also depend on the properties of the mineral surface. By applying a potential to a sulfide mineral, either directly or by use of an oxidant, its anodic dissolution can be controlled. Before any dissolution can occur, the mixed potential must exceed the equilibrium potential (or rest potential) of the mineral.

2.1.2 Electrochemical application to mineral oxidation

Electrochemistry is an important consideration in the study of oxidation of sulfide minerals. Before oxidation can occur, a potential exceeding the mineral rest potential must be applied to the mineral. Quoted rest potentials are dependent on the experimental conditions under which they are measured (e.g. temperature and pH) and are characteristic of the ore used, subject to the stoichiometry of the mineral, the presence of impurities and semiconducting effects. Literature values are subject to a wide variation (Table 2.1). The rest potential is the open circuit potential of the mineral. It has been suggested that to accurately measure the rest potential, the mineral must be allowed to equilibrate with the electrolyte for 12 hours under argon atmosphere to allow the potential to stabilise (Doyle *et al.*, 1989).

When two sulfide minerals are in contact in aqueous solution, the mineral with the lower rest potential becomes anodic and undergoes dissolution, while the mineral with the higher potential is galvanically protected and becomes cathodic. The order of nobility of the minerals is generally consistent with the rest potentials of the minerals, and the commonly accepted galvanic series is as follows: pyrite, chalcopyrite, covellite, chalcocite, galena, sphalerite, going from most noble to most active (Natarajan, 1988, and Table 2.1). The rate of galvanic dissolution also depends on the duration of contact, the anode to cathode surface area ratio, the electrolyte (its conductivity, pH, other redox species present etc.) and the

presence or absence of bacteria. Generally galvanic interactions are reported to be enhanced by bacteria, so bacteria can improve the selective leaching of certain sulfide minerals (Riekkola-Vanhanen and Heimala, 1993).

Minerals	Rest Potential (mV vs sat. Ag/AgCl)	Conditions	Reference
Pyrite	497	inoculated, Fe present	Natarajan (1988)
	494	with *Thiobacillus ferrooxidans*	Jyothi *et al.* (1989)
	494	with *Thiobacillus ferrooxidans*	Natarajan (1992)
	473.70	sample RC1A	Doyle *et al.* (1989)
	462	in nutrient medium	Dutrizac and MacDonald (1974)
	452.80	sample MC11	Doyle *et al.* (1989)
	449.50	sample MD11	Doyle *et al.* (1989)
	422		Peters (1976)
	419.30	sample HP2A	Doyle *et al.* (1989)
	391.75	sample LS1A	Doyle *et al.* (1989)
	387	inoculated, Fe-free	Natarajan (1988)
	365.70	sample HP4A	Doyle *et al.* (1989)
	347	uninoculated	Natarajan (1988)
	344	in nutrient medium	Jyothi *et al.* (1989)
	297 to 437		Riekkola-Vanhanen and Heimala (1993)
Arsenopyrite	287 to 427		Riekkola-Vanhanen and Heimala (1993)
Chalcopyrite	357	inoculated, Fe present	Natarajan (1988)
	287	inoculated, Fe-free	Natarajan (1988)
	247	uninoculated	Natarajan (1988)
	247 to 397		Riekkola-Vanhanen and Heimala (1993)
Galena	222	inoculated, Fe present	Natarajan (1988)
	67	inoculated, Fe-free	Natarajan (1988)
	57	uninoculated	Natarajan (1988)
	77 to 197		Riekkola-Vanhanen and Heimala (1993)
Sphalerite	37	inoculated, Fe present	Natarajan (1988)
	27	inoculated, Fe-free	Natarajan (1988)
	12	uninoculated	Natarajan (1988)
	7 to 107		Riekkola-Vanhanen and Heimala (1993)
Pyrrhotite	-103 to 42		Riekkola-Vanhanen and Heimala (1993)

Table 2.1 Rest Potentials for Sulfide Minerals

In mineral leaching systems, the mixed potential is usually of more significance than the rest potential. The mixed potential is that potential where the rate of the anodic reaction equals that of the cathodic reaction. This means that at the mixed potential, the resistance in the external circuit approaches zero. The current flowing at the mixed potential (the mixed current) can theoretically be used to determine the mineral leach rate (Jin *et al.*, 1993). The

value of the mixed potential will depend on the mineral rest potential and the potential of the electrolyte in which it is suspended (e.g. the ferric/ferrous ratio in a ferric leaching system), or in a galvanic couple, the rest potential of the minerals concerned. For minerals in galvanic contact, the mixed potential is intermediate between the individual rest potentials (as noted by Mehta and Murr (1983) for the pyrite/chalcopyrite couple). In the region of the mixed potential, the rates of reverse processes are often ignored. For sulfide minerals, this is generally acceptable because the dissolution reactions can be considered irreversible, but the assumption is not always valid for other processes such as ferric reduction (Nicol, 1993).

The mixed potential and mixed current can be determined by measuring polarization curves for the anode and the cathode under different experimental conditions by varying the resistance in the external circuit from infinity to nearly zero and measuring the electrode potential (Jin *et al.*, 1993). The point of intersection between the anodic and cathodic polarization curves corresponds to the mixed potential and mixed current for the system. Useful information on the reaction mechanism can be obtained from the position of the mixed potential on individual polarization curves, especially if the mixed potential lies within, for example, a passivating region (Nayak *et al.*, 1995). The Tafel slopes for the anodic and cathodic reactions can be useful in distinguishing whether multiple electron transfer is simultaneous or sequential, and can thus be used in determination of a reaction mechanism (Pletcher, 1991, p111). This may be applicable in determining reaction intermediates in a multi-step reaction, like the formation of a final sulfate product from sulfide minerals like pyrite.

Conventional electrochemical techniques, such as cyclic voltammetry, can be used to study sulfide minerals (Briceño and Chander, 1988; Chia *et al.*, 1989; Riekkola-Vanhanen and Heimala, 1993). In these types of studies it is often useful to use mineral electrodes. When making mineral electrodes, it is important to avoid altering the composition and the mineral surface. Generally, sulfides are sensitive to heat, oxidation and the introduction of ions such as Ag^+ and Cu^+ from electrical contacts (Peters, 1976). The form of the electrode affects its behaviour depending on whether a particular crystal face is exposed or if the mineral particles have been mixed with a binder for immobilisation.

Platinum is often used as an inert electrode and can easily attain the redox potential of a mineral suspension. Although it is known to become poisoned, it allows good current flow and is useful in biological studies because it is non-toxic to bacteria. Graphite electrodes have also been used in mineral electrochemical studies (Blake *et al.* , 1994, Linge and Jones, 1993) because they are inert, have a low resistance and are less expensive than platinum.

Cyclic voltammetry is a technique used to show the existence of intermediates (which often cannot be predicted on thermodynamic grounds) in the oxidation or reduction of a sample. In cyclic voltammetry, the potential of the mineral is scanned between two limits while the current is measured, then the direction of the scan is reversed. Species which are oxidised on the forward scan are reduced on the reverse scan. With high scan rates it is possible to identify the existence of short lived intermediates that are not normally detected (Crow, 1994). In leaching systems, the position and shape of the current-voltage curves on consecutive cycles changes due to changes in the structure and composition of the mineral surfaces caused by dissolution and precipitation (Riekkola-Vanhanen and Heimala, 1993). Often the peak current decreases with repeated sweeps because of the disappearance of active sites (Chia *et al.*, 1989). The greater the separation between the peaks for the forward and reverse scans, the more irreversible the electrode process (Crow, 1994), while the current density gives an indication of the extent of passivation. In work done by Riekkola-Vanhanen and Heimala (1983), a low current density for pyrrhotite indicated a rapid activation and passivation of the surface, while chalcopyrite displayed passivation at low potentials, dissolution of the passivation layer at higher potentials and active dissolution of the mineral at even higher potentials. This is just one example to show that the leach or dissolution rates of sulfide minerals are dependent on the mineral electrochemical potential.

The presence of intermediates in an electrochemical process are indicated by the presence of multiple peaks in a cyclic voltammogram. If all the electron transfer processes take place in a single reaction, then only one oxidation and one reduction peak should be seen. Although cyclic voltammetry can detect the existence of these intermediate reactions at suitable scan rates, it is difficult to assign specific reactions to specific peaks. This can be attempted using thermodynamic data. The half-peak potentials estimated from the voltammograms should correspond to the standard potential (E^{o}) for the proposed reaction giving rise to the peak (Chia *et al.*, 1989).

There are a number of factors to bear in mind regarding the polarization studies of sulfide minerals. The polarization curves for irregularly shaped specimens are not as reproducible as for polished specimens. It has been found, however, that there was still a general similarity in results between irregular and polished samples, so polishing had no major effect on the polarization behaviour (Meyer, 1979).

Sulfides often have a low conductivity, so the voltage drop across the mineral could be appreciable. The resistance can be reduced by thinning the sample (Peters, 1976). The semiconductor nature of sulfides could also cause them to have non-ohmic junctions (Peters, 1976).

It must also be realised that when controlling the potential during oxidation of a sulfide mineral, the electron acceptor will probably affect the observed behaviour. It is expected that the mineral will behave differently when an external source (e.g. a Pt counter electrode) is used as the electron sink to when a redox couple participates in the charge transfer process (Doyle *et al.*, 1989).

AC impedance measurements are sensitive for measuring mineral reactivities and the state of the mineral surface (Briceño and Chander, 1988, Doyle *et al.*, 1989). This is however a slow technique so is not suitable for investigating rapidly changing systems, and it is often necessary to allow the mineral/solution interface to stabilise during a conditioning period.

Although electrochemical techniques are useful in the characterisation of sulfide minerals, they generally lack the specificity to identify the species formed at a mineral electrode surface unequivocally. It can be useful to combine them with other techniques like x-ray photoelectron spectroscopy (XPS) for a better overall understanding of the electrochemical processes (Buckley and Woods, 1984).

2.2 Pyrite

2.2.1 Physical characterisation of pyrite

Pyrite is an extremely common sulfide mineral, occurring in most sulfide ore bodies. Natural pyrite, however, is heterogeneous and even within a single sample there can be large differences in stoichiometry, impurity content and physical defects (Doyle *et al.*, 1989). This results in a large range of electronic properties.

Pyrite is an opaque, brass yellow mineral with a metallic lustre. In polished section it is generally isotropic. It has a density of 4.6 - 5.2 $g.cm^{-3}$, a Mohr hardness of 6-6.5 and melts at about 1171 °C. Pyrite is dimorphic with marcasite, which is very similar to pyrite in appearance. The colour of freshly fractured marcasite deepens on exposure to air and a white ferrous sulfate powder develops on the surface due to the inherent instability of marcasite. Marcasite has a less dense crystal structure than pyrite, with a density of 4.88 $g.cm^{-3}$ (Lowson, 1982). The transformation from marcasite to pyrite is significantly exothermic at 700 K, with an enthalpy of transformation of about -4.9 $kJ.mol^{-1}$.

Euhedral pyrite has a well developed crystal form. The most common crystal forms are the cube and the pentagonal dodecahedron (also known as the pyritohedron) (Lowson, 1982). The cubic and pyritohedral faces are usually striated with fine lines caused by oscillatory growth between the two forms. The crystals are usually extensively twinned, both on a macro- and micro-scale, with the direction of twinning controlling the sign of thermoelectric properties.

The crystal structure of pyrite is isomorphic with the natural mineral sulfides of manganese, cobalt, copper, zinc, cadmium, osmium, ruthenium and rhodium. Although strictly it cannot be classified as 'close-packed', pyrite is a very dense material. Each Fe atom is surrounded by six S atoms, and each S atom has one nearest neighbour S atom and three nearest neighbour Fe atoms. Pyrite has a variable sulfur deficiency within $FeS_{2.00}$ to $FeS_{1.94}$ (Lowson, 1982). Marcasite has a lower symmetry than pyrite - it crystallises in an orthorhombic crystal structure.

Framboidal pyrite consists of non-crystalline grains and agglomerates of non-crystalline grains (Lowson, 1982). This type of pyrite is usually heterogeneously dispersed through a host rock, and is often associated with mine tailings. Framboidal pyrite is more reactive than massive pyrite, with Pugh *et al.* (1984) reporting a twofold increase in the reaction rate.

Pyrite is a semiconductor and can occur as n- or p-type material, and even contain p-n junction material. The variable nature of the semiconducting properties has been attributed to the range in stoichiometry, the lead, cobalt and nickel content and a range of heavy metals (Lowson, 1982). In semiconductors, the valence and conduction bands are separate and conduction occurs either by electrons in the conduction band (n-type) or holes in the valence band (p-type). For pyrite, the band gap is estimated to be between 0.95 and 1.2 eV (Doyle *et al.*, 1989). n- and p-type semiconductors exhibit different electrochemical behaviour. For the anodic oxidation of pyrite, holes are required and for the cathodic reduction, electrons are required, so the rates of these reactions will be a function of the rate at which holes and electrons can be supplied to the surface.

For p-type pyrite, the resistivity decreases with temperature, but for n-type pyrite it increases (Lowson, 1982). At room temperature, n-type pyrite has a lower resistivity than p-type and a higher Hall mobility. Generally, the resistivity ranges from 10^{-5} - 10^{0} Ω.m for n-type and 10^{-3} - 10^{0} Ω.m for p-type (Doyle *et al.*, 1989). Besides being a function of the semiconducting type, the chemical resistivity also varies depending on the crystal direction, and the pressure. There is some dispute as to which semiconducting type is more reactive. Doyle *et al.* (1989) found that n-type pyrite generally has a high rest potential and low reactivity, but that once a current does pass, it appears to transform the surface to a p-type material, probably through forming metal deficient layers. Chia *et al.* (1989) found that n-type was more easily oxidisable and that p-type was more stable.

As mentioned above, anodic dissolution requires the injection of holes into the valence band (mainly of sulfur 3p character) (Doyle *et al.*, 1989). Holes can be provided by photons, which explains why the dissolution of many sulfides is promoted by light. When holes are provided by a redox couple, the energy levels of the oxidant must overlap with the energy level of the

valence band of the pyrite. Hence a powerful oxidising agent may be less effective for a particular sulfide than one which gives better overlap of the energy levels (Doyle *et al.*, 1989).

2.2.2 Ferric leaching of pyrite

Pyrite is oxidised by ferric iron according to the following equation:

$$FeS_2 + 8H_2O + 14Fe^{3+} \rightarrow 15Fe^{2+} + 2SO_4^{2-} + 16H^+ \qquad [2.2]$$

It has been stated that pyrite does not respond favourably to ferric leaching (Dutrizac and MacDonald, 1974) because a very slow rate is observed, but this would be expected when the stoichiometry of Equation 2.2 is considered - 14 moles of ferric ions are converted to 15 moles of ferrous ions in reaction with each mole of pyrite, causing a rapid drop in the redox potential according to the Nernst equation (Equation 1.3).

Several researchers have investigated the ferric leaching of pyrite and other sulfide minerals. Experimental details are given in Table 2.2.

Mathews and Robins (1972) used a gas lift percolator with nitrogen as the circulatory gas to study the oxidation of iron disulfide with ferric sulfate. Ferric chloride was also used in some of the tests but similar rates were obtained. The effects of temperature, ore mass, volume, surface area, pH, total iron concentration and ferric iron concentration were investigated. The leach rate was found to be dependent on the ratio of ferric iron to total iron. This result was a confirmation of that obtained by Garrels and Thompson (1960) who postulated that the instantaneous rate was controlled adsorption of ferrous and ferric ions to the pyrite surface and was proportional to the fraction occupied by ferric ions. They used acidic ferric sulfate to leach pyrite and monitored the solution redox potential. They found a rapid drop in potential initially, followed by a linear drop in potential with time from about 200 minutes into the leach. This linear region formed the basis for all their results. Based on their postulate that the behaviour of the system was because of adsorption of ions to the pyrite surface, they suggested that the marked increase in the leach rate when the ferric/ferrous ratio approached very high values was because the fraction occupied by ferric ions at the pyrite surface probably increased in an anomalous fashion as the ferrous ion concentration became very low. They

Table 2.2 Experimental Details for Ferric Leaching of Pyrite (table in three parts)

Reference	Apparatus	Ore pretreatment	Leaching medium	Size fraction	Slurry concentration
Garrels and Thompson 1960	Slurry stirred magnetically	Rinsed with 6N H_2SO_4 and distilled water, then dried with acetone	$Fe_2(SO_4)_3$	+74-149 μm	-
Singer and Stumm 1967	Leaching under N_2,- no detail	None discussed	Fe(III)	-	1 g.ℓ^{-1}
Mathews and Robins 1972	Gas lift percolator with N_2 circulator gas	Prewashed (no detail given)	$Fe_2(SO_4)_3$ in H_2SO_4	+300-420 μm	50 g.ℓ^{-1}
Paciorek *et al.* 1981	Slurry in conical flask agitated by reciprocating shaker	Ground and sieved under N_2	'61' bacterial growth medium	< 38 μm	500 g.ℓ^{-1}
Wiersma and Rimstidt 1984	Vessel with overhead glass stirrer	Dry sieved	$FeCl_3$ in HCl	+75-150 μm	2 g.ℓ^{-1}
McKibben and Barnes 1986	Pyrite clamped between 2 nylon screens in stirred vessel	Very detailed treatment (see text)	$FeCl_3$	+125-250 μm	3.75 g.ℓ^{-1}
Tal 1986	Slurry in beaker stirred magnetically	None discussed	$Fe_2(SO_4)_3$ in H_2SO_4	<38 μm	30 g.ℓ^{-1}
Zheng *et al.* 1986	Ore clamped between two filter discs with circulation of lixiviant	Washed in 6N H_2SO_4 and distilled water, then dried with acetone or under vacuum	$Fe_2(SO_4)_3$ in H_2SO_4	+105-250 μm	25 g.ℓ^{-1}
Kawakami *et al.* 1988	Stirred batch reactor	None discussed	$FeCl_3$ in HCl	< 53 μm	12 g.ℓ^{-1}
Boogerd *et al.* 1991	Slurry in shake flasks	None discussed	bacterial growth medium and $FeCl_3$ in HCl	10 μm	5 - 10 g.ℓ^{-1}
Williamson and Rimstidt 1994	Mixed flow or stirred batch reactor	1 N HCl soak	$FeCl_3$ in HCl	+150-250 μm	2 g

Table 2.2 continued

Reference	Temperature	Activation energy	pH	Initial [Fe]	Time	ln (Fe^{3+}/Fe^{2+}) range
Garrels and Thompson 1960	33 ± 2 °C	-	0 - 2	0.0004 M	24 - 100 hours	-6 to -2
Singer and Stumm 1967	-	-	-	0.003 M	4 hours	-1.2 to 1.8
Mathews and Robins 1972	30 °C - 70 °C	92 $kJ.mol^{-1}$	1.35	0.02 M	2 hours	-0.02 to 1.82
Paciorek *et al.* 1981	28 ± 1.5 °C	-	not controlled	0.0002 M	311 hours	-3.75 to -2.83
Wiersma and Rimstidt 1984	25 °C	92 $kJ.mol^{-1}$	2	0.001 molal	4 hours	-7.63 to -1.53
McKibben and Barnes 1986	30 °C	60.3 $kJ.mol^{-1}$ (McKibben, 1984)	1.89	0.002 M	3 hours	-1.25 to 2.28
Tal 1986	60 ± 1°C	-	not controlled	0.18 M	-	-0.2 to 2.9
Zheng *et al.* 1986	25 °C	-	-	0.009 - 0.09 M	-	-6 to 2.3
Kawakami *et al.* 1988	60 °C	95 $kJ.mol^{-1}$	1	0.5 M	60 hours	-0.08 to 1.89
Boogerd *et al.* 1991	70 °C	-	1.5	0.09 M	9 hours	-0.75 to 1.65
Williamson and Rimstidt 1994	25 °C	-	< 3	0.0001 m		0.57 to 2.47

Typical commercial bioleaching conditions (Van Aswegen, 1993):

temperature	40-45 °C
pH	1.2-1.8
residence time	4 days
W:S	4:1
$[O_2]$	2 ppm

Table 2.2 continued

Reference	constants	Rate law	Rate law in common terms
Garrels and Thompson 1960	-	-	-
Singer and Stumm 1967	-	-	-
Mathews and Robins 1972	$k = 1.47 \times 10^{8}$ for rate in mol.ℓ^{-1}.min^{-1}	$r_{FeS_2} = k \cdot \frac{MA}{V} \cdot \frac{[Fe^{3+}]\exp(\frac{-E_a}{RT})}{[Fe^{tot}][H^+]^{0.44}}$	$r_{FeS_2} = K \cdot \frac{MA}{V} \cdot \frac{[Fe^{3+}]\exp(\frac{-E_a}{RT})}{[Fe^{tot}][H^+]^{0.44}}$
Paciorek *et al.* 1981	-	-	-
Wiersma and Rimstidt 1984	$k = 1.0 \times 10^{-4}$ to 2.7×10^{-4} s^{-1} rate in mol.kg^{-1}solution.s^{-1}	$-\frac{dm_{Fe^{3+}}}{dt} = k'\frac{A}{M'}m_{Fe^{3+}} = km_{Fe^{3+}}$	$r_{FeS_2} = K[Fe^{3+}]$
McKibben and Barnes 1986	$k = -10^{-9.74}$ rate in mol FeS_2.cm^{-2}.min^{-1}	$R_{FeS_2} = k\frac{[Fe^{3+}]^{0.5}}{[H^+]^{0.5}}$	$r_{FeS_2} = K\frac{[Fe^{3+}]^{0.5}A}{[H^+]^{0.5}V}$
Tal 1986	$k = 6.42$ mg pyrite .g^{-1}.h^{-1} $n = 0.682$ rate in mg pyrite .g^{-1}.h^{-1}	$r = k\left(\frac{[Fe^{3+}]}{[Fe^{2+}]}\right)^n$	$r_{FeS_2} = K\left(\frac{[Fe^{3+}]}{[Fe^{2+}]}\right)^n\frac{M}{V}$
Zheng *et al.* 1986	rate in μmol.kg^{-1}.s^{-1} $k_1 = 6.10$ $k_2 = 2.03$ $k_3 = 3.84$ $k_4 = 91.1$	$r = \frac{k_1 - k_2\left(\frac{[Fe^{2+}]}{[Fe^{3+}]}\right)^{\frac{1}{2}}}{\frac{1}{[Fe^{3+}]^{\frac{1}{2}}} + k3 + k4\left(\frac{[Fe^{2+}]}{[Fe^{3+}]}\right)^{\frac{1}{2}}}$	$r_{FeS_2} = K \cdot \frac{k_1 - k_2\left(\frac{[Fe^{2+}]}{[Fe^{3+}]}\right)^{\frac{1}{2}}}{\frac{1}{[Fe^{3+}]^{\frac{1}{2}}} + k3 + k4\left(\frac{[Fe^{2+}]}{[Fe^{3+}]}\right)^{\frac{1}{2}}} \cdot \frac{M}{V}$
Kawakami *et al.* 1988	at 348 K $k_R = 0.056$ min^{-1} $k_L = 0.33$ mol^2.m^{-5}.min^{-1} $K_R = 19.5$ $K_L = 5.6$ rate in mol.m^{-2}.min^{-1}	$\frac{d[Fe^{2+}]}{dt} = (15 - 13\alpha)\frac{6\omega}{\rho d}\left\{\begin{matrix} k_R[R]\frac{[Fe^{3+}]}{[Fe^{3+}] + K_R[Fe^{2+}]} \\ + k_L\frac{[Fe^{3+}]}{([Fe^{3+}] + K_L[Fe^{2+}])^2}\end{matrix}\right\}$	$r_{FeS_2} = K\frac{A.M}{V^2.d}\left\{\begin{matrix} k_R[R]\frac{[Fe^{3+}]}{[Fe^{3+}] + K_R[Fe^{2+}]} \\ + k_L\frac{[Fe^{3+}]}{([Fe^{3+}] + K_L[Fe^{2+}])^2}\end{matrix}\right\}$
Boogerd *et al.* 1991	$k = 64 \pm 6$ at 70 °C rate in mmol.ℓ^{-1}.day^{-1}	$\frac{d[FeS_2]}{dt} = k\frac{[FeS_2]}{30 + [FeS_2]} \cdot \frac{[Fe^{3+}]}{95 + [Fe^{3+}]}$	$r_{FeS_2} = K\frac{[FeS_2]}{30 + [FeS_2]} \cdot \frac{[Fe^{3+}]}{95 + [Fe^{3+}]}$
Williamson and Rimstidt 1994	$k = 10^{-6.07 (\pm 0.37)}$ rate in mol pyrite.m^{-2}.s^{-1} DO present	$r = k\frac{m_{Fe^{3+}}^{0.93}}{m_{Fe^{2+}}^{0.40}}$	$r_{FeS_2} = K\frac{[Fe^{3+}]^{0.93}}{[Fe^{2+}]^{0.40}} \cdot \frac{A}{V}$
	$k = 10^{-8.58 (\pm 0.15)}$ rate in mol pyrite.m^{-2}.s^{-1} N_2-purged	$r = k\frac{m_{Fe^{3+}}^{0.30}}{m_{Fe^{2+}}^{0.47}m_{H^+}^{0.32}}$	$r_{FeS_2} = K\frac{[Fe^{3+}]^{0.30}}{[Fe^{2+}]^{0.47}[H^+]^{0.32}} \cdot \frac{A}{V}$

Nomenclature used specifically in Table 2.2

A	surface area of reacting solid	m^2
α	molar fraction of pyrite forming sulfur	
d	initial particle diameter	m
E_a	activation energy	$kJ.mol^{-1}$
k	rate constant	sec^{-1}
m	molality	$mol.kg^{-1}$
M	mass of ore	kg
M'	mass of solution	kg
n	reaction order	
ρ	pyrite density	$kg.m^{-3}$
[R]	concentration of reactive sites	$mol.m^{-2}$
$R_{Fe^{3+}}$	rate	$mol.cm^{-2}.min^{-1}$
ω	pyrite concentration	$kg.m^{-3}$

concluded that the rate of oxidation was dependent on the redox potential and not the total iron concentration.

Wiersma and Rimstidt (1984) oxidised pyrite and marcasite at 25 °C with ferric chloride at pH 2 and monitored the solution redox potential of the mineral slurry. The pretreatment of the ore (if any) was not detailed. They observed a very high initial rate (characterised by a rapid drop in the redox potential) for which a number of reasons were suggested: rapid dissolution of fine particles on the mineral surface or dissolution of a disturbed surface layer, rapid adsorption of ferric ions onto reactive sites at the solid surface and the rapid decrease and disappearance of a streaming potential at the indicator electrode produced by the relative movement of the electrode and solution due to stirring. Because of this behaviour, the first 75 minutes of data for each run were discarded. The rate law was first order with respect to ferric iron, and a determination of the activation energy indicated that the leaching rate was controlled by a surface (chemical) reaction.

McKibben and Barnes (1986) derived a rate law for the oxidation of pyrite by ferric chloride at 30 °C. This work was unusual in that the pyrite sample was clamped between two nylon screens and the leach solution was circulated. The pretreatment of the ore was very thorough to reduce the possibility of measuring anomalously high dissolution rates of fine mineral powders on the ore surface or a thin damaged outer zone of material. The ore was first crushed and soaked overnight in hot HF to remove silicates, washed in de-ionised water, and stored in air before being sieved. The pyrite was cleaned ultrasonically in ethanol for 30 seconds, then rinsed in 1 M nitric acid for 1 minute, followed by successive rinsing with distilled water and ethanol, with a final ethanol rinse to dehydrate the surface. The material was then dried with air and stored briefly. Immediately prior to using the ore, it was rinsed with 0.1 M HCl to remove any oxidised coating, and then with water. The ore was analysed by SEM at particular stages of the preparation. After sieving, a fine powder was visible on the surface and there was irregular pitting, possibly from the HF treatment or the rupture of fluid inclusions during the crushing. After the nitric acid treatment there was no adhered powder and surface pitting and linear fractures were variable from grain to grain. After leaching, much of the mineral surface appeared smooth and undisturbed, but the pit edges and cleavage fractures seemed more ragged and etched. It is possible that some pits may have formed

during the oxidation. It was apparent that oxidation had occurred non-uniformly, occurring mainly at the sites of sites of high excess surface energy.

The rate laws were derived using the initial rate method, which only makes use of the initial reaction period. This technique does not require that a rate law be assumed and also the changes in surface area and volume over short times can be considered negligible. The specific rate of oxidation was found to be proportional to the square root of the ferric concentration.

The effect of the redox potential on the leaching rate has not been directly examined in many instances. Tal (1986), however, determined the leach rate of pyrite in a slurry at 60 °C while maintaining the redox potential at a constant value using MnO_2. There was an increase in leach rate with redox potential as expected, but the ratio of ferric to ferrous iron was never higher than 23.5, which is much lower than that observed in bacterial leaching. In Tal's work, leach rates were given as a function of the ferric/ferrous ratio, but it was not obvious how these rates were calculated.

Zheng *et al.* (1986) also found that the rate was dependent on the potential, and also on the total iron concentration. A ferric sulfate lixiviant was circulated through a packed bed of pyrite and the potential of this solution was maintained by addition of potassium permanganate. The rate of oxidation of ferrous iron by the permanganate was related to the rate of pyrite oxidation. The average potential of the inlet and outlet were used in the calculations. They found that the rate of pyrite leaching increased with the potential and total iron concentration, but became constant at high potentials and high total iron concentrations. Again the range of potentials in this work was too low to be relevent to bioleaching (all less than 500 mV (Ag/AgCl)). Zheng *et al.* modelled the reaction using the Hougen-Watson 'dual-site' model (Hougen and Watson, 1947), which assumes that the rate determining step is a chemical one. Competition of ferrous and ferric iron for adsorption on dual active sites on the pyrite surface controls the rate.

Moses *et al.* (1987) used a stirred batch reactor to study the leaching of pyrite with ferric chloride in HCl over a range of pH values from 2 to 9. Pretreatment of the ore was given special emphasis and three different methods were discussed. Incomplete cleaning did have a

noticeable effect on the leach rate, and different sulfate products were dominant depending on the method of pretreatment. By comparing the rates in aerobic and anaerobic systems, it was concluded that ferric iron is the preferred oxidant even when oxygen is present.

Kawakami *et al.* (1988) investigated the oxidation of a pyrite slurry by ferric chloride in HCl. The effect of temperature, pH, pyrite loading, particle size and initial ferrous and ferric concentration were investigated. The oxidation rate increased with an increase in temperature (from 60 - 90 °C) and with pH (from 0 - 2) but the apparent increase with pH may have been associated with complexation. An increased initial ferric iron concentration increased the rate up to a maximum at 1 M (again possibly due to complexation) and the rate was inhibited by an increasing ferrous concentration. A decrease in particle size resulted in an increased rate, but the dependence on pyrite loading was complicated. In this work, the reaction stoichiometry was found to give a ratio of sulfate to elemental sulfur of about 1.3, regardless of experimental conditions. In all the experimental work, there was a very fast initial rate which decayed quickly with time, which they postulated as being due to a high initial reactivity and the rapid disappearance of reactive sites. On this basis a kinetic model was proposed which assumed a fast short term reaction at 'reactive sites' and a slower long term dissolution at 'nonreactive sites'.

More recently work was done by Boogerd *et al.* (1991) to determine the reaction stoichiometry and kinetics in the chemical reaction between pyrite and ferric chloride in a bacterial growth medium. They found that the initial reaction rate was a function of temperature, ferric ion concentration and pyrite concentration, with an apparent saturation with respect to ferric iron and pyrite concentration at each temperature. They derived an empirical equation to describe this initial rate where it was assumed that no ferrous iron was initially present. The initial rates were apparently derived from the experimental measurement of ferrous iron concentration with time, with the initial rate taken as the change in concentration over the first hour of leaching. The fact that the rate is likely to be changing rapidly within the first hour was not taken into consideration, and the consequent rapid production of ferrous iron into the system was not considered in the derivation of the rate equation.

More information on the reaction mechanism between ferric iron and pyrite has been given by Williamson and Rimstidt (1994). These authors used pyrite suspended in nylon mesh, surrounded by an oxidising solution of ferric ions, and varied the sulfate and chloride concentration, the ionic strength and the dissolved oxygen concentration. In some experiments, the solution was purged with nitrogen. It was found that the reaction rate was enhanced by dissolved oxygen at high redox potentials but was faster in the absence of oxygen at low redox potentials. The concentration of dissolved oxygen had no effect, implying that a different reaction mechanism was operative. This is reflected by the reaction orders obtained with and without dissolved oxygen. The rate was not influenced by the sulfate or chloride concentration, or the ionic strength. The results obtained do not support a simple, site-specific adsorption model. On the basis of this and the correlation between rate and redox potential, these authors suggested that there was an electrochemical mechanism involving distinct anodic and cathodic sites with electron transfer being rate limiting. An electrochemical mechanism is also more consistent with the fractional reaction orders obtained, whereas a molecular, chemically controlled mechanism does not adequately account for this.

The redox potentials corresponding to the measured or calculated ferric/ferrous ratio were low in all the literature studied, much lower than the redox potential usually maintained by bacteria in bioleaching systems (~670 mV vs Ag/AgCl (Boon, 1996)). It is necessary to generate ferric leach data at higher redox potentials so that the leach rates of the chemical ferric leach sub-process can be directly compared with those in bioleaching systems. Also a wide range of experimental methods has been used, with different conditions applied (e.g. pH, temperature, presence of counterions), so it is difficult to compare the resulting leach rates and kinetic models directly. Some of the literature data has been reworked, however, in a later chapter.

2.2.3 Electrochemical studies on pyrite

Pyrite is a suitable mineral to use as an electrode. It is relatively chemically inert and it attains its equilibrium potential quickly and reproducibly (Pesic, 1993) but the effects of the mixed potential which is established and the change in surface properties during oxidation must also be considered.

The anodic polarization of pyrite has been investigated by many workers (e.g. Meyer, 1979, Doyle *et al.*, 1989). The fact that pyrite is a semiconductor does not seem to have any significant effect on the polarization behaviour (Biegler and Swift, 1979; Mishra and Osseo-Assare, 1988). There has also been some work on the cathodic reduction of oxygen on pyrite surfaces (Biegler *et al.*, 1976). This becomes important when galvanic coupling occurs between pyrite and another sulfide mineral, since pyrite invariably behaves as the cathode in such situations. Pyrite has a low overvoltage for hydrogen and oxygen evolution (Peters, 1976).

As can be seen in Table 2.1, the rest potential of pyrite lies in the range 297 - 497 mV (Ag/AgCl), which is generally higher than for the other common sulfide minerals. A higher potential is thus required to oxidise pyrite than most other sulfides.

It has been shown by scanning potential and cyclic voltammetry experiments that there are many intermediates in the oxidation of pyrite (Chia *et al.*, 1989, Meyer, 1979). The reaction products for the anodic oxidation are expected to depend on the applied potential, the pH and other factors such as the activities of the ions involved (Doyle *et al.*, 1989).

Doyle *et al.* (1989) found that multiple fast scans indicated the presence of a metal deficient surface layer formed on the first anodic polarization. Nayak *et al.* (1995) reviewed the literature and found that the current-voltage curves had two prominent regions, the first below about 0.9 V (SHE) where a positive potential sweep gave a small peak or plateau current, and the second at higher potentials where the current rose exponentially. In experimental work done by Nayak *et al.* (1995), a positive sweep on a pyrite electrode in 0.1 M sulfuric acid indicated an initial passivating region (from about 0.330 - 0.625 V SCE) (i.e. the current density was lower than expected). On the reverse sweep this phenomenon was not observed. The existence of a thin layer of elemental sulfur was suggested as a reason for the passivation, although this was not actually observed. When the dissolution reaction is coupled with a ferric reduction, the mixed potential is likely to fall within this passivating region.

Nayak *et al.* (1995) also did separate polarization experiments for pyrite in acid and platinum (inert) in ferric sulfate. On the basis of their results, they deduced that the initial dissolution of pyrite in very dilute ferric solutions would be influenced by the pyrite rest potential, and at

higher ferric concentrations by the mixed potential. In this second case, the leach rate would decrease with time, so the initial dissolution would be of a transient character.

There has been some discrepancy as to whether the primary sulfur reaction product of pyrite oxidation is elemental sulfur or sulfate ions, but at higher potentials, there is general consensus that sulfate ions are the dominant sulfur species formed (Koch, 1975; Bailey and Peters, 1976; Meyer, 1979). This would be expected thermodynamically. Sand *et al.* (1995) have claimed that other intermediate sulfur products, like thiosulfates, are formed during bioleaching with *Thiobacillus ferrooxidans or Leptospirillum ferrooxidans.* Thiosulfates disproportionate under acidic conditions, producing elemental sulfur and bisulfate ions (HSO_3^-) (Vogel, 1957, p333), which can undergo further oxidation to sulfate ions. High potentials will favour the formation of sulfate ions.

From constant current and constant potential experiments, Chia *et al.* (1989) deduced that pyrite oxidation was controlled by solid-state diffusion. Fornasiero *et al.* (1992) deduced that the oxidation rate is surface controlled on the basis of electrokinetic measurements.

After oxidation, pits and crevices can be seen on some parts of the pyrite surface while other parts seem unaffected (Meyer, 1979). The extent of surface deformation will depend on the exact conditions of oxidation, and the length of time for which dissolution had occurred.

2.3 Bioleaching

2.3.1 Direct and indirect mechanisms

There are two proposed mechanisms for the bacterial leaching of sulfide ores. The direct mechanism assumes that the bacteria attach to the surface of the mineral particles and facilitate leaching in some direct enzymatic way. This involves physical contact of the microorganism with the mineral (Rossi, 1990, p.99). Evidence against direct leaching has been reviewed (Sand *et al.*, 1995) with some of the evidence against it being that the bacteria contain a considerable amount of iron, even if the mineral substrate is iron deficient, implying that ferric iron plays a crucial role in leaching. No rigorous evidence has been given supporting the direct mechanism (Rossi, 1990, p.100). Biochemical evidence supporting the direct

mechanism is not sufficient to describe satisfactorily the interaction that is required between the bacteria and the mineral surface for destruction of the mineral lattice to take place (Rossi, 1990, p.104). Even in the absence of iron, it is possible for another indirect mechanism to occur (Crundwell, 1996). Acid attack of the mineral is possible, producing dissolved hydrogen sulfide which can be oxidised by the bacteria.

In the indirect mechanism the bacteria oxidise ferrous iron in solution to ferric iron, which in turn leaches the mineral. This two step process can be described by the following two equations: an electrochemical leaching reaction and a bacterial regeneration of ferric ions.

Chemical ferric leach for the case of pyrite:

$$FeS_2 + 8H_2O + 14Fe^{3+} \rightarrow 15Fe^{2+} + 2SO_4^{2-} + 16H^+ \qquad [2.3]$$

Bacterial oxidation of ferrous iron regenerating ferric:

$$4Fe^{2+} + O_2 + 4H^+ \rightarrow 4Fe^{3+} + 2H_2O \qquad [2.4]$$

Keller and Murr (1982) stated that it was not possible to have significant chemical leaching of pyrite by acidic ferric sulfate at 30 °C until ferric ion concentrations of more than 2 $g.\ell^{-1}$ were present, but that leaching was significant under the same conditions when bacteria were present. There was, however, no indication of the ratio of ferric to ferrous iron in this work. It was noted by Crundwell (1996) that this type of experiment could not be used to distinguish between the direct and indirect mechanism, because in the absence of bacteria, the reaction is often limited by a lack in ferric iron. Nicol (1993) presented findings supporting the indirect mechanism for the oxidation of pyrite in acidic sulfate solutions by *Thiobacillus ferrooxidans*. The redox potential during the bacterial oxidation of a pyrite flotation concentrate was monitored with time, then a sterile experiment was run with the redox adjusted to the same values with H_2O_2, and the leach rates were found to be very similar for the bacterial and sterile runs. Boon (1996) found that in batch culture experiments with pyrite and leptospirillum-like bacteria, the specific oxygen utilisation rate was the same at equal redox potentials for bacteria growing on ferrous iron and pyrite so concluded that ferrous iron was the primary substrate for the bacteria and that the pyrite was chemically leached by ferric iron.

Although kinetic models for the direct and indirect mechanism both appear satisfactory in describing the kinetic behaviour of a bioleaching system, it is necessary to distinguish between the two mechanisms because the physical meaning of the kinetic parameters is different. In the indirect mechanism, different strains of bacteria can be characterized independently of mineral oxidation kinetics, allowing for the separate optimisation of each sub-process in the two step mechanism.

2.3.2 Role of bacteria

In the indirect mechanism, it has been postulated that the role of bacteria in the leaching medium is to keep the redox potential high by regenerating ferric ions. (In some sterile leaching work (Tal, 1986; Fowler, 1996) the redox has been maintained by adding an oxidant such as hydrogen peroxide.) In a pyrite bioleaching system, the redox potential is usually maintained at about 670 mV vs Ag/AgCl (Boon, 1996).

In the presence of bacteria, it has been claimed that the oxidation of pyrite can occur at rates of 20 - 1000 times faster than if no bacteria are present (Dutrizac and MacDonald, 1974, Boon and Heijnen, 1993). In using a strain of thermophilic bacteria, Larsson *et al.* (1991) tried to gain evidence in support of a bioleaching mechanism. They used a two compartment cell with a membrane impermeable to the bacteria and to pyrite separating the two compartments, and monitored the leach rate when the bacteria were separated from the ore and when they were in contact. The leach rate was much higher when the mineral and the bacteria were not physically separated, but on close examination it was found that most of the bacteria were not attached to the mineral surface. This finding provided no support for the direct mechanism but showed that it is obviously advantageous to have the bacteria in close proximity to the ore. This would ensure that the redox potential at the surface of the mineral particle would be kept high, so that a high leach rate could be maintained. The authors did not consider the possibility that the rate could have been limited by transport of iron through the membrane separating the bacteria and the ore. Keller and Murr (1982) also observed an increased leach rate in the presence of bacteria but again rarely observed any bacterial attachment. It has been suggested that the presence of bacteria modifies the electrochemical properties of the pyrite, probably due to the presence of substances on the mineral surface. These substances can also disturb bacterial activity and the dissolution of pyrite. This change in mineral properties is

evident, for example, in the lowering of the rest potential during the bacterial lag phase (Mustin *et al.*, 1992).

The activity of the bacteria is influenced by the conditions under which they are grown. Bacterial strains have optimum conditions of temperature, pH etc., and the ferric and ferrous concentrations also affect their activity. Increasing the ferric concentration will decrease the bacterial specific growth rate because of inhibition (Kelly and Jones, 1978). The opposite occurs for an increase in ferrous concentration (Boon and Heijnen, 1993), but there has been evidence of substrate inhibition in the presence of excess ferrous iron (Nemati and Webb, 1996).

2.3.3 Effect of electrochemistry on bacteria

Since it is postulated that bioleaching can be described by two electrochemical half reactions (Equations 2.3 and 2.4), it would be expected that electrochemical techniques could be used to investigate the fundamentals of bioleaching. The effect of applied potentials and currents on the growth and activity of bacteria and on bioleaching rates has been investigated using a number of different experimental apparatus, generally involving either a single or double compartment electrochemical cell.

Different electrochemical measuring techniques have been used to deduce the rate of oxidation of ferrous to ferric iron by the bacteria and the rate of leaching of the sulfide mineral. In many cases the redox potential of a bioleaching system is monitored. An example of such work is that by Pesic *et al.* (1989) where a single electrochemical cell with pyrite and platinum indicator electrodes were used. The potential of the indicator electrodes and the redox potential of the solution was monitored during the oxidation of ferrous ions with oxygen in the presence of *Thiobacillus ferrooxidans*. The reaction rates were determined using the Nernst equation, with the equilibrium potential E° and the value RT/zF obtained by calibration. Aguirre *et al.*(1989) made use of an amperometric technique to study the bacterial oxidising ability. By controlling the potential at very small values to ensure that most of the iron present was in the ferrous form, the current required for the continuous reduction of ferric ions was a direct indication of the bacterial activity. Current can be measured very accurately even at small values, so this method can be more useful than other methods like the monitoring of

ferrous concentration, oxygen concentration or redox potential where big changes in initial substrate concentration are required for accurate measurements.

Boon *et al.* (1995) determined the effect of the solution redox potential on the ferrous oxidation kinetics of *Thiobacillus ferrooxidans* and found that the rate of oxygen utilisation was a function of the ferric to ferrous ratio, the dependence taking the form of Equation 2.5.

$$-q_{O_2} = \frac{q_{O_2}^{max}}{1 + \frac{K_s}{[Fe^{2+}] - [Fe^{2+}]_t} + \frac{K_s}{K_i} \cdot \frac{[Fe^{3+}]}{[Fe^{2+}] - [Fe^{2+}]_t}} \qquad [2.5]$$

In similar experiments where pyrite was added stepwise to a bacterial culture at 30 °C, the experimental data indicated a relationship between the rate of ferrous production and the ferric/ferrous ratio that was of an inverse form to the ferrous oxidation kinetics. There was considerable scatter in the results (Figure 2.1) but it is clear that the rate of bioleaching increases with an increase in the redox potential.

Besides simply monitoring the potential, it is useful to impose and/or control it. This type of work can be used to determine reaction rates as a function of the potential. This is important in trying to measure the kinetics of the bacterial and chemical leach sub-processes in the indirect mechanism of bioleaching.

Two compartment electrochemical cells have been used to constantly regenerate ferrous iron which the bacteria can use as a substrate. Blake *et al.*(1994) cultured bacteria in the cathodic compartment of a cell, and when the bulk of their ferrous substrate had been oxidised, the electrochemical reduction of ferric iron was initiated by delivering a current of 30 A at a voltage of 4 - 7 V. In this way the bacteria would be able to receive an unlimited supply of substrate and, in theory, would be able to grow until some other factor became growth limiting. When sufficient reduction had occurred, the current was stopped to prevent excessive acidification from occurring. There was an enhanced bacterial yield when the bacteria were exposed to an applied current. Similar experiments were conducted by Harvey (1996). In his work the redox potential was controlled, and ferric iron produced bacterially was reduced at the cathode. The current used to maintain the constant redox and the plateau

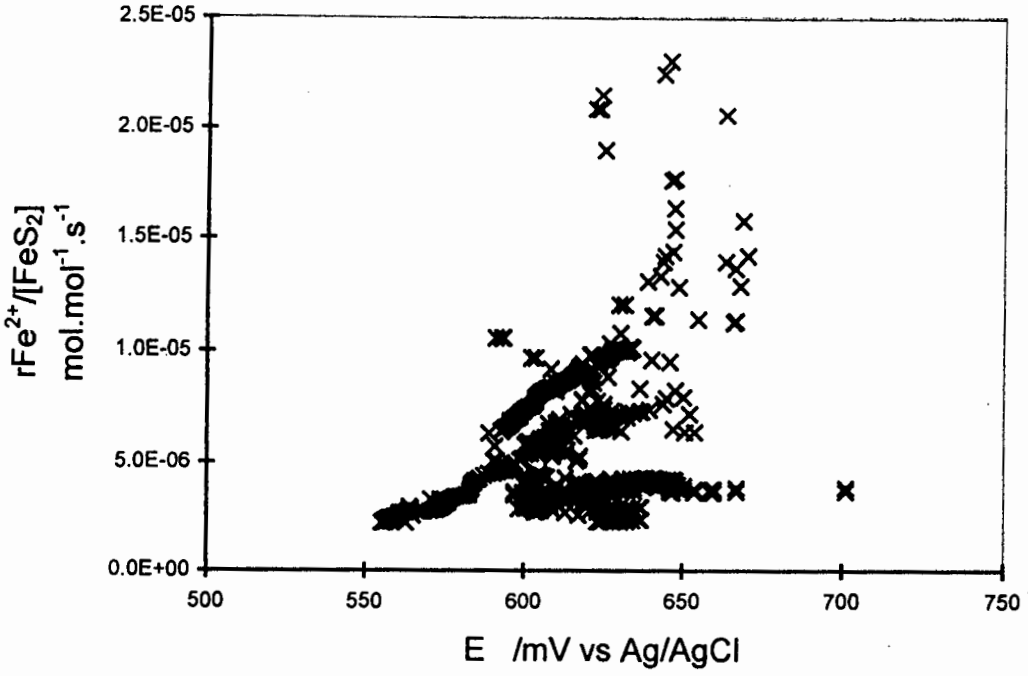

Figure 2.1 Rate of ferrous iron production as a function of redox potential in a pyrite bioleaching system (Hansford, 1995)

current reached after about 8 hours was used to determine the oxidation rate, as it was assumed that this current corresponded to the exponential growth phase of the bacteria. The rate of ferrous oxidation was found to increase with increasing ferrous concentration and decreasing ferric concentration. In an application of this type of work, Natarajan (1992) applied a potential to a culture of *Thiobacillus ferrooxidans* and then used the treated bacteria in bioleaching tests under applied potentials. Bacterial growth was enhanced when the applied potential was such that ferric ions were reduced to ferrous, as a substrate for the bacteria. Bioleaching was also enhanced under application of such negative potentials.

Another interesting application of electrochemical techniques to bioleaching is the study of leaching of mineral electrodes in the presence and absence of bacteria and applied potentials. After such treatment, the surface morphology of pyrite electrodes was examined by Vargas *et al.* (1993) and the pitting observed was only pronounced when both bacteria were present and the anodic polarization potential of the pyrite electrode was high. A similar result was found by Muñoz *et al.*(1995) where a thermophilic microorganism was used in conjunction with an

anodic applied potential to leach chalcopyrite. Pitting was predominant at weak areas of the mineral. Besides the presence of pits which were similar in size and shape to the bacteria, there were also some pits more than ten times larger than the bacteria (Vargas *et al.*,1993), but there was no evidence of bacteria in these pits. It was postulated that this phenomenon was due to an enhancement of the anodic dissolution once a pit had been initiated.

2.4 Ionic Speciation and its Effect on Redox Potential

In bioleaching systems, the concentration of iron is usually of the order of 10 - 30 $g.\ell^{-1}$. At such high concentrations, iron solutions can no longer be considered ideal solutions, as the thermodynamics of ideal solutions strictly only apply to infinitely dilute solutions.

In ideal solutions, the activities of the various electro-active species can be approximated by their concentrations. In non-ideal solutions it becomes necessary to use the activities themselves. This involves either estimating the activity coefficients or calibrating for the system in use.

At high concentrations, and even more so at elevated temperature, ionic speciation must be taken into consideration. Ferrous and ferric iron form many complexes in an aqueous acidic sulfate medium, as is the case in bioleaching. The stability constants of these species vary (Dry and Bryson, 1988), but generally stronger complexes are formed by ferric iron, probably because of its greater charge density. Some of the major species present in bioleaching conditions are $FeSO_4^+$, $FeHSO_4^{2+}$, $FeSO_4$ and $FeHSO_4^+$ (Dry and Bryson, 1988). The formation of complex species has the effect of reducing the activity of free ferric and ferrous ions, which reduces the rate of reaction. This is because complexed ferric sulfate ions have a reduced positive charge relative to Fe^{3+} ions, causing inhibition of electron transfer (Zheng *et al.*, 1986). Also they are large and not readily adsorbed on the pyrite surface.

The Nernst equation relates the measured potential to the ratio of activities of a redox couple. It is only valid for a single redox couple, so it must be assumed that a single reaction (e.g. ferric to ferrous conversion) dominates the redox reaction and that others such as the formation of complexes, have a negligible effect on the overall exchange current density, and

therefore the redox potential (Dry, 1984). When the Nernst equation is used for the ferric/ferrous couple in bioleach systems, the extent of ionic speciation needs to be predicted for both ferric and ferrous species, and it is likely that the proportion of free ferric iron will decrease to a greater extent than free ferrous iron as the total ionic strength and temperature increases. The prediction of uncomplexed ferric and ferrous activities can be difficult, and not necessarily very accurate.

2.5 Summary

Based on a review of the literature, much work has been done on the oxidation of sulfide minerals using chemical, electrochemical and bioleaching techniques. Electrochemical principles can be applied to bioleaching, and can be used to investigate each of the two sub-processes in the indirect mechanism. Although there has been a fair amount of investigation into the ferric leaching of pyrite, there is no leach rate data at potentials as high as those occurring in bioleaching. It is necessary to gain more information regarding the ferric leaching reaction in the bioleaching potential regime to validate the indirect mechanism.

3. MATERIALS AND METHODS

3.1 Ore

The pyrite used in all the tests was from Durban Roodepoort Deeps (DRD) gold mine. The presence of pyrite was confirmed by XRD analysis. Elemental analysis gave 33.3 % Fe and 50.5 % S by weight (for pure iron disulfide 47 % Fe and 53 % S is expected). The particle size distribution (obtained by a Malvern instrument SB.0D) is given in Table 3.1.

Particle size (μm)	% of particles
106	14.3
99 - 144	39.8
92 - 123	59.1.
85 - 132	72.2
79 - 142	81.4

Table 3.1 Particle Size Distribution

The ore was treated in a number of different ways before use, and the pretreatment procedures are detailed in Section 5.2.

3.2 Leaching Solutions

Analytical grade sulfuric acid and de-ionised water were used to prepare a dilute acid solution of pH 1.5. The iron solutions were prepared by dissolving laboratory grade ferric sulfate and AR grade ferrous sulfate in this acid. The exact concentrations of ferrous and ferric iron were determined routinely by titration (Appendix 1), and atomic absorption spectrophotometry was periodically used to confirm the titration results.

In some cases the solution potential of the ferric sulfate was raised by electrolysis. This was done in a two compartment cell (Appendix 2) with the two compartments separated by an ion exchange membrane, or simply by using a glass cylinder as the cathodic compartment and a beaker as the anodic compartment, with the two separated by a fritted glass disc. Both the

anode and the cathode were made of graphite. The catholyte was dilute sulfuric acid and the anolyte was the required concentration of ferric sulfate solution in acid, prepared as above. Using a power supply, a current was applied between the electrodes causing the production of ferric iron at the anode, and hydrogen at the cathode. During the time span of the electrolysis there was no significant diffusion of ferric iron through the fritted disc.

3.3 Solution Redox Potential

If it is assumed that the ferric/ferrous exchange current density at the surface of a leaching particle is large enough to make the effect of the corrosion current due to leaching of the particle negligible, the surface potential of the particle can be considered equal to the redox potential of the solution at the surface (Dry, 1984). A measurement of the solution redox potential can thus be used to approximate the mineral surface potential.

A platinum wire-Ag/AgCl combination redox probe (Crison) was used to monitor the solution redox potential. The electrode was filled with 3M LiCl solution, rather than the more commonly used KCl solution. This was done because when the electrode is used in a ferric/ferrous system over extended time periods, ferric ions in particular can penetrate the frit and lead to the formation of precipitates such as jarosites inside the probe. When the probe did appear to be contaminated, the filling solution was removed and the probe soaked in HCl, then rinsed with distilled water and LiCl before being refilled.

The measured solution potential can be related to the ratio of free ferric to free ferrous iron in an iron solution via the Nernst equation (Equation 1.3). The Nernst equation, however, relates the potential to the free ferrous and ferric activities, and the literature parameters E° and RT/zF are ideal values, so the probe must be calibrated for the system in use. Since the redox potential is temperature dependent, as is the equilibrium between ferric and ferrous iron, the calibrations were carried out at constant temperature (of 25 °C, 40 °C and 60 °C) in a jacketed vessel (Figure 3.1). The temperature was controlled by an external water bath. Also, since the proportion of free ferric and ferrous species is dependent on the total iron concentration as well as the temperature and counter-ions present, calibrations were performed at different total iron concentrations. Ferric and ferrous sulfate solutions of similar

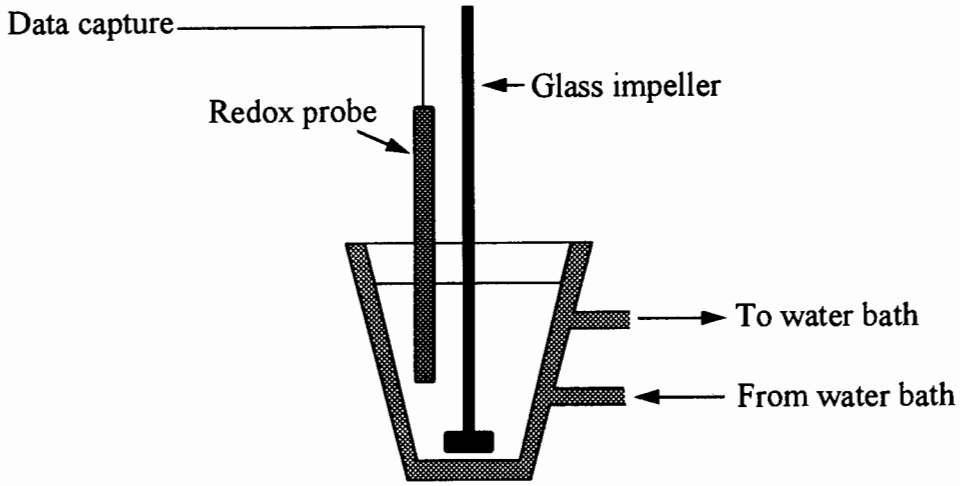

Figure 3.1 Vessel for probe calibration and leaching

concentrations were made up. An aliquot of ferric sulfate of a suitable potential was pipetted into the jacketed vessel, the redox probe inserted and the system allowed to reach thermal equilibrium. Aliquots of the ferrous sulfate solution were added by pipette, the solution was well agitated by an overhead glass impeller and the measured redox potential was recorded once the system had stabilized. The measured redox potential was plotted against the natural logarithm of the ferric to ferrous ratio, and the slope and intercept obtained by regression gave the Nernst parameters RT/zF and E° respectively. All the potential values are quoted with respect to the Ag/AgCl reference electrode.

Because the Nernst equation can strictly only be used for equilibrium situations, the response time of the probe was determined to see if it would be suitable to use in a dynamic system. The probe was moved from a solution of one potential to that of another potential and the time taken for the probe output to reach a steady value was measured.

The redox potential was logged by a PC based data capture system at one second intervals. The measurement system is shown in Figure 3.2. A high input impedance optically isolated amplifier was used to couple the electrode to the ADC on a single board microcomputer (Randall *et al.*, 1993). The digitised value was transferred to the PC by serial communications on request and logged to a data file for subsequent processing.

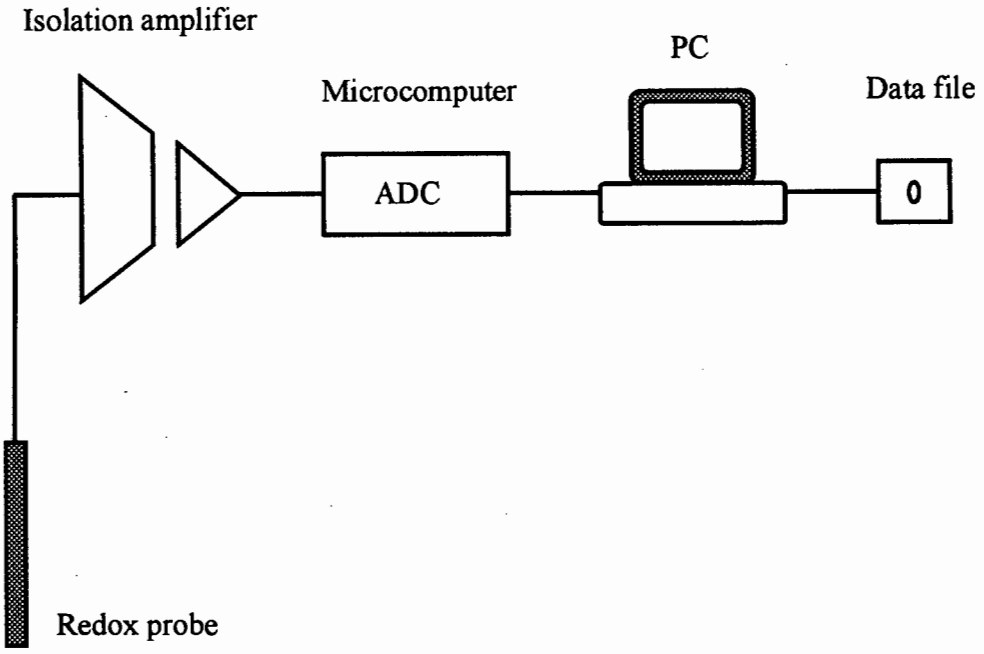

Figure 3.2 Redox potential measuring system

3.4 Experimental Procedure

The dynamic leach experiments were carried out in the same 100 mℓ jacketed glass vessel used for probe calibration (Figure 3.1). The temperature was controlled at 25 °C using an external water bath, and the solution was agitated using a glass impeller driven by an overhead electric motor. 50 mℓ ferric sulfate solution were pipetted into the vessel and the probe inserted. The system was constantly stirred and once thermal equilibrium was reached, a known amount of ore (usually about 0.4 g) was added to the system and the redox potential monitored for the duration of the leach. The leaching experiments were generally carried out over a period of about 20 - 30 minutes.

The leach rate was determined from an assumed reaction stoichiometry between ferric iron and pyrite, the total iron concentration and the measured redox potential. It was assumed that no precipitation of reaction products occurred, and that the particle size of the pyrite did not change over the course of the reaction, which is a reasonable assumption over short times.

3.5 Rate Determination

There is evidence in the literature that the sulfur moiety in pyrite can form a number of products with valency ranging from 0 to +6 (i.e. S^o to SO_4^{2-}) (Sand *et al.*, 1994). There is also evidence that the various oxidation states of sulfur can co-exist in the same system. To accommodate this in an overall equation, where parallel reactions occur in different proportions, the variable n is introduced.

A general form of the reaction between pyrite and ferric iron can be denoted as follows

$$\mathbf{FeS_2 + (3n+2)Fe^{3+} + 2nH_2O \rightarrow (3n+3)Fe^{2+} + 2SO_n^{-n/2} + 4nH^+} \qquad [\,3.1\,]$$

for n = 0 to 4.

With n = 0, only elemental sulfur is formed.

$$\mathbf{FeS_2 + 2Fe^{3+} \rightarrow 3Fe^{2+} + 2S} \qquad [\,3.2\,]$$

With n = 4, only sulfate ions are formed.

$$\mathbf{FeS_2 + 14Fe^{3+} + 8H_2O \rightarrow 15Fe^{2+} + 2SO_4^{2-} + 16H^+} \qquad [\,3.3\,]$$

We define r_{FeS_2} as follows:

$$\mathbf{r_{FeS_2} = \frac{d[FeS_2]}{dt} = -\frac{d[Fe^{3+} + Fe^{2+}]}{dt}} \qquad [\,3.4\,]$$

where

$$\mathbf{\frac{d[Fe^{2+}]}{dt} = -(3n+3)r_{FeS_2} = r_{Fe^{2+}}} \qquad [\,3.5\,]$$

and $$\frac{d[Fe^{3+}]}{dt} = (3n+2)r_{FeS_2} = r_{Fe^{3+}} \qquad [3.6]$$

The Nernst equation

$$E = E_o + \frac{RT}{zF}\ln\frac{[Fe^{3+}]}{[Fe^{2+}]} \qquad [3.7]$$

gives

$$\frac{dE}{dt} = \frac{RT}{zF}\cdot\frac{d}{dt}\ln\frac{[Fe^{3+}]}{[Fe^{2+}]} = \frac{RT}{zF}\left(\frac{1}{[Fe^{3+}]}\cdot\frac{d[Fe^{3+}]}{dt} - \frac{1}{[Fe^{2+}]}\cdot\frac{d[Fe^{2+}]}{dt}\right) \qquad [3.8]$$

Substituting [3.5] and [3.6] in [3.8] :

$$\frac{dE}{dt} = \frac{RT}{zF}\cdot r_{FeS_2}\cdot\left(\frac{(3n+2)}{[Fe^{3+}]} + \frac{(3n+3)}{[Fe^{2+}]}\right) \qquad [3.9]$$

or rearranging $$r_{FeS_2} = \frac{\frac{zF}{RT}\cdot\frac{dE}{dt}}{\frac{(3n+2)}{[Fe^{3+}]} + \frac{(3n+3)}{[Fe^{2+}]}} \quad (\text{in mol.}\ell^{-1}.s^{-1}) \qquad [3.10]$$

where $$[Fe^{2+}] = \frac{[Fe^{total}]}{1 + \frac{[Fe^{3+}]}{[Fe^{2+}]}} \qquad [3.11]$$

and $$[Fe^{3+}] = \frac{[Fe^{total}]\cdot\frac{[Fe^{3+}]}{Fe^{2+}]}}{1 + \frac{[Fe^{3+}]}{Fe^{2+}]}} \qquad [3.12]$$

The rate of pyrite dissolution can thus be calculated if the rate of change of potential with time is known from the measurement of potential as a function of time, provided suitable calibration constants in the Nernst equation can be found and if the stoichiometry (i.e. n) is known and remains constant throughout the reaction. In this work it was assumed that all the solubilized sulfur was present as sulfate ions, i.e. n = 4. The rate expression [3.10] is thus reduced to

$$r_{FeS_2} = \frac{\frac{zF}{RT} \cdot \frac{dE}{dt}}{\frac{14}{[Fe^{3+}]} + \frac{15}{[Fe^{2+}]}} \qquad [3.13]$$

zF/RT was determined from the probe calibration and the ferric and ferrous concentrations were determined from the measured potential and the total iron concentration. An iterative method was used to determine the time-dependent total iron concentration and is detailed in Appendix 3.

In an experimental situation there is considerable scatter in the measured values of potential, so that dE/dt is prone to oscillations which are not characteristic of the system itself. It was thus necessary to 'smooth' the curves of E versus t which were obtained. A satisfactory curve fit of the raw E versus t data could not be found, so the data were converted to the form (E(0)/E(t)-1) where E(0) was the initial potential and E(t) was the potential at time t. This function was fitted by a function of the form $y = A (\ln(t))^B$, by varying the parameters A and B. In some cases where the experimental variables were changed a great deal, a better fit was obtained by the function $y = A (\ln(t))^B + C$. The objective function for the curve fitting procedure was satisfactorily small, typically in the range 0.0001 to 0.001 for about 1200 data points. An example of the curve fitting procedure is given in Appendix 4.

The fitted values of A and B (and C) were used to calculate the values for E and dE/dt. These were substituted into Equation 3.13 to calculate the rate of dissolution of pyrite in moles of pyrite per litre of slurry per second. The rate was normalised by dividing by the initial molar concentration of pyrite used in each experiment, assuming a molecular weight of 120 $g.mol^{-1}$. The rates were plotted against the calculated redox potential E.

4. PROBE BEHAVIOUR

4.1 Calibration

The redox probe was calibrated at different iron concentrations and at 25 °C, 40 °C and 60 °C. The calibration curves of measured potential E versus $\ln([Fe^{3+}]/[Fe^{2+}])$ were linear at 25 °C. Linear regression was used to determine the Nernst parameters, E^o and RT/zF. Typical values are shown in Table 4.1. The parameters differ considerably from the ideal values for standard conditions and change with the total iron concentration. This deviation from ideality is to be expected because the activities of the free ferric and ferrous iron are affected by the total ionic strength. The amount of speciation, particularly of ferric iron, increases with an increase in total iron concentration, particularly in a sulfate medium. Complexation with various sulfur species will also decrease the amount of free ions present, and hence affect the measured potential.

Total [Fe] mol.ℓ^{-1}	RT/zF mV	E^o mV vs Ag/AgCl	correlation coefficient, R^2
0.41	25.89	443.4	0.999
0.29	24.96	446.9	0.999
0.18	24.33	449.4	0.999
0.12	23.61	454.2	0.997
0.06	23.10	458.7	0.998
standard values	25.7	573	

Table 4.1 Measured Nernst parameters at 25 °C

At 40 ° C the calibration curve deviated significantly from linearity while at 60 °C it appeared parabolic. An increase in temperature is expected to have a large effect on the activity of the ions present. This would be more noticeable at high redox potentials where the ferric form is dominant. Therefore the concentration of ferrous and ferric ions as determined analytically (at 25 °C) would not equal the actual concentrations of these species at elevated temperatures.

To be able to use the solution redox potential to determine the concentration of ferric and ferrous species above 25 °C one needs to be able to accurately determine or predict the activities of these ions at the required temperatures. For this reason, all further work was carried out at 25 °C where the redox potential could be reliably interpreted. Future work would need to include temperatures over the range of about 10 - 50 °C, to cover the range in conditions found industrially. There is software available to predict ionic equilibria (e.g. JESS, MINTEQ, ASPEN) and although their application can be limited, these programs could be of use in such work.

4.2 Response Time

The Nernst equation can strictly only be applied to solutions in equilibrium. In the leach system, the solution potential changes continuously so it was necessary to have some indication of the probe response time. The response time was defined as the time taken for the probe to reach 99% of its final steady state value. The results are given in Table 4.2. For a falling redox potential (as occurs during leaching), the probe responds very quickly, with larger changes in potential requiring a longer stabilisation period, as expected. In general, the probe responds sufficiently quickly to allow the Nernst equation to be used in this pseudo-equilibrium situation where the potential is decreasing in a continuous manner. Rimstidt and Newcomb (1992) also used a combination Pt-Ag/AgCl redox probe and found the response time to be between ten and twenty seconds.

Initial Potential mV vs Ag/AgCl	Final Potential mV vs Ag/AgCl	Time seconds
671	608	1
671	608	2
671	590	2
608	590	2
696	670	1
689	607	2
687	590	2
751	650	3
802	682	4
953	672	6
682	734	5
590	671	7
608	671	6
668	677	5
607	687	11

Table 4.2 Probe response time

5. DYNAMIC LEACH TESTS

5.1 Initial Transient Behaviour

Typical behaviour of the solution redox potential with time is shown in Figure 5.1. The initial drop in the potential was very fast, and slowed down with time. When the rate of change of redox potential was converted to a rate of dissolution using Equation 3.13, the initial large change was apparent as a very high initial rate reached within the first 10-30 seconds, then the rate decreased as the potential decreased (Figure 5.2). After the initial anomalously high rates, the rate of leaching or the corrosion current continued to decrease as the solution redox potential decreased, but at a much slower rate, suggesting that the rate of reaction between pyrite and ferric iron is a function of the solution potential.

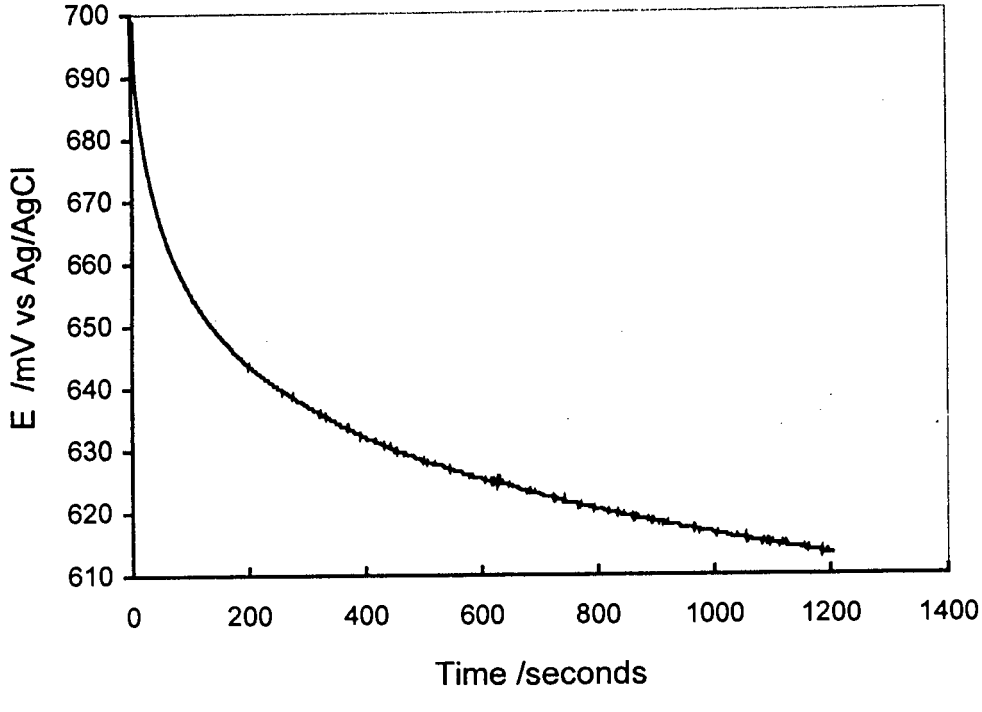

Figure 5.1 Redox potential versus time

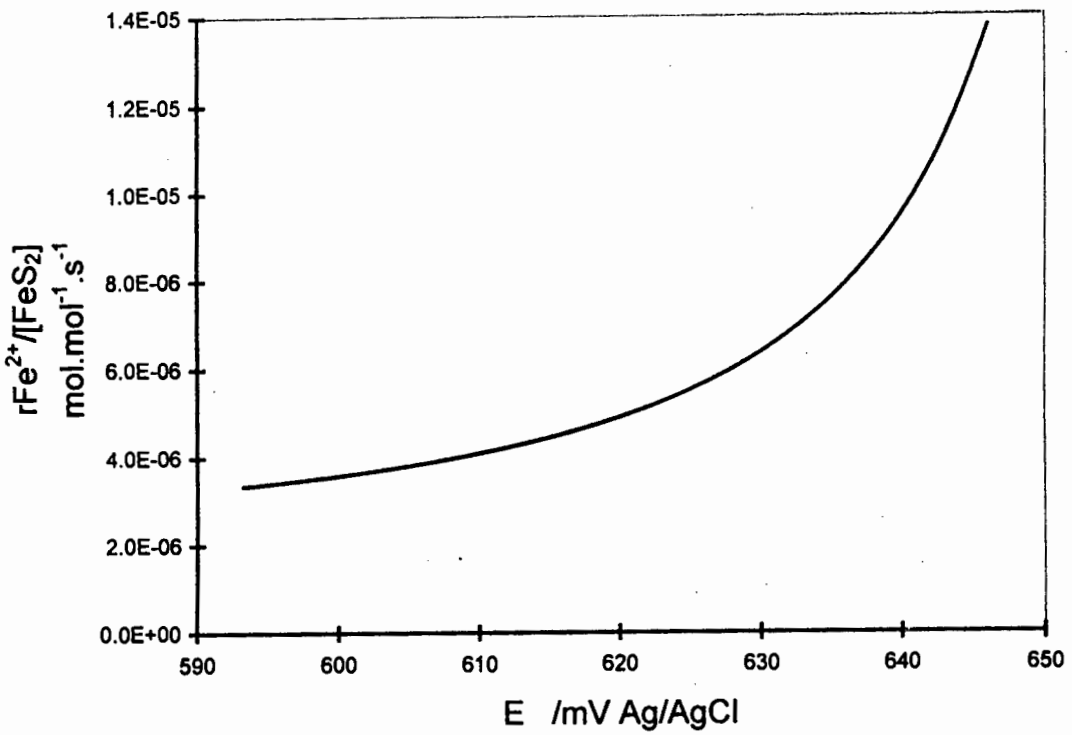

Figure 5.2 Rate versus redox potential

The initial change in potential, and therefore the calculated initial reaction rate, seemed to be anomalously high. A series of leaches was carried out, using initial ferric sulfate solutions of different initial redox potential, with all other parameters constant. The graphs of Figures 5.3 and 5.4 indicate that there is a transient effect, regardless of the starting potential, but that there is an underlying tendency for the rate to increase as the redox potential increases. In order to generate leach data for redox potentials in a particular range, it is necessary to start leaching at a higher potential so that the initial transient can be ignored. Doyle *et al.* (1989) allowed a 12 hour equilibration period for pyrite electrodes in an electrolyte before any electrochemical experiments, because some of the pyrite samples did not have stable potentials initially.

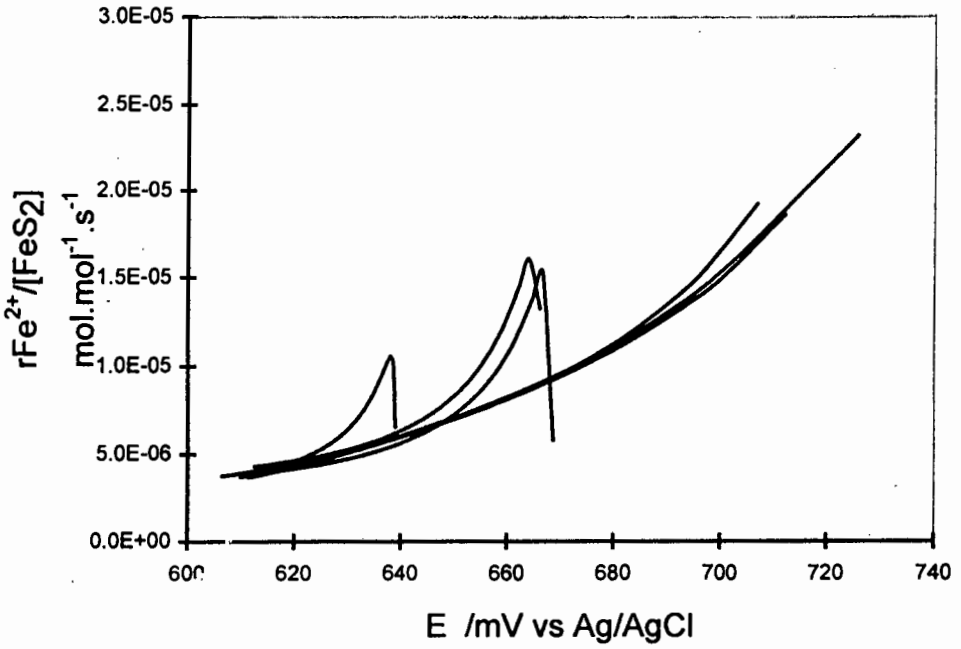

Figure 5.3 Leaching from different initial potentials

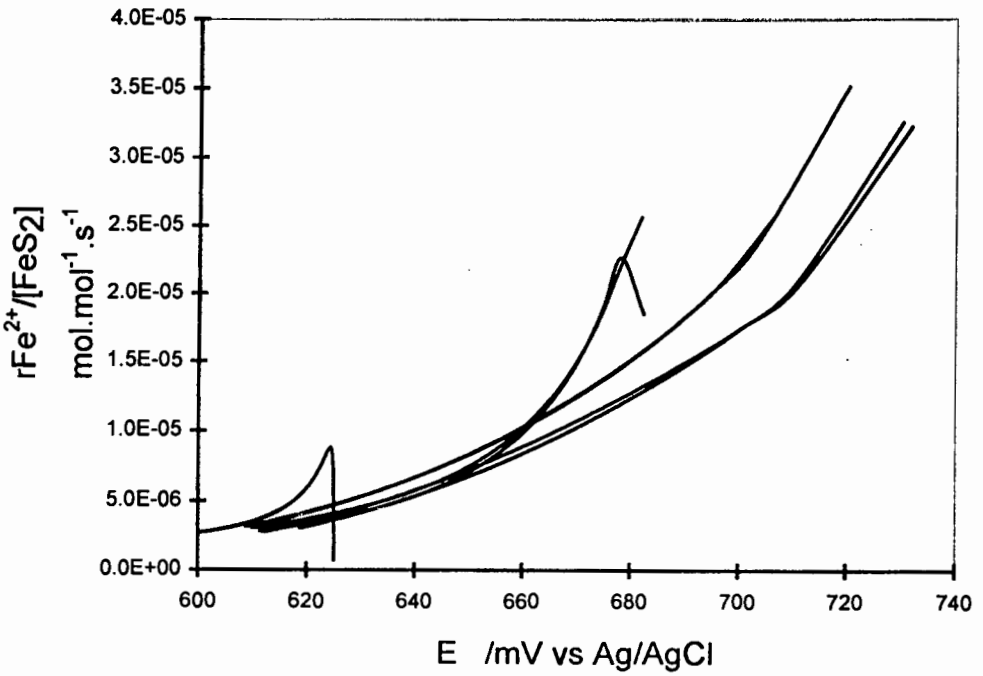

Figures 5.4 Leaching from different initial potentials

The causes of this transient and finding ways to eliminate it were investigated. To test whether the initial high rate was the effect of fresh contact between the ore and the solution, consecutive leaches were carried out. In these tests, the ore was leached for 20 to 30 minutes, then the solution was decanted and fresh ferric sulfate solution was added, without washing the ore. The results are shown in Figures 5.5 - 5.7. The very first leach in each set did behave slightly differently, with a slightly higher initial rate, yet subsequent leaches were very similar. This indicates that, perhaps with the exception of the first leach, the dissolution of fine surface particles or reactive surface layers does not contribute a great deal to the transient rate. It is more likely, however, that the first leach shows a slightly different behaviour because of the initial difference in the potential of the leaching solution and the pyrite particles. This will be discussed in more detail later.

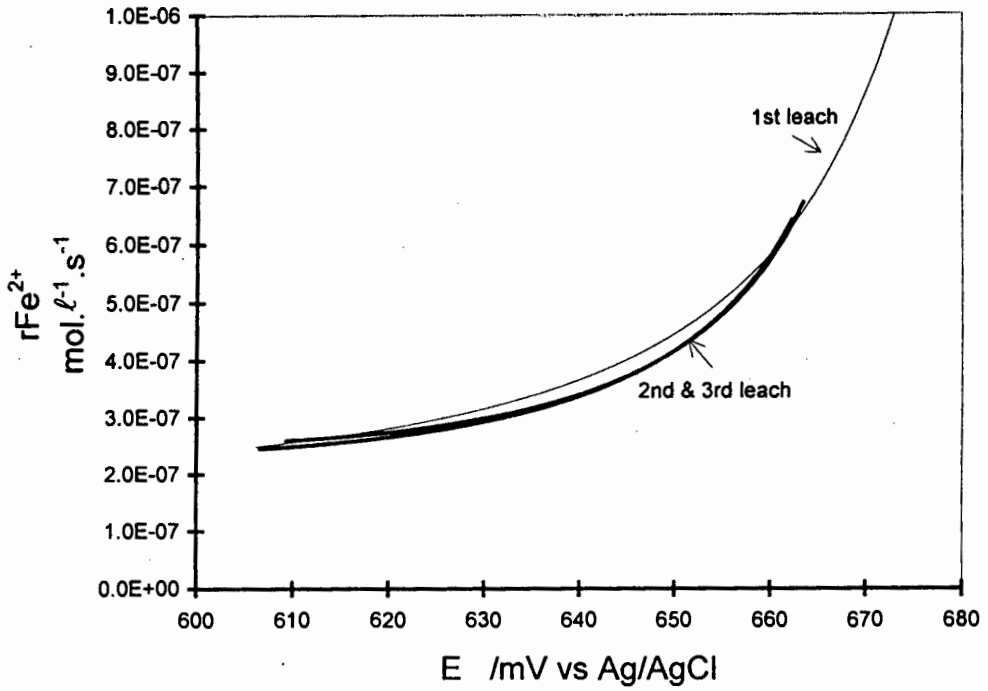

Figure 5.5 Rate versus potential for three consecutive leaches

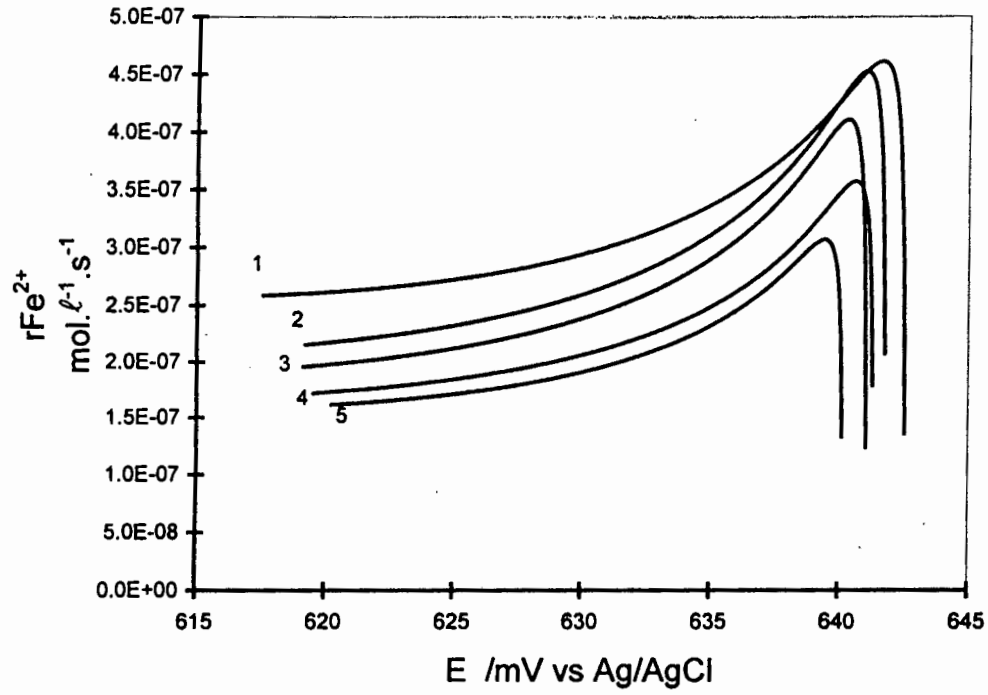

Figure 5.6 Rate versus potential for five consecutive leaches

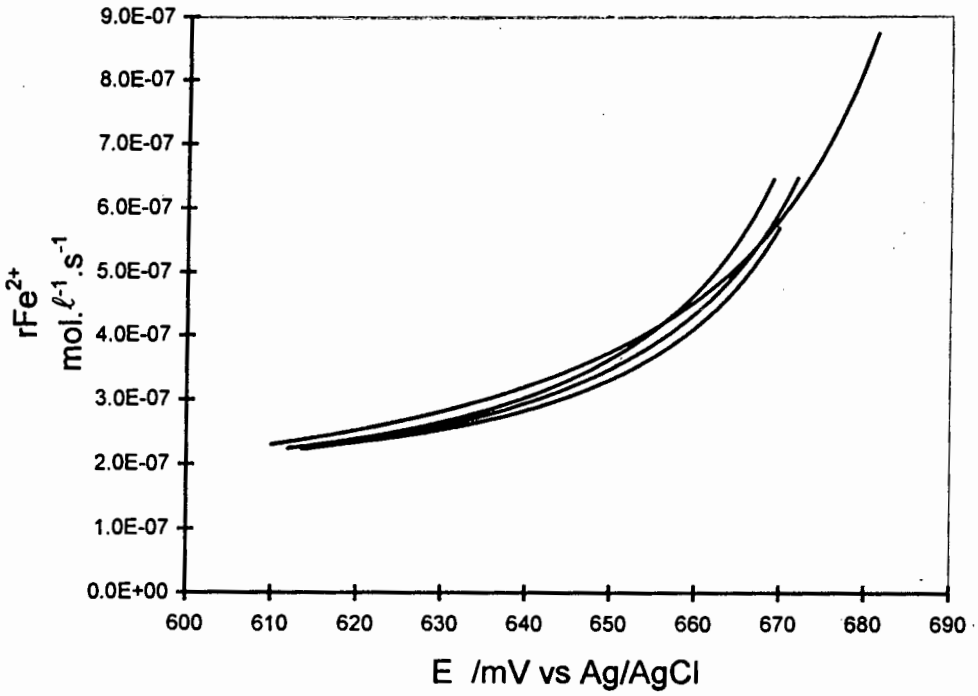

Figure 5.7 Rate versus potential for four consecutive leaches

The degree of reproducibility of the transient is shown on Figure 5.8. The graphs of potential versus time for leach tests started at different starting potentials are not perfectly superimposed. The potential drops a little too quickly, then the curves coincide. This indicates that the transient is dependent on the initial redox potential of the solution, although the curves coincide after very short times, times shorter than the transient period.

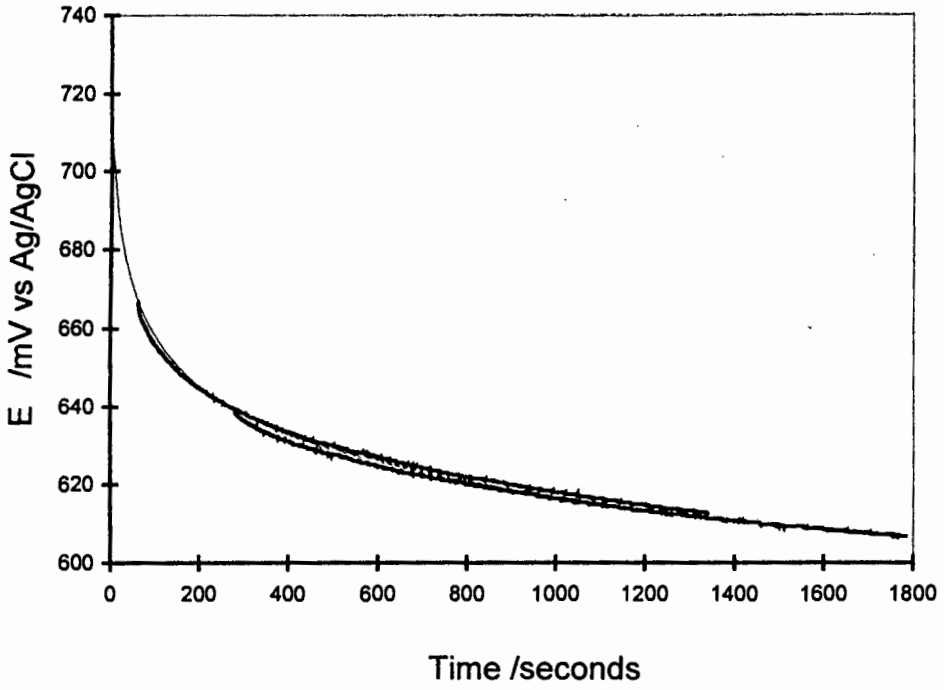

Figure 5.8 Reproducibility of transients

A charging effect might also be used to partially explain the transient rate (Bockris and Reddy, 1970). When the ore is added to a ferric/ferrous solution, non-Faradaic charging occurs at the ore-solution interface, forming a double layer of charge. There is a potential difference across this double layer, causing the flow of current both from the mineral to the ferric/ferrous couple and from the ferric/ferrous couple to the mineral. The net current flow is from the mineral to the ferric/ferrous couple, since the solution potential is initially greater than the mineral surface potential. This results in the mineral becoming increasingly positively charged, and the solution increasing its negative charge, and this has the effect of further reducing current flow because of the reduced potential across the double layer. Eventually the net current should

reach zero when the potential on either side of the barrier is equal, but the mineral is not ideally polarizable but also disintegrating and charged particles are leaving the lattice across the double layer. This results in a net corrosion current, the magnitude of which depends on the rate at which the charged species can leave the mineral. The charging currents could account for the initial rapid drop in solution redox potential, with a greater initial rate expected for a large difference in potential between the mineral and the ferric/ferrous solution. The fact that pyrite is a semiconductor and that a large mineral surface area is exposed would make the length of this initial transient period significant.

It is also likely that fine particles and rough areas on the pyrite surface will dissolve at elevated rates compared to massive pyrite. Other workers who have found high initial rates have attributed them to these surface effects. Wiersma and Rimstidt (1984) noticed a sharp drop in redox potential when ore was added to ferric chloride. Adding more ferric chloride to a half completed run did not produce the same initial sharp decrease as in the beginning, but the potential increased then continued to decrease with the same slope as it had before the addition. Pretreatment of the ore was not detailed in this work, so it is quite likely that the oxidation of surface species caused high initial rates. Linge and Jones (1993) observed large initial rates in the leaching of arsenopyrite and attributed these high rates in the first half hour to an initial oxidation of surface oxides. There was also an ongoing, slower dissolution with an irreproducible rate. In the experimental work of this thesis, the ore was pretreated (Section 5.2) to reduce the possibility of surface fines and oxide layers, but it is still possible that some more reactive sites on the pyrite surface were selectively leached initially (possibly accounting for the small difference in potential versus time curves for the first leach in a cycle of leaches).

Another possible reason for observing an initial transient is the formation of a sulfur rich layer on the pyrite surface. This has been discussed by Chander and Briceño (1987), Sato (1992) and Ralph (1997). A step-wise mechanism is proposed whereby ferrous iron is preferentially released from the ore faster than the sulfur moiety can be oxidised. The sulfide attempts to reach equilibrium with the solution by adjusting the metal/sulfur ratio, thus altering the metal/sulfur activity ratio in the surface layer (Sato, 1992). This results in the formation of a sulfur rich layer on the ore, which is consistent with the observation by Doyle *et al.* (1989) that a metal deficient surface layer was formed on the initial anodic polarization of pyrite. The

ferrous iron which is released to the solution is responsible for the rapid drop in potential. When the stable limit of non-stoichiometry of the sulfide is reached, it can no longer adjust its composition so dissolution of the mineral continues according to the expected stoichiometry. This hypothesis can also be used to explain why the initial sharp drop in rate is reduced when the ore is pretreated by washing and drying. During the washing procedure, the sulfur rich layer forms and persists during drying and for a short period of storage. If it is then added to a ferric/ferrous solution, the initial drop in potential is reduced. If the treated ore is stored in the presence of oxygen for extended periods, the sulfur rich layer becomes depleted by oxidation, so the initial surge is again observed. Williamson and Rimstidt (1994) also hypothesised that the differences in reaction rates when the ore was washed were due to a change in the electrochemical behaviour of the solid, rather than a change in the solution properties, but did not have enough data to give conclusive evidence supporting this.

Nayak *et al.* (1995) claimed that the initial dissolution of pyrite in ferric sulfate is expected to be a transient phenomenon, characterised by a decay in reaction rate with time. This was deduced from polarization studies on pyrite: the mixed potential during the reaction between pyrite and ferric iron generally falls in the transient passivation region for pyrite oxidation. Meyer (1979) also found a similar transient curve on the initial polarization of pyrite from the rest potential. These results provide support for an electrochemical explanation for the transient. If this is indeed the case, then different masses of ore and different exposed surface areas should influence the duration of the transient.

Further investigation of the transient could involve leaching ore, then removing the ore at a certain point and adding it to a leaching solution at the same potential as that from which it had just been removed. One would expect there to be no significant charging current in this case. Also conventional electrochemical experiments such as cyclic voltammetry could be used to investigate the irreversibility of the reaction between pyrite and the ferric/ferrous couple.

Although the transient has not been thoroughly investigated or conclusively explained, further investigation is beyond the scope of this work. The initial high rates are likely to be artefacts of the double layer charging, so the initial transient behaviour should not be used to interpret

the leach kinetics of pyrite. All the initial data has been shown and has been used in the calculation of the rate of leaching, but has not been used in any kinetic interpretations of the reaction.

5.2 Pretreatment Procedures

The pyrite used in the leaching experiments was treated in a number of different ways after it was found that when untreated ore was added to a ferric sulfate solution a very rapid drop in the solution potential resulted. Various washing procedures were used, to remove fines from the ore surface, and to remove highly reactive sites on the surface, such as rough, jagged edges. The ore was washed with distilled water, ferric sulfate or sulfuric acid, and dried in air, with or without using acetone to dehydrate the surface. A suspension of the ore in ethanol was treated by ultrasound. The graph in Figure 5.9 shows the potential versus time data for untreated pyrite and pyrite washed with distilled water and dried with acetone. Within the variability of the experiments, there was no significant difference between the different pretreatment procedures, but all lessened the initial sharp drop observed when untreated ore was used. For convenience it was decided to simply wash the ore in distilled water, then rinse it in acetone and allow it to dry in air for further testwork.

Williamson and Rimstidt (1994) also noted a change in reaction rate when they rinsed their pyrite with a few millilitres of distilled water between experiments. The rate constant dropped from one experiment to the next. The large reduction in the rate constant could not be explained by the negligible change in surface area of the pyrite. On the basis of these and other experiments, Williamson and Rimstidt postulated that the change in rate constant with time which they observed was because of a change in the electrochemical behaviour of the pyrite, rather than that of the solution.

Other harsher methods could be investigated, such as soaking the ore in warm HF (McKibben and Barnes, 1986) and it could be useful to examine the ore before and after treatment by SEM, but such studies have been done and have shown that without pretreatment the pyrite surface is coated with fine particles and that surfaces are rough, hence susceptible to rapid leaching. Some SEM work done on the pyrite before and after leaching in this work showed

similar characteristics on the ore surface (Section 5.8) though with the short term leaching experiments there was no noticeable deformation of the surface after leaching.

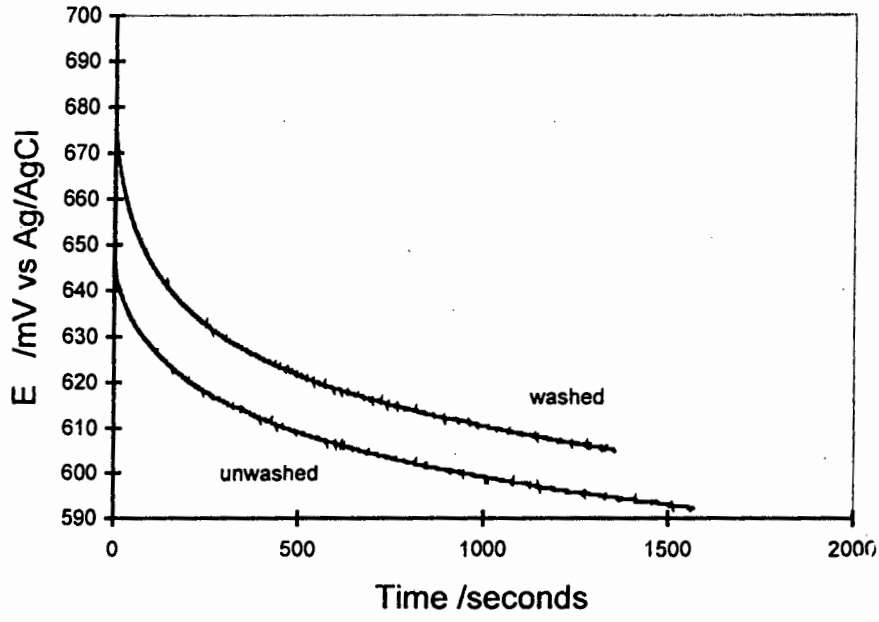

Figure 5.9 Redox potential versus time for washed and unwashed ore

5.3 Mass Transfer

At low stirring rates, the reaction between ferric iron and pyrite was under mass transfer control. As the stirring rate was increased, there was no significant effect on the rate (Figure 5.10). A stirring speed which was beyond the mass transfer control regime was chosen and used for all the experiments.

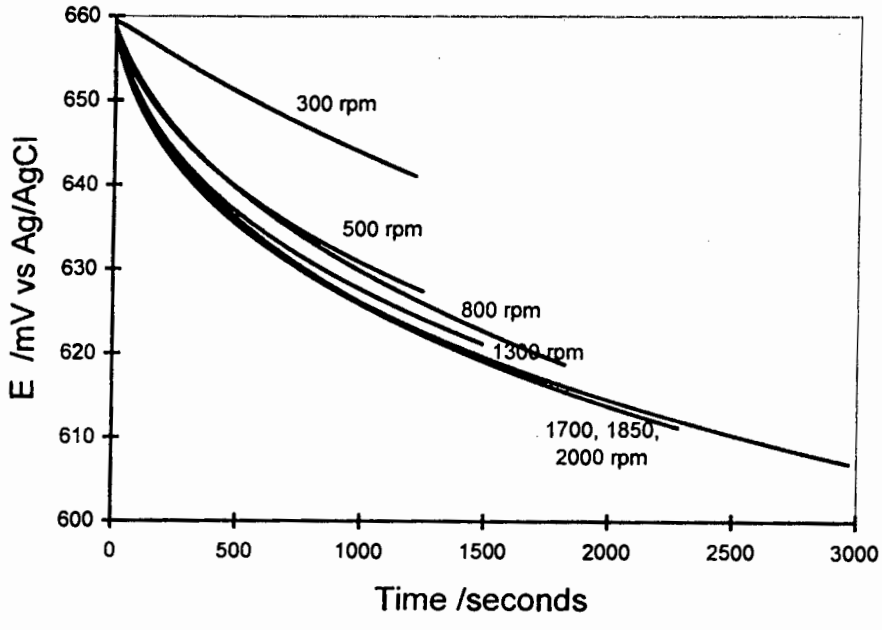

Figure 5.10 Effect of stirring rate on the measured potential

5.4 Reproducibility of Data

A single experiment was replicated to determine the spread in results. Variability in this work was expected, because crushed pyrite is not homogeneous, in terms of its elemental composition, surface structure and semiconductor properties. Figure 5.11 shows the variability of the reaction rates obtained for a set of experiments where 0.413 $\pm$ 0.004 g pyrite where leached in 50 ml 0.38 M ferric sulfate. The variability in reaction rate normalised to the pyrite concentration (assuming a molecular mass of 120 $g.mol^{-1}$) is of the order of 7 %. This variability represents the uncertainty in the experimental work, since it is much larger than any errors associated with the calibration procedure.

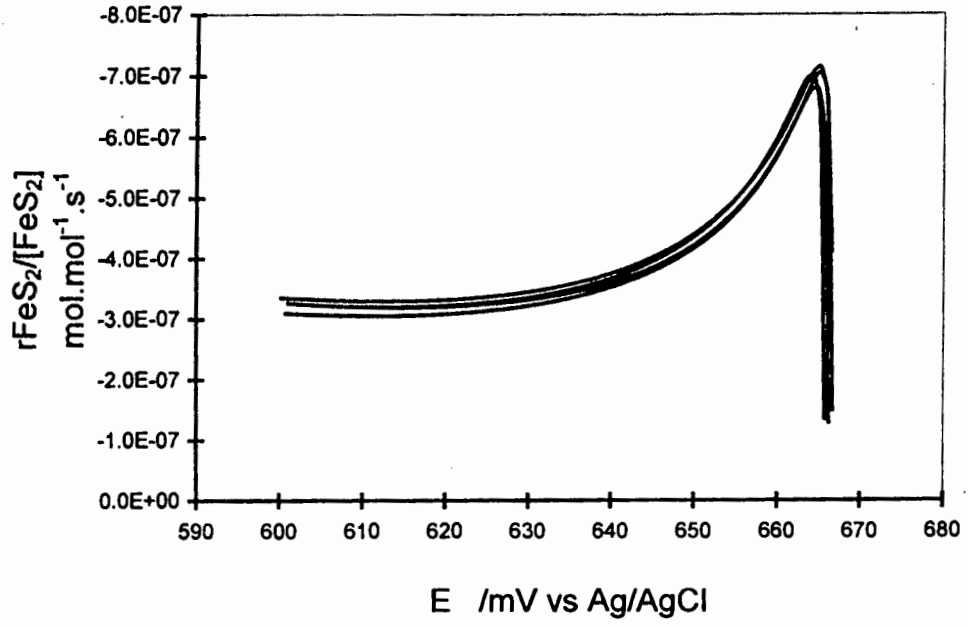

Figure 5.11 Reproducibility of experiments

5.5 Total Iron Concentration

Leaching tests using ferric sulfate solutions of different total iron concentrations but with the same starting redox potential were carried out. The effect of the total iron concentration is shown in Figures 5.12-5.13. The rate does not appear to depend on the total iron content. Garrels and Thompson (1960) also found the rate to be independent of the total iron concentration, and in the work of Zheng *et al.* (1992) it also appears that at iron concentrations higher than about 0.05 M the rate becomes independent of the iron concentration. If there is sufficient ferric iron in the system so as not to be rate limiting, the same rate will cause a larger drop in redox potential when the total iron concentration is less,

because an increase in the amount of ferrous iron will have a greater effect on the ratio of ferric to ferrous iron. The fact that the rate is independent on the total iron content indicates that the reaction is not under chemical or diffusional control, but that it is likely to be under electrochemical control, with charge transfer at the mineral surface being rate limiting.

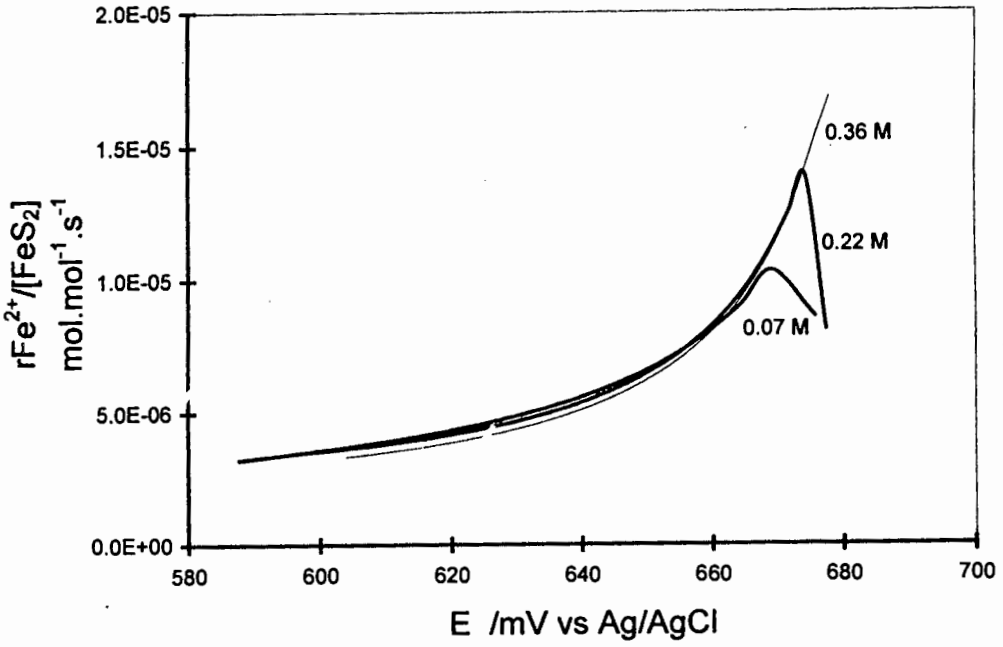

Figure 5.12 Effect of total iron concentration on leach rate

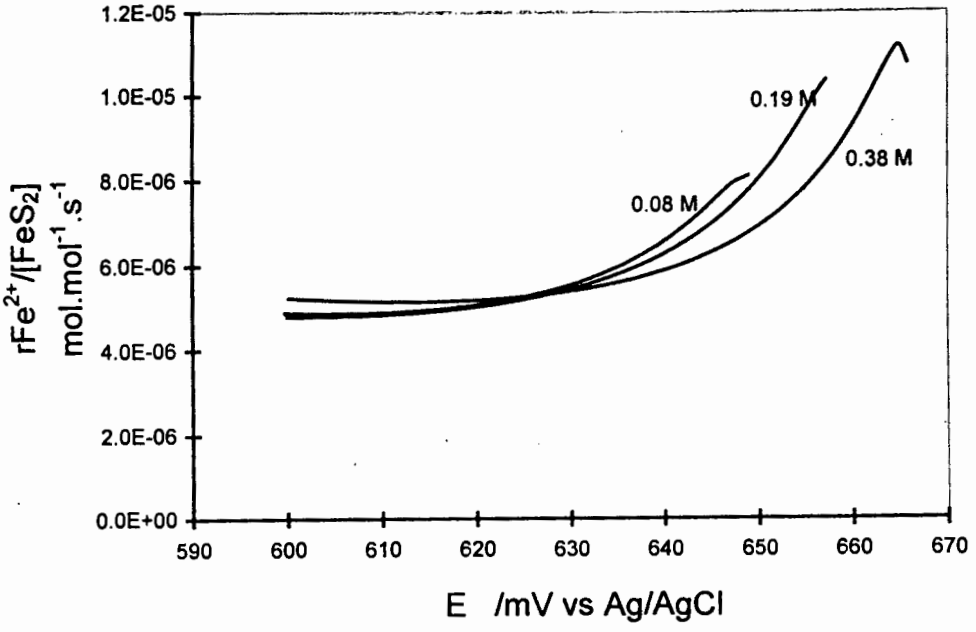

Figure 5.13 Effect of total iron concentration on leach rate

5.6 Ore Mass

A higher concentration of pyrite, corresponding to a higher surface area, causes a faster drop in the potential. This change in the potential drop is to be expected if there is a charging effect responsible for the transient rates. When the rate is normalised with respect to the pyrite content there is no significant effect of ore concentration on the specific rate over the time span of the experiments (Figures 5.14 and 5.15). This, along with the fact that the total iron concentration does not affect the rate, indicates that the rate-limiting step is probably electron transfer between the ferric iron and the pyrite rather than chemical control by the reactants.

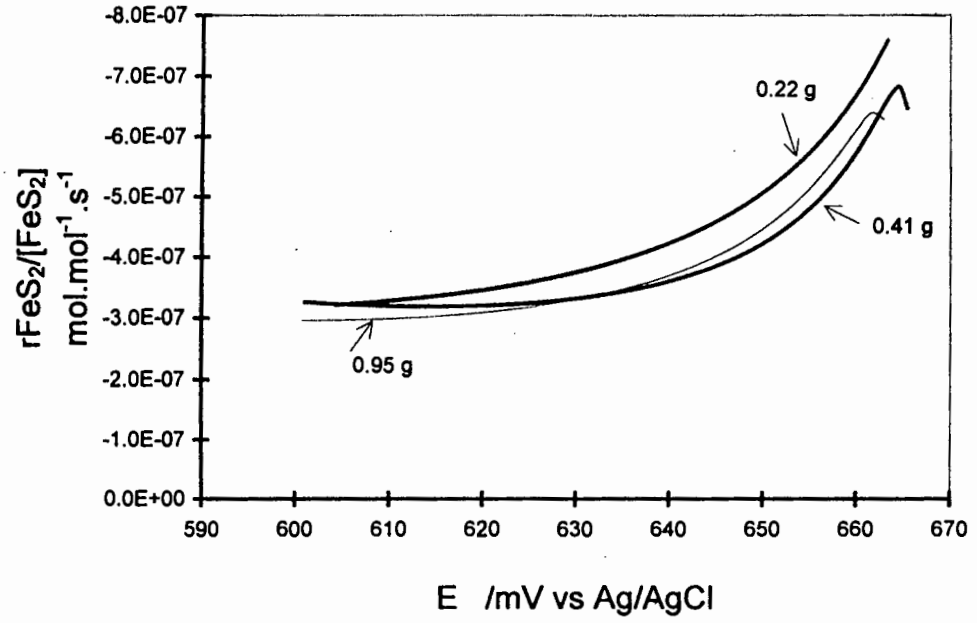

Figure 5.14 Effect of ore mass on leach rate

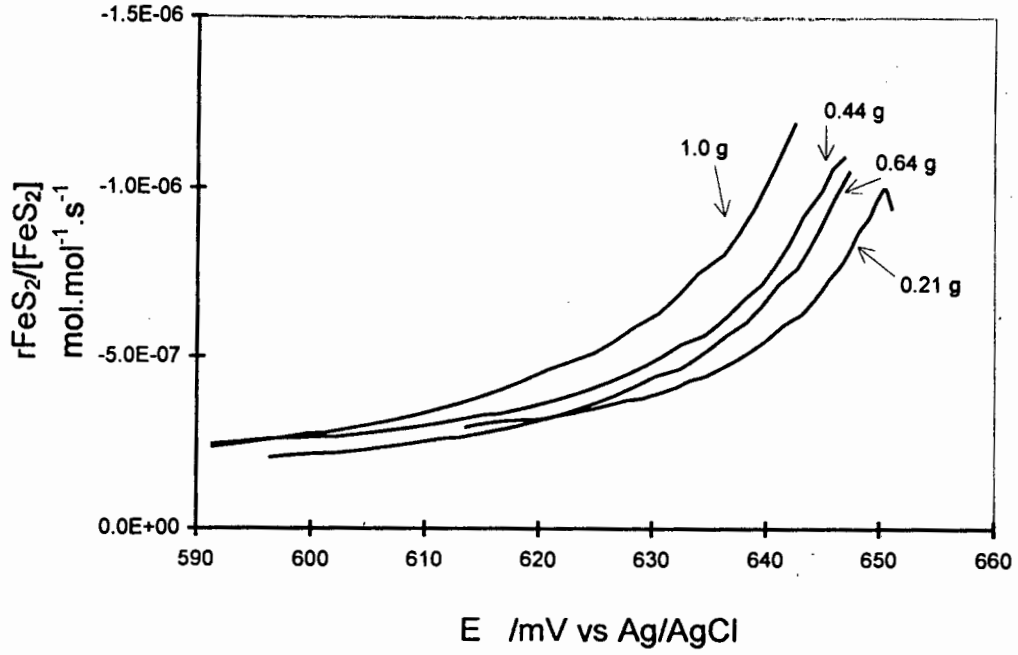

Figure 5.15 Effect of ore mass on leach rate

5.7 Reaction Stoichiometry

In all of the above work, it was assumed that the reaction stoichiometry remained constant and that sulfate ions were the only sulfur product. The formation of elemental sulfur is possible, especially at low potentials and it is possible that the reaction stoichiometry could change during the course of the reaction, or under different experimental conditions. The effect of using different values for n, the stoichiometric coefficient in Equation 3.1, on r_{FeS_2} is shown in Figure 5.16. The leach rate when n had a value of 4 (only sulfate formation) was lower than when n was assigned a value of 0 (only elemental sulfur production). Thus the leach rates which were obtained in this work represent the lowest possible values, even if reactions of different stoichiometries were proceeding simultaneously. It is interesting to note that the rate of production of ferrous iron is hardly affected by a change in the reaction stoichiometry, because of the relationship between $r_{Fe^{2+}}$ and r_{FeS_2}. There is an increase in $r_{Fe^{2+}}$ of less than 0.03 % as n decreases from 4 to 0. This may indicate that the transfer of an electron to ferric iron is rate limiting, and that the overall reaction rate is not limited by the oxidation of the sulfur species.

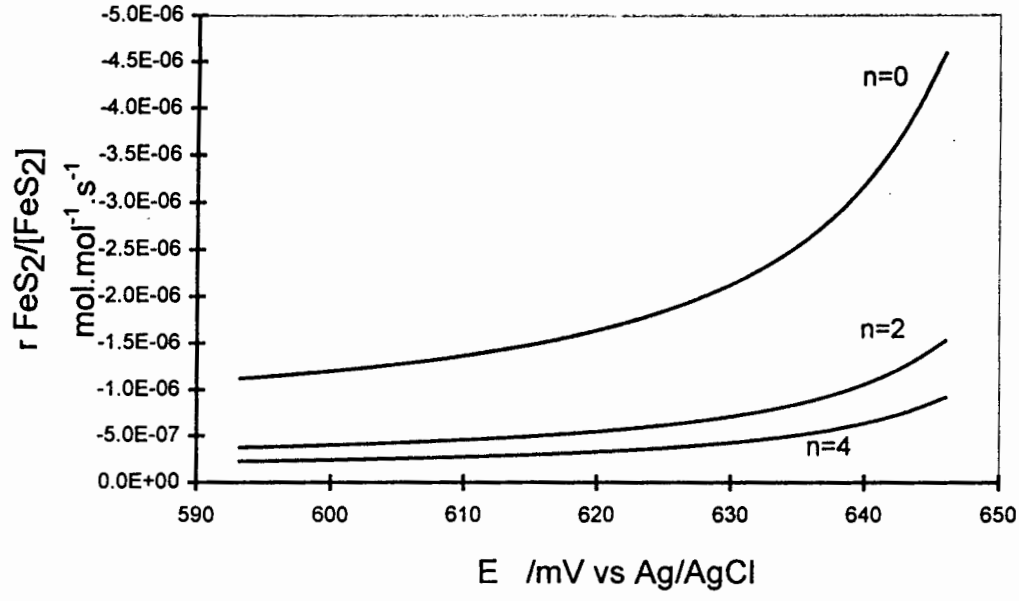

Figure 5.16 Effect of reaction stoichiometry on leach rate

5.8 Scanning Electron Microscopy

Before leaching (after washing) most of the pyrite grains appeared smooth, with only a small amount of surface deposits (Figure 5.17). After about 20 minutes of leaching, there was little change to the surface appearance, although many of the grains appeared smoothed or abraded.

A sample of washed ore was added to a ferric sulfate solution (0.4 M) of redox potential about 630 mV and allowed to leach in a sealed bottle for 6 weeks. After this time, the surface was noticeably deformed, with many pits (Figures 5.18-5.20). The surface structure was very similar to that of a bacterially leached pyrite sample, indicating that bacterial action is not necessary for pitting to occur. A micrograph of bioleached pyrite (Drossou, 1986) is shown for comparison (Figure 5.21).

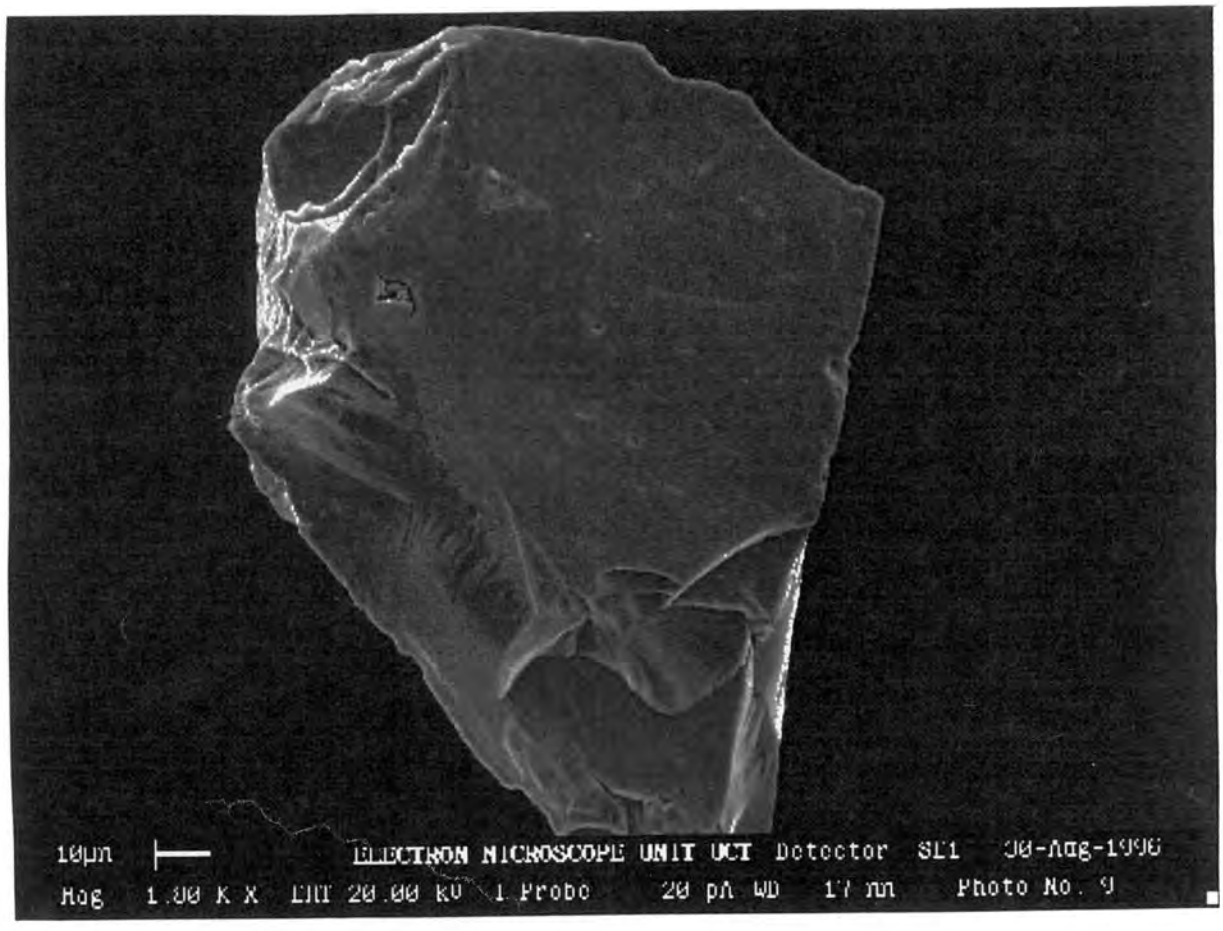

Figure 5.17 Pyrite before leaching, showing smooth surface

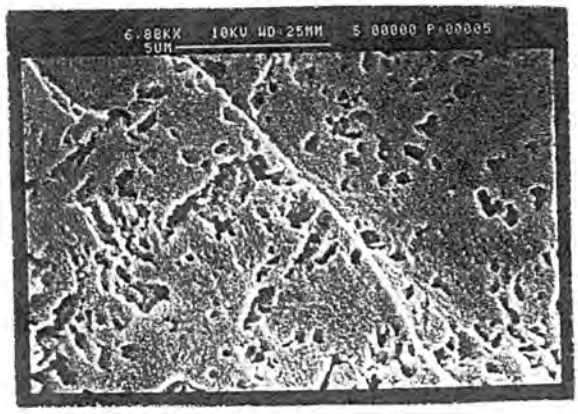

Figure 5.18

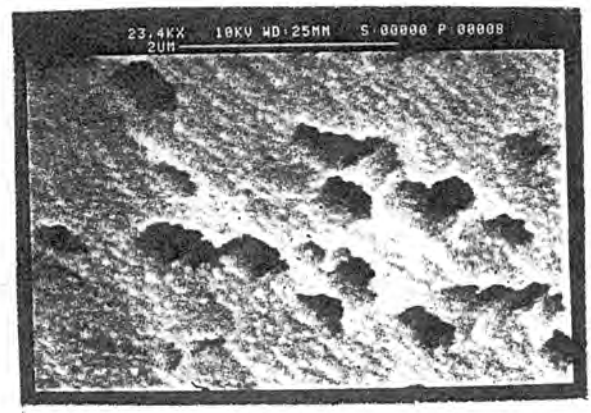

Figure 5.19

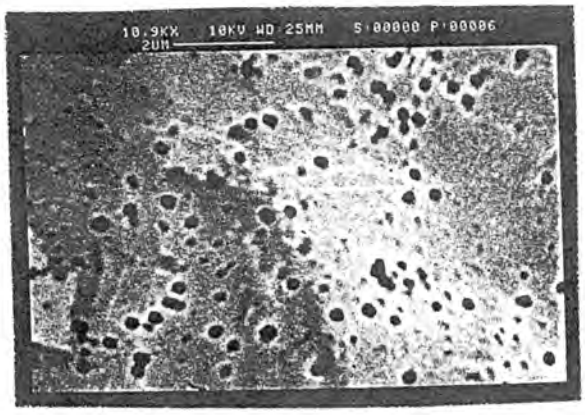

Figure 5.20

Figures 5.18 - 5.20 Pyrite after leaching for 6 weeks, showing pits in the surface

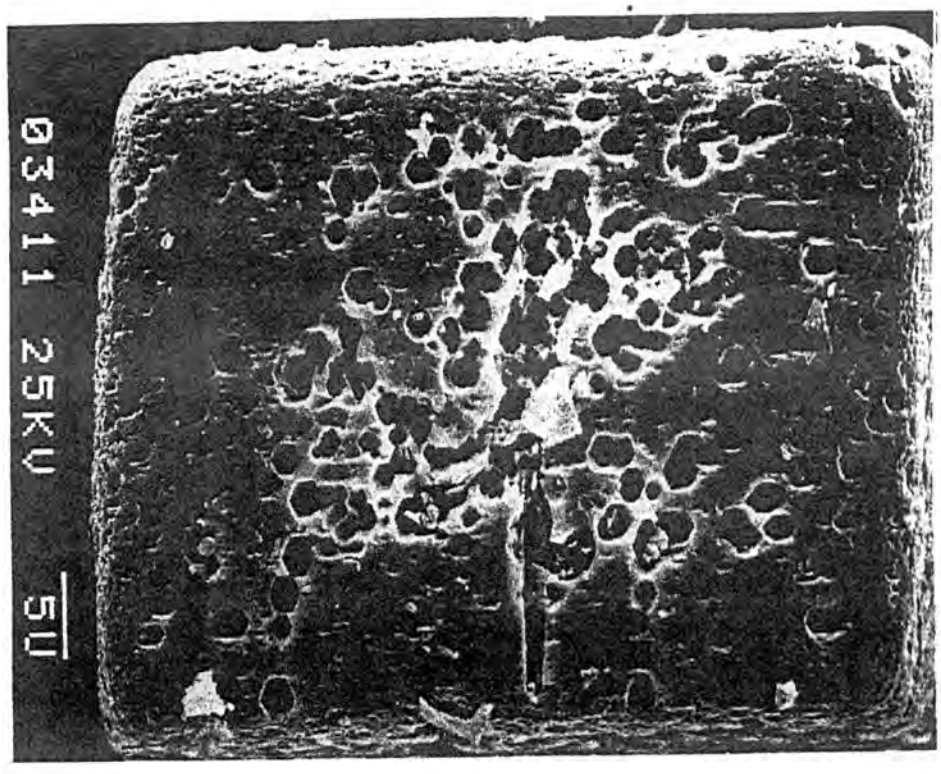

Figure 5.21 Pyrite bioleached for 28 days, showing pits (Drossou, 1986)

6. KINETICS OF FERRIC LEACHING OF PYRITE

6.1 Comparison of Literature Data

As has been discussed in the literature review, there has been much investigation into the ferric leaching of pyrite. However, the leaching has been carried out at much lower potentials than those occurring in bioleaching, and the leach rate has not been linked quantitatively (or sometimes even qualitatively) to the redox potential. Previously published work was re-examined in two ways, to determine whether the rates of reaction between ferric iron and pyrite found in the literature can be considered to be a function of the redox potential, as hypothesised in this thesis. The first was to re-analyse raw experimental data and express the rate as a function of the ferric to ferrous ratio. In analysing the literature data it was preferred to use the raw data presented and not any derived rate laws or calculated initial rates, because different assumptions were used by different researchers, making any meaningful comparison difficult. Secondly, the rate laws stated in the literature were used to find the leach rates at particular values of the ferric/ferrous ratio. Even though the rate laws were not derived for the potential range prevalent in bioleaching, the qualitative trend in the leach rates over a large range of potentials was predicted using these laws, to see what types of dependence the rate had on the potential.

6.1.1 Re-analysis of Raw Data

Data in previously published work by the following authors was re-analysed :

Wiersma and Rimstidt (1984)

Mathews and Robins (1972)

McKibben and Barnes (1986)

Tal (1986)

Zheng *et al.* (1986)

Kawakami *et al.* (1988)

Boogerd *et al.* (1991)

In most cases concentration versus time data were available, and the rate of leaching was determined by taking the tangent to ferrous concentration versus time profiles, and converting the rates to units of moles of ferrous iron produced per square metre of pyrite per second. Conversion between different units is given in Appendix 5. In most cases, assumed rate laws were not used because the method of analysis has been found to have a great effect on the results (Rimstidt and Newcomb, 1992). Even the use of a simple function to fit concentration versus time data can introduce large errors. For example, Rimstidt and Newcomb (1992) used data from relatively short times to determine the initial rate of leaching of pyrite by ferric iron, but found that they could use a linear relationship between the ferric concentration and time for the first 15 minutes of their experiments, or a parabolic fit for the first hour of their experiments. Neither fit predicted the measured initial concentration, or the experimental data after the initial period. The Arrhenius equation and experimentally determined activation energies were used to convert rates obtained at higher temperatures to 25 °C. Table 2.2 in Chapter 2 lists the experimental conditions under which the data were obtained, as well as activation energies where these were available. Figure 6.1 shows a compilation of the re-analysed data.

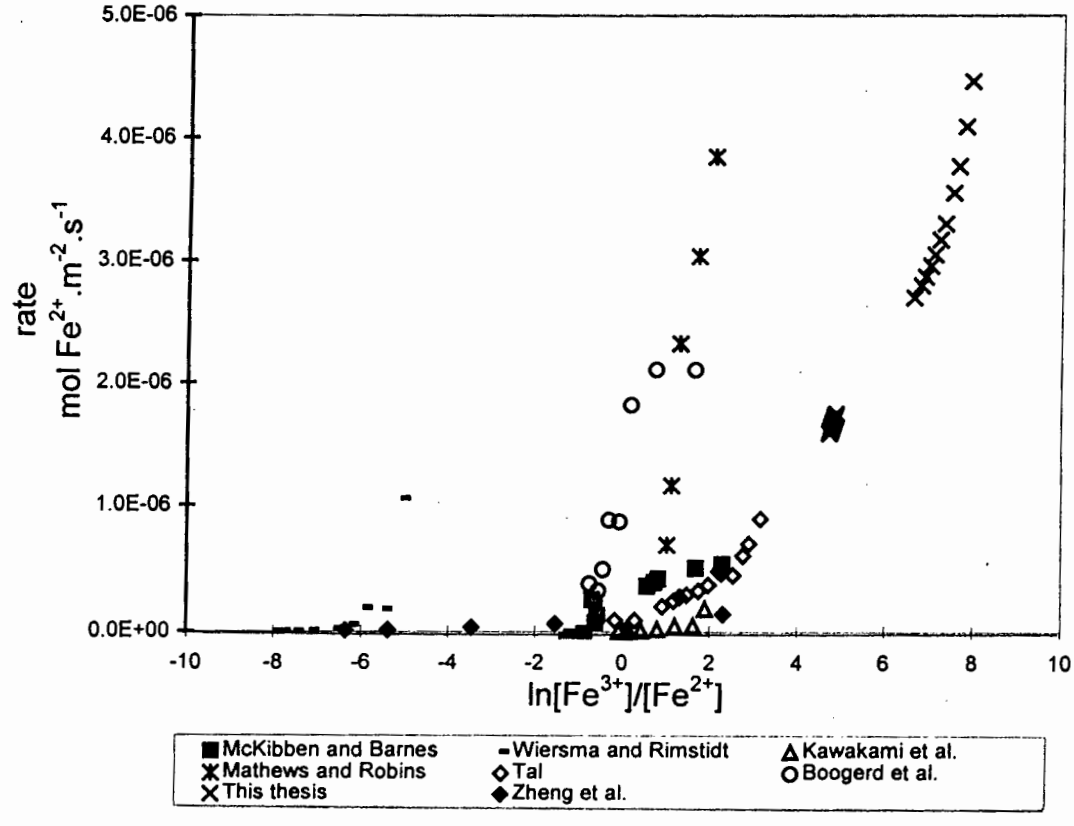

Figure 6.1 Pyrite leaching rates from literature data

Wiersma and Rimstidt (1984) used a dynamic redox potential measurement technique to determine the leach rate. Their work, however, was different to the experiments of this thesis in a number of ways: ferric chloride was used as the leaching agent, the iron concentration was of millimolar level, the solution redox potential was less than 520 mV versus Ag/AgCl, the solids concentration was about five times lower and the experiments were carried out over much longer times. Wiersma and Rimstidt also observed a very sharp initial change in the redox potential and therefore they ignored the first 75 minutes of each experiment when deriving leach kinetics. The same trend was observed as in this thesis, that is, a very high initial rate which decreases as the redox potential decreases. Wiersma and Rimstidt found that the leach rate was first order with respect to ferric iron concentration, but it must be emphasised that the initial data was ignored, and also the range of redox potentials used were much lower than those in this thesis.

It was assumed that $[Fe^{tot}]_{initial} = [Fe^{3+}]_{initial}$ and that the average particle diameter was 112.5 μm. The potential versus time data were analysed in the same way as in this thesis, with the first available data point after 492 seconds, but the theoretical E° and RT/zF values as used by the authors (E° = 573 mV (Ag/AgCl) and RT/zF = 25.69 mV) were used, as the potential measuring system was not calibrated for the system. A change in these parameters does cause a significant change in the rate.

The data of Mathews and Robins (1972) was available as a plot of ferric iron concentration versus time, on a logarithmic scale. Because of the choice of scale, large errors were introduced when reading data off the graph. The set of data re-analysed was obtained at 30 °C and an activation energy of 92 $kJ.mol^{-1}$ given by Mathews and Robins was used to extrapolate the data to 25 °C. The leach rate was calculated from the change in ferric iron concentration with time, then multiplied by -15/14 to get the rate of ferrous production. The first data point available was after 5 minutes, and the rate of leaching increased very sharply with the redox potential.

McKibben and Barnes (1986) found that the initial rate of oxidation of pyrite by ferric iron was proportional to the square root of the ferric iron concentration. Ferrous iron versus time

and total iron versus time data were re-analysed for a single experimental run, and the redox potential was seen to influence the leach rate (Figure 6.1).

In the re-analysis, it was assumed that $[Fe^{tot}]$ remained constant at 2mM, that $[Fe^{2+}]_{initial} = 0$ and that the average particle diameter was 187.5 μm. The first available data point was after 100 minutes. From the available data, the ferric iron concentration profile was determined, hence the ratio of ferric to ferrous iron could be determined. The rate of leaching could not be deduced simply from the change in ferrous iron concentration with time because of the scatter in results. Instead, the curve of ferrous iron concentration versus time was fitted with a parabola, as suggested by McKibben and Barnes, with the function $[Fe^{2+}] = -9x10^{-11}t^2 + 2x10^{-5}t + 0.035$ being the most suitable (Figure 6.2). The rate of reaction was found by differentiating this function i.e. $d[Fe^{2+}]/dt = -18x10^{-11}t + 2x10^{-5}$. McKibben and Barnes found the initial reaction rate as the value of $d[Fe^{2+}]/dt$ at time zero. In the re-analysis of this data, the whole experiment was considered, not just the initial rate. Details of the data manipulation are given in Appendix 6. Negative leach rates were obtained below about 409 mV (Ag/AgCl). The leach rates were extrapolated to 25 °C using an activation energy of 60.3 $kJ.mol^{-1}$ (McKibben, 1984). This activation energy is lower than that of Mathews and Robins (1972), Wiersma and Rimstidt (1984) and Kawakami *et al.* (1988) but is similar to that of King and Perlmutter (1977) who obtained an activation energy of 52.75 $kJ.mol^{-1}$ for pyrite leaching in a $FeCl_3$ - HCl system. The specific rate of leaching increased as the ferric to ferrous

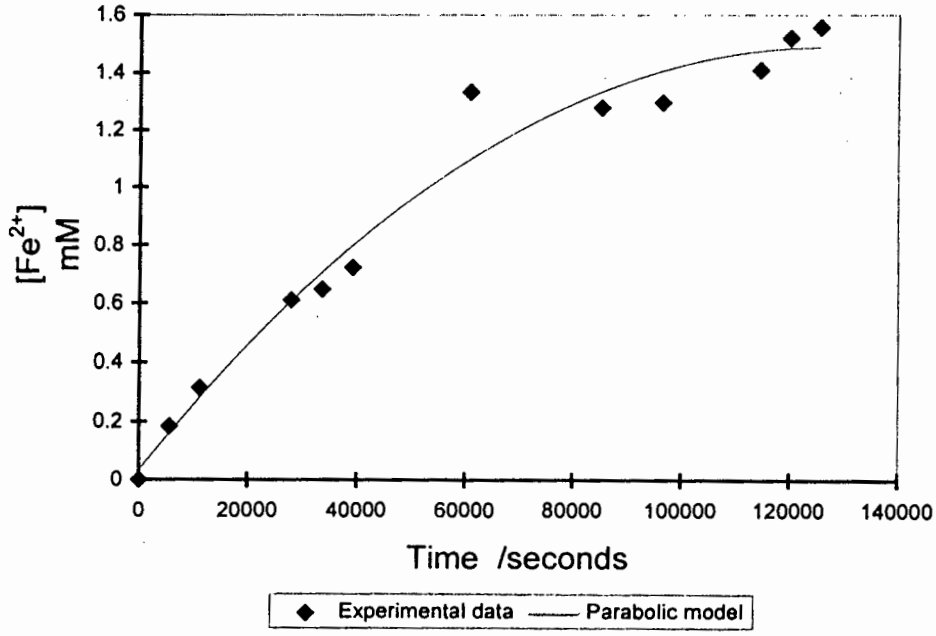

Figure 6.2 Ferrous iron concentration versus time, from McKibben and Barnes (1986)

ratio increased, when an entire experimental run was considered. McKibben (1984) found that the initial rate did not depend on the ferric/ferrous ratio, but it must be noted that he used the initial rate, which has been shown in this thesis to be a transient phenomenon and should not be used to deduce rate laws.

Tal (1986) held the solution potential constant using H_2O_2 and quoted leach rates at particular values of the ferric/ferrous ratio. Each point on the graph of Tal's data on Figure 6.1 represents a single experiment. Due to the lack of raw data, the data quoted by Tal could not be reworked. The rates were quoted as (mg pyrite).(g pyrite)$^{-1}$.(hour)$^{-1}$. To convert these rates to rates per unit surface area, an average particle diameter of 30 μm was assumed, since the particle size distribution was given as 87% less than 38 μm. Also, since no activation energy was given, it was assumed that the activation energy was 95 kJ.mol^{-1}, in accordance with data of Mathews and Robins (1972), Wiersma and Rimstidt (1984) and Kawakami *et al.* (1988). The rate of leaching was found to increase as the redox potential increased.

In the work of Kawakami *et al.* (1988), ferrous concentration versus time data were analysed. The rate was calculated as the change in ferrous iron concentration divided by the change in time. It was assumed that the total iron concentration remained constant at 0.5 M and that the average particle diameter was 50 μm. The activation energy was 95 kJ.mol^{-1}. The first available data point was at 30 minutes and this first data point gave an anomalously high rate, but this may have been due to the fact that it was assumed that the initial ferrous concentration was zero, whereas even a small ferrous concentration could have significantly affected the leach rate. Again the leach rate increased with redox potential. This is consistent with the observation by the authors that ferrous iron inhibited the leach rate.

Boogerd *et al.* (1991) did kinetic analysis of leaching using initial leach rates. In an analysis of the data in this work, the quoted initial rates were not used, but the ferrous iron versus time and total iron versus time data that were presented were used to find the dissolution rate versus solution redox potential. The first data point available was after one hour of leaching. The ferric iron concentration was calculated from the experimentally determined total iron and ferrous iron concentrations. The leach rate was calculated as the change in ferrous iron concentration with time. Details are given in Appendix 7. No activation energy was given in

this work, but there was data available for initial rates at various temperatures. From this data, activation energies were calculated and it was found that the activation energy increased with a decrease in temperature. At around 30 °C the activation energy was in the region of 100 $kJ.mol^{-1}$, but because of the large spread in values, a value of 95 $kJ.mol^{-1}$ (in accordance with Mathews and Robins (1972), Wiersma and Rimstidt (1984) and Kawakami *et al.* (1988)) was used to extrapolate the leach rates from 70 °C to 25 °C. The rates calculated from this data are higher than other literature values for a similar range in ferric/ferrous ratio, but the trend is still the same i.e. the leach rate increases with an increase in redox potential.

Although Zheng *et al.* (1986) did not provide raw data in their work, they did provide data of rate versus redox potential. Unfortunately they did not give any form of calibration to convert from potential to the ferric/ferrous ratio, and did not explicitly mention the electrode to which their quoted potential values were referenced. The qualitative dependence of rate versus potential for a set of experiments run at 25 °C with a total iron concentration of 0.09 M were included in Figure 6.1 for comparative purposes. Again the rate increased with the redox potential.

The objective for re-analysing previously published data was to investigate the validity of the hypothesis that the rate of ferric leaching of pyrite is a function of the redox potential. As can been seen in Figure 6.1, there was a large variation in the results obtained by different investigators but generally the pyrite leach rate increased with an increase in the ferric/ferrous ratio or redox potential. In most cases there was an anomalously high initial leach rate characterised by a sudden large drop in the redox potential. In many cases this was explained by the existence of reactive sites on the ore surface so in many of the original analyses, the initial period was ignored because of these high rates. In the case of McKibben and Barnes (1986) and Boogerd *et al.* (1991) the leach rate appeared to reach a maximum at high potentials. Zheng *et al.* (1986) also predicted that a maximum rate would be reached at high potentials and this was reflected in their model, but the available data points for rate versus potential could also be interpreted as by Tal (1986) where no upper limit of rate is observed over the range of potentials used in the experiment. It must be emphasised that a variety of experimental techniques were used, and factors such as the leaching medium (ferric sulfate or ferric chloride), particle size, iron concentration, temperature and pyrite source could all have an effect on the observed leach rate. The spread in the results is thus to be expected.

6.1.2 Rate Laws in the Literature

Rate laws of previously published work and their corresponding rate constants were used to find the leach rates at particular ferric/ferrous ratios. The rate of pyrite leaching has been related to a range of parameters, including ferric iron, total iron and the ferric/ferrous ratio. It must be noted that the rate laws in the literature were derived for conditions often far from those encountered in bioleaching, so they would not be expected to be valid in bioleaching regions. They were still extended to regions outside of those for which they were derived, to see the qualitative dependence of the rate law over a large potential range.

Wiersma and Rimstidt (1984) found the rate depended linearly on the ferric iron concentration. In their work the initial ferric iron concentration was 0.001 molal, and it was assumed that the total iron concentration remained constant at this value. A graph of rate versus $\ln([Fe^{3+}]/[Fe^{2+}])$ is shown in Figure 6.3 for a number of total iron concentrations. The rate is very dependent on the total iron concentration, but follows the shape of a switching function, reaching a saturation level at high potentials and tending to zero at low potentials. This rate law was derived for values of ln([Fe3+]/[Fe2+]) between about -8 and -5, which

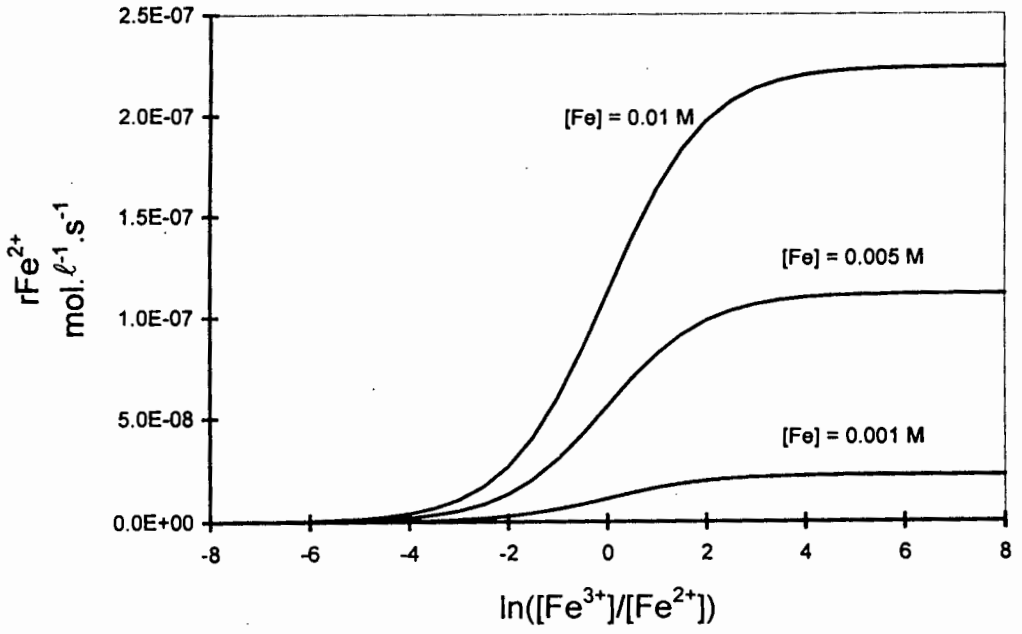

Figure 6.3 Rate versus ferric/ferrous ratio, using $r = K[Fe^{3+}]$ from Wiersma and Rimstidt (1984)

correspond to very low potentials (<500 mV (Ag/AgCl)) and in this region the rate law predicts very small rates. In Figure 6.1, where raw data was analysed, the initial rates appeared high, but this is probably due to the transient effect noted by Wiersma and Rimstidt and also observed in this thesis.

The rate law of Mathews and Robins (1972) relates the rate to the ratio of ferric to total iron. Where the total iron is assumed to stay constant, this is essentially the same form of rate law as that of Wiersma and Rimstidt (1984) and the behaviour is the same.

Boogerd *et al.* (1991) used an empirical rate equation of the following form:

$$r_{FeS_2} = K \cdot \frac{[FeS_2]}{30 + [FeS_2]} \cdot \frac{[Fe^{3+}]}{95 + [Fe^{3+}]} \qquad [6.1]$$

Figure 6.4 shows a comparison of the rate law predictions with the experimental results which were analysed as discussed above in Section 6.1.1. The rate law is of the same qualitative trend as the experimental points, reaching a maximum value at higher ferric/ferrous ratios, but it does not fit very well quantitatively. It must be remembered though that the rate law was derived from the initial rates of many such sets of data, and the parameters obtained would be those suitable for most of the experimental data, and not necessarily comply to one experimental run.

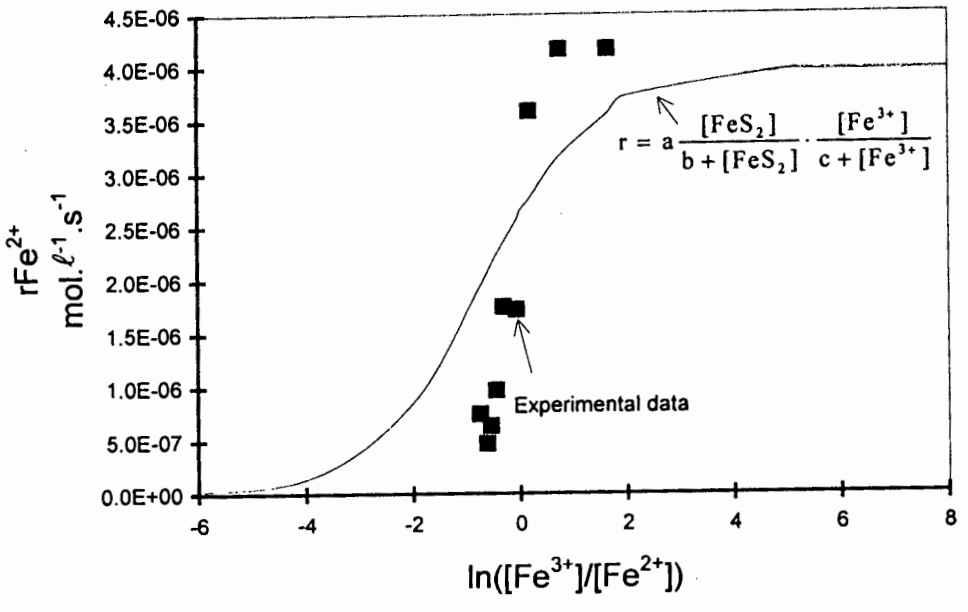

Figure 6.4 Experimental data and predicted rate from Boogerd *et al.* (1991)

It was stated by McKibben (1984) that there was no dependence of the initial leach rate of pyrite on the redox potential. Initial rates, however, are prone to include the effects of transients, so this statement is possibly incorrect. McKibben and Barnes (1986) derived a rate law from initial rate data. Their ferrous iron concentration versus time data were fitted with a parabola, and the initial rate was the value of the derivative of the parabolic function as time tended to zero. A rate determined in this manner would be affected by the presence of an initial transient, as this would affect the function used to fit the data. As can be seen from Figure 6.5 the rate law predicts rates which are much higher than those obtained by re-analysing experimental data. This is not surprising. however, since the rate law predicts initial rates, which are expected to be higher.

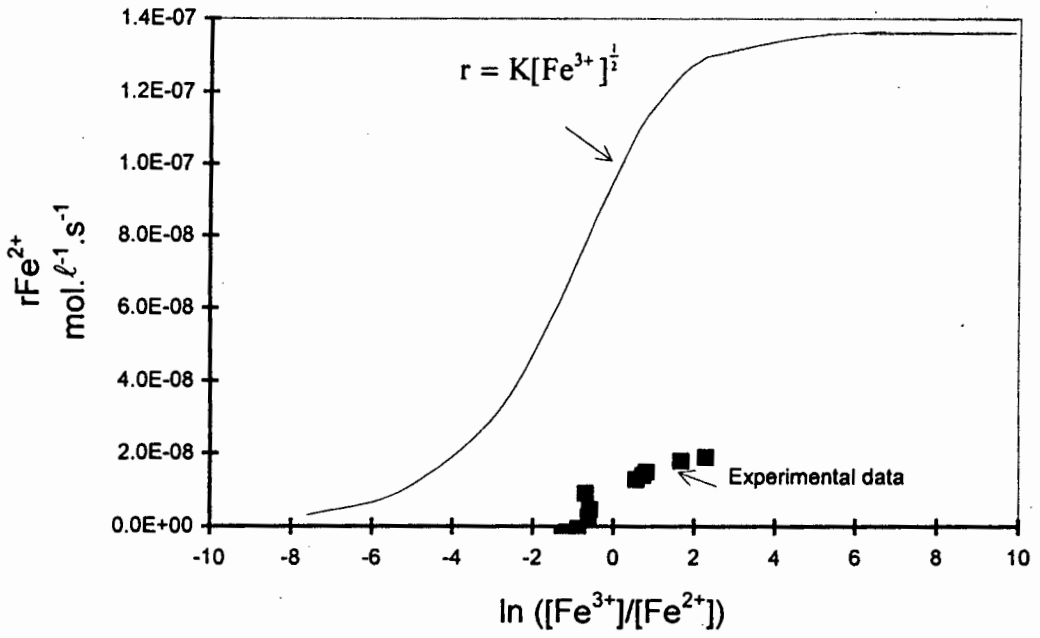

Figure 6.5 Experimental data and predicted initial rate from McKibben and Barnes (1986)

The rate law suggested by Tal (1986) is different to those mentioned above. The dependence was as follows:

$$r_{FeS_2} = K\left(\frac{[Fe^{3+}]}{[Fe^{2+}]}\right)^{0.682} \qquad [6.2]$$

This rate law predicts a continuous increase of rate with the ferric/ferrous ratio (Figure 6.6), in the same way that the electrochemically based Butler-Volmer equation would (Section 6.3), without reaching a limiting value. The qualitative trend for the experimental data was as

predicted, but correlation was not good for higher redox potentials. Tal acknowledges that at higher potentials there is some discrepancy in the rate law.

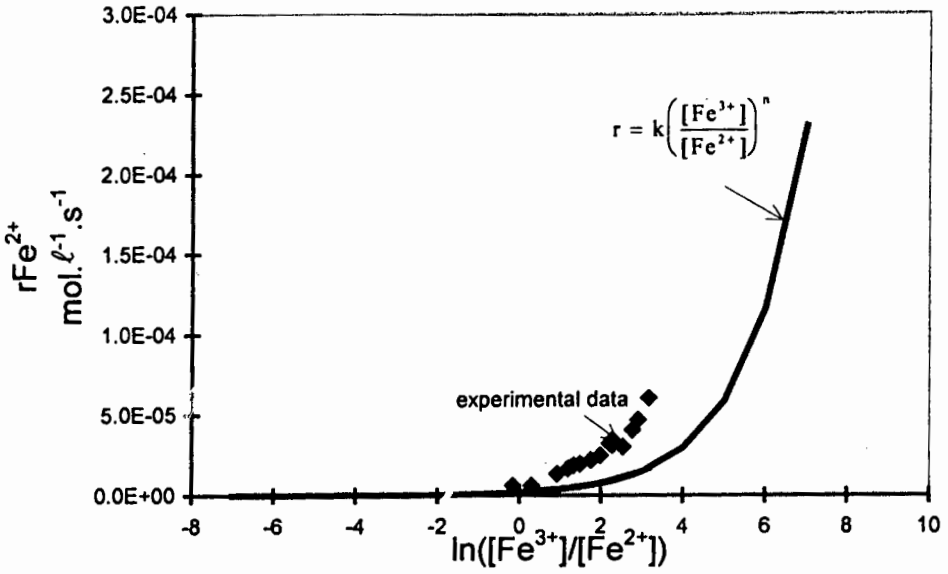

Figure 6.6 Experimental data and rate law of Tal (1986)

Zheng *et al.* (1986) expressed the rate of ferric leaching of pyrite as a function of the ferric/ferrous ratio as well as the total iron concentration. The rate law at constant sulfate concentration is as follows:

$$r_{FeS_2} = K \cdot \frac{k_1 - k_2\left(\frac{[Fe^{2+}]}{[Fe^{3+}]}\right)^{\frac{1}{2}}}{\frac{1}{[Fe^{3+}]^{\frac{1}{2}}} + k_3 + k_4\left(\frac{[Fe^{2+}]}{[Fe^{3+}]}\right)^{\frac{1}{2}}} \qquad [6.3]$$

This model is the Hougen-Watson 'dual-site' rate expression based on the Langmuir-Hinshelwood adsorption isotherm. In this model, ferric and ferrous iron compete for adsorption on dual active sites on the surface and the driving force for the reaction is assumed to be the surface concentration of adsorbed species rather than the concentration of species in solution. This rate law thus predicts chemical control of the rate (rather than diffusional or electrochemical). The rate law fits the given data of Zheng *et al.* very well (Figure 6.7) but predicts that the rate becomes constant at high potentials (in the region of 700 mV (SHE)). This is not necessarily the case, for the data published do not explicitly show this behaviour.

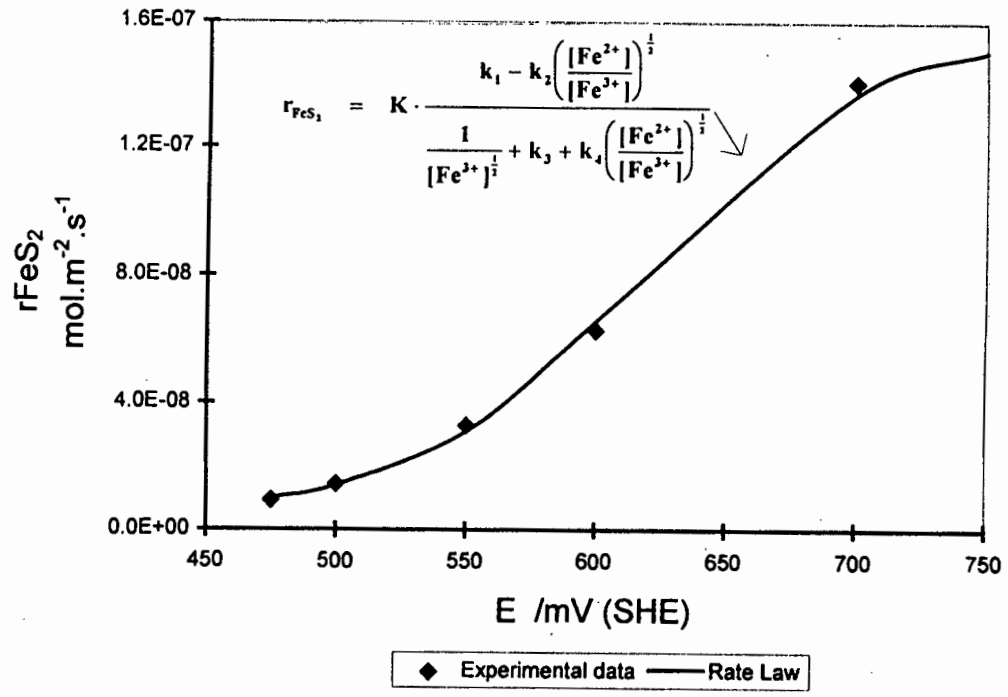

Figure 6.7 Experimental data and rate law of Zheng *et al.* (1986)

Another dependence on the ferric/ferrous ratio has been given by Williamson and Rimstidt (1994). These authors compiled rate data over a large range of ferrous and ferric concentrations and a range of ln([Fe3+]/[Fe2+]) of about -3.6 to 5.7. Two different rate laws were proposed, allowing for the presence of dissolved oxygen and for purging with nitrogen. These laws are as follows:

$$r_{FeS_2} = 10^{-6.07} \frac{[Fe^{3+}]^{0.93}}{[Fe^{2+}]^{0.40}} \cdot \frac{A}{V} \qquad [6.4]$$

in the presence of dissolved oxygen

$$r_{FeS_2} = 10^{-8.58} \frac{[Fe^{3+}]^{0.30}}{[Fe^{2+}]^{0.47}[H^{+}]^{0.32}} \cdot \frac{A}{V} \qquad [6.5]$$

for a nitrogen-purged solution.

These rate laws predict a rate which increases with redox potential, not reaching a saturation level. In the presence of dissolved oxygen, the rate increases at a slower rate (Figure 6.8). This type of rate dependence is similar to that expected in an electrochemical system where the Butler-Volmer equation applies. Williamson and Rimstidt suggest that there is indeed an electrochemical mechanism involved in the oxidation of pyrite, involving electron transfer as the rate determining step.

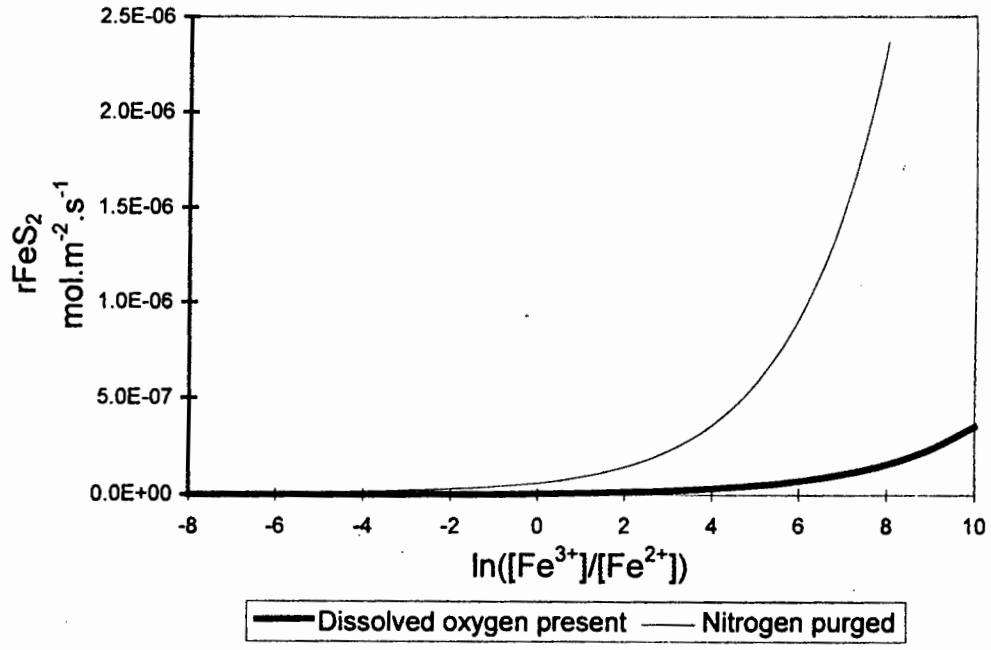

Figure 6.8 Rate law predictions of Williamson and Rimstidt (1994)

The above analysis of literature leaching rates and rate laws indicates that it could be valid to express the rate as a function of the ferric/ferrous ratio (or potential), rather than as a function of other commonly used parameters such as ferric iron. Most of the rate laws show a similar trend when related to the ferric/ferrous ratio, even though they were not derived at high potentials. The rate is low at low potentials, then has a rapid increase, reaching a maximum in most cases. It is also evident that there are no rate laws in the literature which are suitable to predict the rate of ferric leaching of pyrite in the case of bioleaching, where the potentials are high.

In addition to reworking the experimental data of other researchers, representative data of this thesis were analysed according to the derived literature rate equations. McKibben and Barnes (1986) deduced that the pyrite dissolution rate depended on the square root of the ferric iron concentration. Using their method, the ferrous concentration versus time data was fitted with a parabola, and the initial rate determined by taking the derivative of the fitted equation at time zero. A parabolic fit of representative data of this thesis was not satisfactory at short times. Nevertheless, the log of the initial rate determined in this way was plotted against the log of the initial ferric iron concentration, and qualitatively the same trend was observed as by McKibben and Barnes : the initial rate increased with the ferric iron concentration. Such a

plot is shown in Figure 6.9, where the slope of the graph is 0.35, indicating that the initial rate is a function of the ferric iron concentration raised to the power 0.35, which is less than that of McKibben and Barnes. This type of comparison, however, is purely qualitative, because the experiments of McKibben and Barnes were run over much longer times where the ferric iron concentration changed substantially, and also the parabolic fit used did not fit my data well at very short times, because of the initial transient effect. If one considers a plot of rate versus the square root of ferric concentration, without plotting the transient, the non-linear dependence is clear (Figure 6.10).

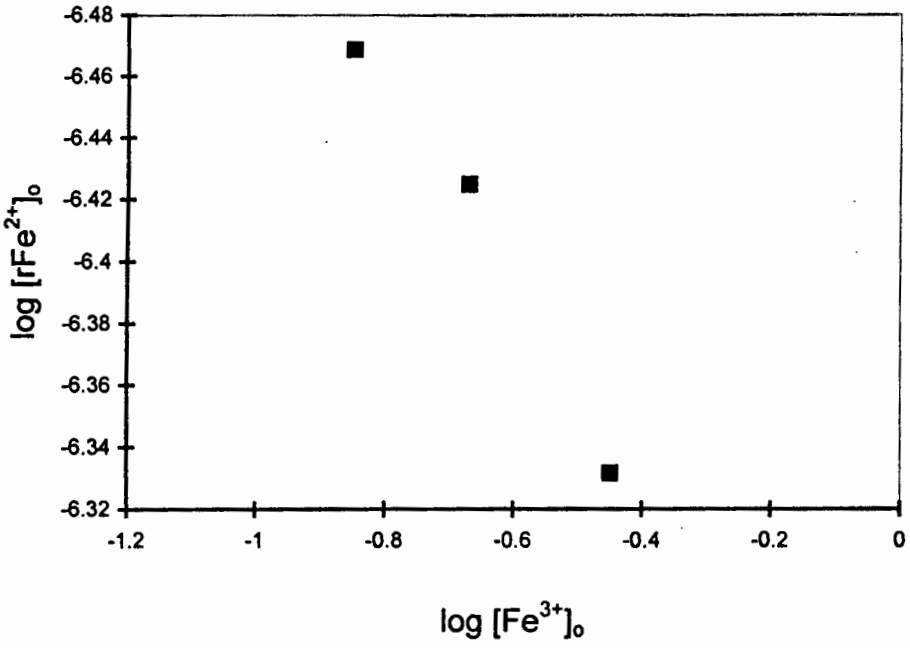

Figure 6.9 Log(initial rate) versus log(initial ferric concentration)
Data from this thesis used to test the model of McKibben and Barnes (1986)

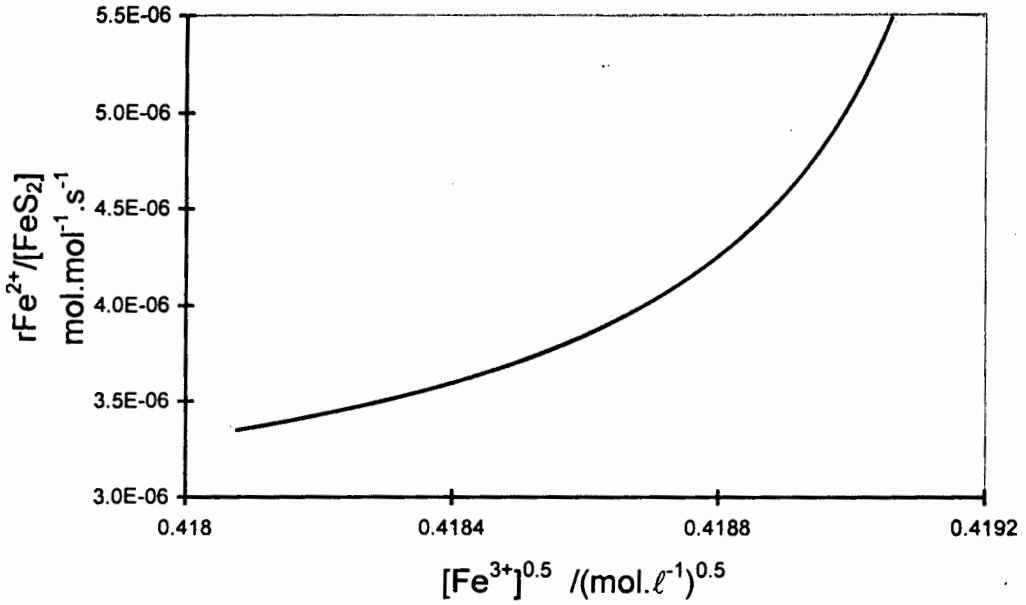

Figure 6.10 Rate versus $[Fe^{3+}]^{½}$ using data from this thesis

Wiersma and Rimstidt (1984) claimed a dependence of the rate on the ferric concentration, but this also did not appear to be the case. Perhaps at low redox potential values and after long times (from which they deduced the dependence) this could be considered an approximate rate dependence.

Mathews and Robins (1972) also predicted a linear dependence on ferric iron. They proposed the rate equation

$$\frac{d[Fe^{3+}]}{dt} = -k[Fe^{3+}] \qquad [6.6]$$

which can be integrated to

$$\ln \frac{[Fe^{3+}]}{[Fe^{3+}]_o} = -kt \qquad [6.7]$$

implying that a plot of the logarithm of the ratio of ferric iron to the initial ferric iron concentration against time should be linear. Figure 6.11 shows that in the case of my work, this is not the case, even after sufficient time for any transient effects to be over. Again the time scale of Mathews and Robins experiments was much longer and the ratio of ferric to total iron changed a great deal, unlike in this thesis where the change was very small. In this thesis, the initial ferric iron concentration could be approximated by the total iron concentration because of the high redox potentials used.

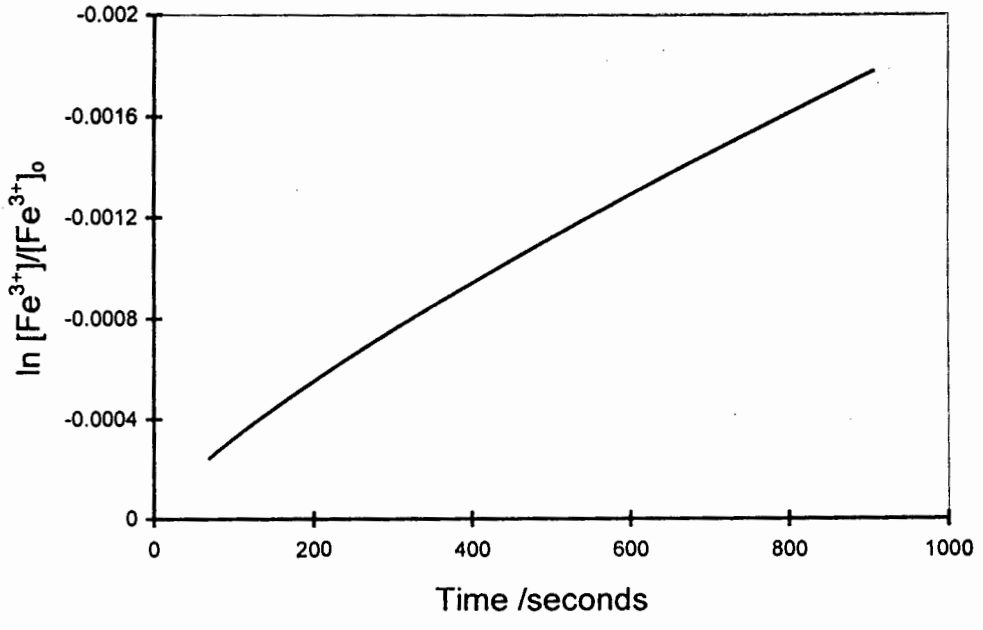

Figure 6.11 Log (ferric/total iron) versus time using data from this thesis

Tal's data (1986) fitted the rate law

$$r = k\left(\frac{[Fe^{3+}]}{[Fe^{2+}]}\right)^n \qquad [6.8]$$

In plotting the logarithm of the rates obtained in my work against the logarithm of the ferric/ferrous ratio, this rate law was not validated, but possibly over longer times and at lower values of the ferric/ferrous ratio it would hold.

Boogerd *et al.* (1991) used an empirical model to describe ferric leaching of pyrite. Their model was of the form

$$r = a \cdot \frac{[FeS_2]}{b + [FeS_2]} \cdot \frac{[Fe^{3+}]}{c + [Fe^{3+}]} \qquad [6.9]$$

and this equation fitted my data reasonably well, although the parameters a, b and c were very different to those of Boogerd *et al.*. Unfortunately this type of model is not particularly useful since it is empirical and not mechanistically based.

Williamson and Rimstidt (1994) and Zheng *et al.* (1986) suggested that the rate of ferric leaching of pyrite was a function of the ratio of ferric to ferrous iron. Williamson and Rimstidt suggested that an electrochemical mechanism was operative, with charge transfer being rate limiting. Two different but similar rate laws were proposed, one in the presence of dissolved oxygen and one in a nitrogen purged system. The rate law in the presence of dissolved oxygen was found to fit only some of the data of this thesis well, but predicted a rate higher than the initial transient rate, which is not feasible. Zheng *et al.* (1986) proposed that the rate was a function of the potential and the total iron concentration, but their model was based on a purely chemical mechanism. The form of the model was suitable to predict the results in this thesis, but did not serve to elucidate any electrochemically based mechanism. Also the model makes use of four variable parameters, and these took on a wide range of values when the model was used to fit data of different experimental runs in this thesis.

6.2 Bioleaching versus Sterile Rates

As a comparison between typical bioleaching rates and the chemical leaching rates obtained in this work, a typical curve of specific rate of dissolution versus the redox potential was superimposed on the plot of Figure 2.1 (Hansford, 1995) and is shown in Figure 6.12. Excluding the initial transient, the potential range covered in this work falls in the region of the potentials found in pyrite bioleaching systems. Higher potentials will still need to be investigated. Bearing in mind that the chemical and bioleaching experiments were carried out with different experimental arrangements and with different pyrite, there is a remarkable agreement in the magnitude of the rates. Although other bioleaching data is available in the literature (e.g. Mustin *et al.*, 1992, Chang and Myerson, 1982), it is not of a suitable form to test whether the potential is the rate-controlling parameter. The comparison with the data of Hansford (1995), however, indicates that it is possible to achieve characteristic bioleaching rates in an abiotic system provided that the redox potential is kept sufficiently high.

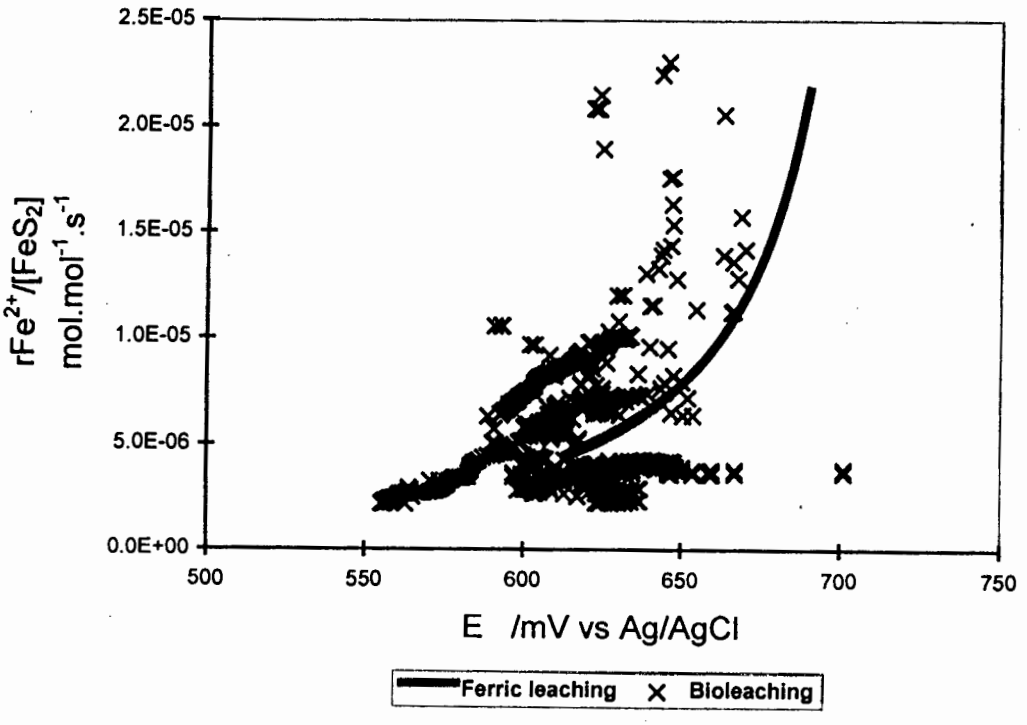

Figure 6.12 Bioleach and chemical leach rates versus redox potential

6.3 Kinetic Models

There are several ways in which the reaction rate between ferric iron and pyrite can be measured, and several ways in which the data can be analysed. Unfortunately, the rate laws and rate constants derived from different experimental techniques (as seen in the literature analysis in this thesis) and different methods of analysis (Rimstidt and Newcomb, 1992) are subject to a wide variation, qualitatively and quantitatively. Ideally, the rate law should be consistent with all experimental data, irrespective of how it was derived, and should be valid over a large range of experimental conditions.

Often rate laws are empirical and not explicitly related to the reaction mechanism. Usually this is the case because the reaction mechanism is complex or poorly understood. In the reaction between ferric iron and pyrite, various models have been proposed (Table 2.2) but few are mechanistically based. Those which are deserve further discussion.

Zheng *et al.* (1986) found the Hougen-Watson 'dual-site' rate expression provided a suitable fit to their data. This approach is valid when the rate determining step is purely chemical and assumes that the driving force for the reaction is the surface concentration of adsorbed species rather than the concentration of species in solution. Essentially the model describes the competition of ferric and ferrous iron for adsorption on dual active sites on the pyrite surface. When a ferric ion is adsorbed onto two adjacent active sites an activated ferric complex is formed. This is decomposed by electron transfer to produce an activated complex of ferrous iron, which also decomposes to allow the desorption of ferrous ions back into the solution. The rate limiting step is the chemical reaction on the pyrite surface. The model predicts that the rate of pyrite oxidation increases with an increase in the redox potential, and this was supported experimentally. The model also predicts that at high potentials the rate will be independent of the potential, but the experimental data available did not show this. It was noted by Zheng *et al.* that their experimental data could also be fitted by several other curves. The same model was used to fit some typical data of this thesis, but it was found that the rate constants were subject to a large variation, and were also completely different to those obtained by *Zheng et al.*. In some cases the model did not appear suitable.

Williamson and Rimstidt (1994) had a different approach to modelling their rate data. Instead of fitting a theoretically based equation to the experimental data, they determined rate laws by multiple linear regression and then explained the possible mechanistic implications. Williamson and Rimstidt expressed the rate as a function of the ratio of ferric to ferrous iron, i.e.

$$r_{FeS_2} = K\frac{[Fe^{3+}]^a}{[Fe^{2+}]^b} \qquad [6.10]$$

In formulating a mechanism it was necessary to know whether the process was electrochemical or one involving molecular adsorption. They found that a simple Langmuir isotherm model for competitive site-specific adsorption between ferric, ferrous and hydrogen ions was not suitable to explain the kinetics since they could not demonstrate saturation of the mineral surface by ferric iron , even over a six order of magnitude range in ferric iron concentration. It was possible to fit the rate by a Freundlich type isotherm with a multilayer, non site-specific interaction between pyrite and aqueous ferric iron. This, together with the correlation of the rate with the potential supports an electrochemical mechanism, with electron transfer being rate limiting. This is consistent with the activation energies in the literature which indicate that there is a chemical rather than a physical rate determining step. The mechanism postulated implies that electrons from the mineral are transferred to the ferric iron within a zone of solvent near the mineral surface.

The model of Boon *et al.* (1995) for bacterial ferrous oxidation, Equation 2.5, is based on microbial enzyme kinetics with product inhibition. An inverse of this type of model was adapted to describe the chemical oxidation rate, i.e.

$$r = \frac{r^{max}}{K + B\frac{[Fe^{2+}]}{[Fe^{3+}]}} \qquad [6.11]$$

This model is a simple function of the ferric/ferrous ratio, predicting an increase in the rate with the redox potential. The form of the model, however, suggests a saturation of the rate at a particular point, without suggesting a reason for this behaviour. The rate could become limited due to mass transfer limitations, insufficient reactant concentration or electron transfer control, yet these factors are not considered in such a model. In the chemical leaching system

it is also necessary to take account of the fact that leaching will only occur once the rest potential of the mineral has been reached. Also, the rate is predicted to tend to zero as the potential tends to zero, yet it is known that leaching can only occur once the potential at the mineral surface is higher than the rest potential of the mineral. This is not reflected by this model. The model does fit the experimental data of this thesis well in most cases, and the range in the values of the parameters r^{max}, B and K is not too large. The model is also very simple, with a simple dependence on the ferric/ferrous ratio.

The results of this work and that of others (e.g. Garrels and Thompson, 1960; Williamson and Rimstidt, 1994) suggest that the reaction between ferric iron and pyrite is under electrochemical control. The leaching of other sulfide minerals has also been described by electrochemical theory. Crundwell (1987) described the kinetics of the oxidative dissolution of sphalerite by an electrochemical mechanism where charge transfer from the mineral to the aqueous oxidant is rate limiting. Verbaan and Huberts (1988) also used an electrochemical model to describe the kinetics of leaching synthetic nickel sulfide (Ni_2S_3). Electrochemical models are generally based on the Butler-Volmer equation which quantitatively describes reactions which are limited by charge transfer at an interface. The Butler-Volmer equation (for a single electron transfer reaction in Equation 6.12) is a kinetic expression relating the current flow to the overpotential at a surface. The current is essentially the rate of electron transfer at the surface, in this case the corrosion current, which controls the reaction rate in an electrochemical reaction. It would be mechanistically valid to model the ferric leaching of pyrite by an equation of the form of the Butler-Volmer equation.

$$\mathbf{i} = \mathbf{i_o}\left(\exp\left(\frac{(1-\alpha)F\eta}{RT}\right) - \exp\left(\frac{-\alpha F\eta}{RT}\right)\right) \qquad [\,6.12\,]$$

The values η and α in Equation 6.12 determine the interrelationship between the rate of the charge transfer reaction and the potential difference across the interface. η is the overpotential, which is the difference between the equilibrium potential and the applied potential. α is the transfer coefficient (or in the case for single step reactions, the symmetry factor) and is an intrinsic characteristic of the charge-transfer reaction and determines what fraction of the

electrical energy resulting from the displacement of the potential from equilibrium affects the rate of electrochemical transformation (Bockris and Reddy, 1970). Not all of the potential difference across the double-layer at the interface actually causes the reaction. For a single step reaction, the symmetry factor is defined as the distance along the reaction co-ordinate between the initial and activated states divided by the distance along the reaction co-ordinate between the initial and final states. It has a value of about 0.5 for single electron transfers. When this is the case, the current/overpotential curves is symmetrical, so equal magnitudes of the overpotential on either side of zero produce equal currents, and equal oxidative and reductive currents should produce equal overpotentials. Significant deviation of the transfer coefficient from 0.5 is likely only under conditions where experimental confirmation is difficult due to the effects of mass transport limitations on any measurement (Pletcher, 1991). The symmetry factor for the reduction of ferric iron to ferrous iron at a platinum electrode has been shown to be 0.58 (Bockris and Reddy, 1970).

In the Butler-Volmer equation the current or rate of charge transfer is predicted to increase (or decrease) continually as the potential increases (or decreases, respectively) without reaching a saturation current. This is unlikely in reality, since at extreme potentials the rate is likely to be limited by processes other than the rate of charge transfer at the solution/mineral interface, e.g. diffusion of reactive species to the interface, the build-up of a passivating film, the occurrence of side reactions etc. The Butler-Volmer equation does take the rest potential of the mineral into account. Although at extremely high redox potentials a Butler-Volmer type model is inadequate, the potentials reached in bioleaching are not likely to lie outside the region of validity for this type of model.

Some of the experimental data of this thesis were modelled by a Butler-Volmer type equation, of the following form by minimising the sum of squares of the error between the experimental data and the model predictions:

$$\mathbf{r} = \mathbf{r_o}\left(\exp\left(\alpha\beta(\mathbf{E}-\mathbf{E'})\right) - \exp\left((1-\alpha)\beta(\mathbf{E}-\mathbf{E'})\right)\right) \qquad [\,6.13\,]$$

Four parameters can be varied: η, α, E' and β (=zF/RT). Theoretical values for α and zF/RT can be used but these do not necessarily represent the system correctly. Figure 6.13 shows a comparison between the model prediction and a typical set of data.

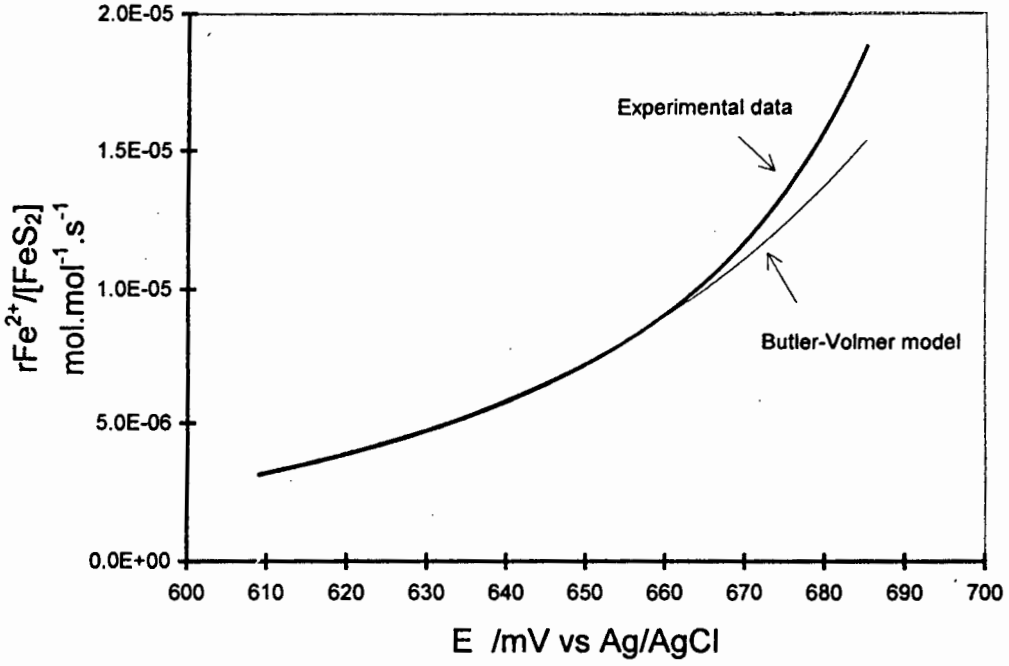

Figure 6.13 Fit of the Butler-Volmer Equation (Equation 6.13) to experimental data.

Model parameters: $\alpha = 0.46$

$r_o = 4.8 \times 10^{-8}$ (mol Fe^{2+}).(mol FeS_2)$^{-1}$.s^{-1}

E' = 413 mV (Ag/AgCl)

zF/RT = 39 mV^{-1}

If all the parameters are allowed to vary simultaneously, the initial values assigned to the parameters have a great effect on their final solutions. A number of solutions is possible for an equally good fit of the Butler-Volmer function to the experimental data. The range of possible solutions is too large to be able to make any deductions from this method.

In an attempt to find reasonable constant values for all the parameters, the variables were fixed at chosen values, or held between chosen limits.

First α and zF/RT were held constant at their theoretical values, 0.5 and 39 mV^{-1} respectively. With this restriction, no feasible fit could be found for most of the experimental data. This indicates that the system is not ideal and strictly theoretical treatment is not feasible. Limiting α to between 0.4 and 0.6 and zF/RT to between 37 and 42 mV^{-1} produced more acceptable results in general. r_o was still subject to a large variation ($1.2x10^{-8}$ - $7.4 x10^{-8}$ mol Fe^{2+}.(mol $FeS_2)^{-1}.s^{-1}$, 50 % variation) and E' fell in the range 286 - 422 mV (Ag/AgCl) (15 % variation).

When only α was held constant at 0.5, the other parameters were subject to a large variation, depending on their initial values. In many cases the final solutions were not feasible. This was also the case when both α and E' were held constant. When only β = zF/RT was held constant at 0.039 V^{-1} (its theoretical value), the curve fitted the experimental data well in each case, but there was a large range in values of the parameters r_o ($3.5x10^{-8}$ to $8.5x10^{-8}$ mol Fe^{2+}.(mol $FeS_2)^{-1}.s^{-1}$), α (0.38 to 0.68) and E' (310 to 542 mV vs Ag/AgCl). There was no apparent trend in the values of the constants with the total iron concentration or ore concentration. When E' was fixed in addition to zF/RT, α retained its value while r_o adjusted to give the best fit. The higher E', the higher r_o.

There was no apparent trend in the values of the constants with the total iron concentration or ore concentration. Although no constant values could be found for the parameters, they do fall in a reasonable range, and are not physically meaningless.

7. CONCLUSIONS

In this thesis the ferric leaching of pyrite was investigated within the context of the multi-step, indirect mechanism of bioleaching.

A survey of the literature showed that although there is considerable previously published work on the ferric leaching of pyrite, the investigations were carried out at potentials much lower than those in bioleaching. Also, few researchers had related their observed leach rates to the ferric/ferrous ratio or redox potential. This indicated that further work was necessary to determine the rate of reaction between pyrite and ferric iron at high redox potentials as a function of the potential.

An experimental technique was developed to determine the leach rate as a function of the redox potential. The experimental work showed that the redox potential dropped sharply when pyrite was added to an acidic ferric sulfate solution. The sharp initial drop was found to be of a transient character, probably due to a number of effects. These could include the rapid dissolution of highly reactive surface sites, a non-Faradaic charging effect and the formation of a non-stoichiometric, sulfur-rich surface layer.

The leach rate increased as the potential increased. The total iron concentration and the mass of ore used did not appear to have any significant effect on the rate. The effect of the surface area of the ore was not investigated, but it would be useful to compare leach rates expressed as a rate per unit surface area.

The leach rates were similar in magnitude to bioleaching rates at similar potentials. This observation supports the indirect mechanism of bioleaching as it indicates that the presence of bacteria does not cause a higher leach rate because of a direct reaction between the bacteria and the mineral, but rather that the bacteria function to maintain the potential at a high value, improving conditions for the ferric leaching reaction.

Although previously published data were not in a suitable range of redox potentials to be directly comparable with results of this study, rate data in the literature were expressed as a function of the ferric/ferrous ratio, and it was noted that in general the rate increased with the potential. Even when previously published rate laws were plotted as a function of the potential, this trend was observed.

It appears that in the results of thesis and of previously published work, the rate is very low at low potentials, increases in an apparent exponential manner, and in many cases reaches a maximum at high potentials. It is feasible that the rate will reach an upper limit at high potentials, but the cause of the limitation is not clear. The hypothesis based on that suggested by Boon *et al.* (1995) predicts such an upper limit, but possible reasons for this limitation are not obvious. A model following the Butler-Volmer equation is mechanistically more realistic.

In future work it is recommended that the leach rate is determined at constant potential either by using an *in situ* regeneration of ferric iron by use of an electric current, or by circulating the lixiviant through a packed or fluidised bed of ore and regenerating ferric iron outside the reaction vessel.

It is also necessary to investigate the effect of temperature, bearing in mind that the solution properties (e.g. complexation) are temperature dependent. Temperature is an important parameter, especially in commercial applications, since an increase in temperature will increase the reaction rate, which can lead to an increase in productivity.

REFERENCES

Aguirre R., J.V. Wiertz, R. Badilla-Ohlbaum, 1989, An amperometric method for measuring iron oxidising activity of *Thiobacillus ferrooxidans* , in *Bioleaching : From Molecular Biology to Industrial Applications*, Ed. R. Badilla-Ohlbaum, T. Vargas, L. Herrera, Proceedings of UNDP-UNIDO, Project CHI/88/003, Santiago, Chile, p107-117.

Ahonen L., O.H. Touvinen, 1989, Effect of temperature on the microbiological leaching of sulfide ore material in percolators containing chalcopyrite, pentlandite, sphalerite and pyrrhotite as main minerals, *Biotechnol. Letters*, **11**, p331-336.

Bailey K.L., E. Peters, 1976, Decomposition of pyrite in acids by pressure leaching and anodization: the case for an electrochemical mechanism, *Can. Met. Quarterly*, **15** (4).

Biegler T., D.A.J. Rand, R. Woods, 1976, Oxygen reduction of sulphide minerals, Part I, *J. Electroanal. Chem.*, **60**, p151.

Biegler T., D.A. Swift, 1979, Anodic behaviour of pyrite in acid solutions, *Electrochimica Acta*, 24, p415-420.

Blake R.C. II, G.T. Howard, S. McGinness, 1994, Enhanced yields of iron-oxidising bacteria by *in situ* electrochemical reduction of soluble iron in the growth medium, *Appl. and Environ. Microbiol.*, **60** (8), p2704-2710.

Bockris J. O'M., A.K.N. Reddy, 1970, *Modern Electrochemistry*, Volume 2, Pub. MacDonald, London.

Boogerd F.C., C. van Beemd, T. Stoelwinder, P.Bos, J.G. Kuenen, 1991, Relative contributions of biological and chemical reactions to the overall rate of pyrite oxidation at temperatures between 30 °C and 70 °C, *Biotech. and Bioeng.*, **38**, p109-115.

Boon M., J.J. Heijnen, 1993, Mechanism and rate limiting steps in bioleaching of sphalerite, chalcopyrite and pyrite with *Thiobacillus ferrooxidans* , *Biohydrometallurgical Technologies*, Ed. Torma, Wey, Lakshmanan, The Minerals, Metals and Materials Society, p217-235.

Boon M., G.S. Hansford, J.J. Heijnen, 1995, The role of bacterial ferrous iron oxidation in the bio-oxidation of pyrite, *Biohydrometallurgical Processing*, Volume I, Ed. T. Vargas, C.A. Jerez, J.V. Wiertz, H. Toledo, University of Chile.

Boon M., 1996, Theoretical and experimental methods in the modelling of bio-oxidation kinetics of sulphide minerals, PhD Thesis, Technische Universiteit Delft.

Briceño A., S. Chander, 1988, An electrochemical characterization of pyrites from coal and ore sources, *Int. J. Min. Proc.*, **24**, p73-80.

Brierley J.A., 1994, Biooxidation-heap technology for pretreatment of refractory sulfidic gold ore, In Biomine '94, Conference Proceedings, Perth, Western Australia, September 1994, p10.1-10.8.

Buckley and Woods, 1984, An x-ray photoelectron spectroscopic investigation of the surface oxidation of sulfide minerals, Meeting abstract, *J. Electrochem. Soc.*, **131** (3).

Chander S., A. Briceño, 1987, Kinetics of pyrite oxidation, *Min. and Met. Proc.*, **171**.

Chang Y.C., A.S. Myerson, 1982, Growth models of the continuous bacterial leaching of iron pyrite by *Thiobacillus ferrooxidans*, *Biotech. and Bioeng.*, **24**, p889-902.

Chia L.M., W.K. Choi, R. Guay, A.E. Torma, 1989, Electrochemical aspects of pyrite oxidation by *Thiobacillus ferrooxidans* during leaching of a Canadian uranium ore, *Biohydrometallurgy* 1989, Ed. J. Salley, R.G.L. McCready, P.L. Wichlacz, p35-43.

Crow D.R., 1994, *Principles and Applications of Electrochemistry*, fourth edition, Pub. Blackie Academic and Professional, Glasgow, Great Britain.

Crundwell F.K., 1987, Kinetics and mechanism of the oxidative dissolution of a zinc sulfide concentrate in ferric sulphate solutions, *Hydrometallurgy*, **19**, p227-242.

Crundwell F.K., 1988, The role of charge-transfer mechanisms in the oxidative and non-oxidative dissolution of sphalerite, PhD thesis, University of the Witwatersrand.

Crundwell F.K., 1996, The role of iron in bioleaching, Third International Conference on Minerals Bioprocessing and Biorecovery/Bioremediation in Mining, Big Sky, Montana, August 1996.

Dew D.W., 1995, Comparison of performance for continual biooxidation of refractory gold ore flotation concentrates, *Biohydrometallurgical Processing*, Volume I, Ed. T. Vargas, C.A. Jerez, J.V. Wiertz, H. Toledo, University of Chile, p239-251.

Doyle F.M., A.H. Mirza, W. Ye, M. Mianowska, 1989, Effect of the physical and chemical characteristics of ore pyrite on leaching kinetics, in *Bioleaching : From Molecular Biology to Industrial Applications*, Ed. R. Badilla-Ohlbaum, T. Vargas, L. Herrera, Proceedings of UNDP-UNIDO, Project CHI/88/003, Santiago, Chile, p23-44.

Drossou M., 1986, The kinetics of the bioleaching of a refractory gold-bearing pyrite concentrate, MSc thesis, University of Cape Town.

Dry M.J., 1984, Kinetics of leaching of a low grade matte in ferric sulphate solution, PhD thesis, University of the Witwatersrand.

Dry M.J., A.W.Bryson, 1988, Prediction of redox potential in concentrated iron sulphate solutions, *Hydrometallurgy*, **21**, p59-72.

Dutrizac J.E., R.J.C. MacDonald, 1974, Ferric ion as a leaching medium, *Minerals Sci. Engng*, **2**, p59-100.

Fornasiero D., V. Eijt, J. Ralston, 1992, An electrokinetic study of pyrite oxidation, *Colloids Surfaces*, **62**, p63-73.

Fowler T., 1996, Kinetics of the ferric sulphate leaching of sphalerite and sphalerite/pyrite mixtures, MSc thesis, University of Cape Town.

Garrels R.M., M.E. Thompson, 1960, Oxidation of pyrite by iron sulphate solutions, *Am. J. Science*, Bradley Volume, **258A**, p57-67.

Hansford G.S., 1995, unpublished data.

Harvey P, 1996, The growth of iron-oxidising bacteria in an electrolytic cell under constant redox potentials, PhD thesis, University of the Witwatersrand.

Hougen O.A., K.M. Watson, 1947, *Chemical Processes Principles*, Volume III, Pub. Chapman and Hall, London.

Jin Z-M., G.W. Warren, H. Henein, 1993, An investigation of the electrochemical nature of the ferric chloride leaching of sphalerite, *Int. J. Min. Proc.*, **37**, p223-238.

Jyothi N., K.N. Sudha, K.A. Natarajan, 1989, Electrochemical aspects of selective bioleaching of sphalerite and chalcopyrite from mixed sulfides, *Int. J. Min. Proc.*, **27**, p189-203.

Kawakami K., J. Sato, K. Kusunoke, K. Kusakabe, S. Morooka, 1988, Kinetic study of oxidation of a pyrite slurry by ferric chloride, *Ind. Eng. Chem. Res.*, **27**, p571-576.

Keller L., L.E. Murr, 1982, Acid-bacterial and ferric sulfate leaching of pyrite single crystals, *Biotech. and Bioeng.*, **24**, p83-96.

Kelly D.P., C.A. Jones, 1978, Factors affecting metabolism and ferrous iron oxidation in suspensions and batch cultures of *Thiobacillus ferrooxidans*: relevance to ferric iron leach solution regeneration, In *Metallurgical Applications of Bacterial Leaching and Related*

Microbiological Phenomena, Ed. L.E. Murr, A.E. Torma, J.E. Brierley, Academic Press, New York, p19-30.

King W.E., D.D. Perlmutter, 1977, Pyrite oxidation in aqueous ferric chloride, *AIChE Journal*, **23** (5), p679-685.

Koch D.F.A., 1975, Electrochemistry of sulfide minerals, *in Modern Aspects of Electrochemistry*, **10**, p211.

Larsson L., G. Olsson, O. Holst, H.T. Karlsson, 1991, Mechanisms of pyrite oxidation, IX Int. Symposium, *Biohydrometallurgy*, Ed. J.C. Duarte, R.W. Lawrence, Tróia, Portugal.

Linge H.G., W.G. Jones, 1993, Electrolytic oxidation of arsenopyrite slurries, *Minerals Eng.*, **6**, p873-882.

Lowson R.T., 1982, Aqueous oxidation of pyrite by molecular oxygen, *Chemical Reviews*, **82** (5), p461-497.

Mathews C.T., R.G. Robins, 1972, The oxidation of iron disulphide by ferric sulphate, *Aus. Chem. Eng.*, August 1972, p21-25.

McKibben M.A., 1984, Kinetics of aqueous oxidation of pyrite by ferric iron, oxygen, and hydrogen-peroxide from pH 1-4 and 20-40 °C, PhD thesis, Pennsylvania State University.

McKibben M.A., H. L. Barnes, 1986, Oxidation of pyrite in low temperature acidic solutions, *Geochim. et Cosmochim. Acta*, **50**, p1509-1520.

Mehta A.P., L.E. Murr, 1983, Fundamental studies of the contribution of galvanic interaction to acid-bacterial leaching of mixed metal sulfides, *Hydrometallurgy*, **9**, p235-256.

Meyer R.E., Electrochemistry of FeS_2, 1979, *J. Electroanal. Chem.*, **101**, p59-71.

Mishra K.K., K. Osseo-Assare, 1988, Aspects of the interfacial electrochemistry of semiconductor pyrite, *J. Electrochem. Soc.*, **135** (10), p2502-2509.

Moses C.O., D.K. Nordstrom, J.S. Herman, A.L. Mills, 1987, Aqueous pyrite oxidation by dissolved oxygen and by ferric iron, *Geochim. et Cosmochim. Acta*, **51**, p1561-1571.

Muñoz J.A., A. Ballester, M.L. Blázquez, F. González, C. Gómez, 1995, Studies on the anodic dissolution of chalcopyrite at constant potential : effect of a new thermophilic microorganism, Proceedings of Copper 95 - Cobre 95 International Conference, Volume III, Santiago, Chile, p409-420.

Mustin C., J. Berthelin, P. Marion, P. de Donato, 1992, Corrosion and electrochemical oxidation of a pyrite by *Thiobacillus ferrooxidans*, *Appl. and Environ. Microbiol.*, **58** (4), p1175-1182.

Natarajan K.A., 1988, Electrochemical aspects of bioleaching multisulfide minerals, *Minerals and Metallurgical Processing*, **5** (2), p61-65.

Natarajan K.A., 1992, Electrobioleaching of base metal sulfides, *Metallurgical Transactions B*, **23B**, p5-11.

Nayak B.B., R.K. Paramguru, H.S. Ray, 1995, Studies on initial dissolution kinetics from polarization data: Part III: Pyrite in ferric sulfate, *Trans. Indian Inst. Met.*, **48**, p35-41.

Nemati M., C. Webb, 1996, The influence of immobilization on temperature effects in the activity of *Thiobacillus ferrooxidans*, submitted for publication in *Biotechnology Letters*.

Nicol M., 1993, The role of electrochemistry in hydrometallurgy, Plenary lecture, IV International Symposium on Hydrometallurgy, Salt Lake City, August 1993.

Paciorek K.J.L., R.H. Kratzer, P.F. Kimble, W.A. Toben, A.L. Vatasescu, 1981, Degradation of massive pyrite: physical, chemical and bacterial effects, *Geomicrobiol. J.*, **2**, p363-374.

Pesic B, 1993, Redox potential technique to study the factors of importance during reactions of *Thiobacillus ferrooxidans* with Fe^{2+}, in *Proceedings of Minerals, Metals and Materials Society*, Ed. A.E. Torma, J.E. Wey, V.L. Lakshmanan, The Minerals, Metals and Materials Society, p545-560.

Peters E., 1976, The electrochemistry of sulphide minerals, in *Trends in Electrochemistry*, Ed. J. O'M. Bockris, D.A.J. Rand, B.J. Welch, Plenum Press, New York, p267-290.

Peters E., F.M. Doyle, 1989, Leaching and decomposition of sulfide minerals, in *Challenges in Minerals Processing*, Ed. K.V.S. Sastry, M.C. Fuerstenau, Pub. Society of Mining Engineers, Inc., Littleton, Colorado, p509-526.

Pletcher D., 1991, *A First Course in Electrode Processes*, Pub. The Electrochemical Consultancy, England.

Pugh C.E., L.R. Hossner, J.B. Dixon, 1984, Oxidation rate of iron sulfides as affected by surface area, morphology, oxygen concentration and autotrophic bacteria, *Soil Science*, **137**, p309-314.

Ralph D.E.R., 1997, personal communication.

Randall E.W.R., P. Moon, A.D.M. Garvin, 1993, Dynamically extendible communications protocol for a serial input/output system, *Jnl Microcomputer Appl.*, **16**, p385-393.

Riekkola-Vanhanen M., S. Heimala, 1993, Electrochemical control in the biological leaching of sulfidic ores, in *Biohydrometallurgical Technologies*, Ed. A.E. Torma, J.E. Wey, V.L. Lakshmanan, The Minerals, Metals and Materials Society, p561-570.

Rimstidt J.D., W.D. Newcomb, 1992, Measurement and analysis of rate data: the rate of reaction of ferric iron with pyrite, *Geochim. et Cosmochim. Acta*, **57**, p1919-1934.

Rossi G., 1990, *Biohydrometallurgy*, Pub. McGraw-Hill, Hamburg.

Sand W., T. Gerke, R. Hallmann, A. Schippers, 1995, Sulfur chemistry, biofilm, and the (in)direst attack mechanism - a critical evaluation of bacterial leaching, *Appl. Microbiol. Biotechnol.*, **43**, p961-966.

Sato M., 1992, Persistency-field Eh-pH diagrams for sulfides and their application to supergene oxidation and enrichment of sulfide ore bodies, *Geochim. et Cosmochim. Acta*, **56**, p3133-3156.

Singer P.C., W. Stumm, 1967, The rate-determining step in the production of acidic mine wastes, *Amer. Chem. Soc., Div. Fuel Chem.*, Preprints, **13** (2), p80-87.

Tal P., 1986, The effect of the iron(III) to iron(II) ratio on the rate of dissolution of pyrite, Council for Mineral Technology: Hydrometallurgy Division Technical Memorandum No. 18255, July 1986.

Taylor B.E., M.C. Wheeler, D.K. Nordstrom, 1976, Stable isotope geochemistry of acid mine drainage : experimental oxidation of pyrite, *Geochim. et Cosmochim. Acta*, **51**, p1561.

Torma A.E., 1993, Mineral Bioprocessing, in Proceedings of Biomine '93, Australian Mineral Foundation, p1.1-1.10.

Tributsch H., J.C. Bennett, 1981, Semiconductor-electrochemical aspects of bacterial leaching. I. Oxidation of metal sulfides with large energy gaps, *J. Chem. Tech. Biotechnol.*, **31**, p565-577.

Van Aswegen P.C., 1993, Bio-oxidation of refractory gold ores - the Genmin experience, in Proceedings of Biomine '93, Australian Mineral Foundation, p15.1-15.14.

Vargas T., A. Sanhueza, B. Escobar, 1993, Studies on the electrochemical mechanism of bacterial catalysis in pyrite dissolution, in *Biohydrometallurgical Technologies*, Ed. A.E. Torma, J.E. Wey, V.L. Lakshmanan, Minerals, Metals and Materials Society, p579-588.

Verbaan B., R. Huberts, 1988, An electrochemical study of the bacterial leaching of synthetic Ni_3S_2, *Int. J. Min. Proc.*, **24**, p185-202.

Vogel A.I., 1954, *A Text-book of Macro and Semimicro Qualitative Inorganic Analysis*, Fourth edition, Pub. Longmans, Green and Co., London.

Wadsworth M.E., 1987, Leaching - Metals Applications, *in Handbook of Separation Process Technology*, Ed. R.W. Rosseau, Pub. John Wiley and Sons, New York, p500-539.

Wiersma C.L., J.D. Rimstidt, 1984, Rates of reaction of pyrite and marcasite with ferric iron at pH 2, *Geochim. et Cosmochim. Acta*, **48**, p85-92.

Williamson M.A., J.D. Rimstidt, 1994, The kinetics and electrochemical rate-determining step of aqueous pyrite oxidation, *Geochim. et Cosmochim. Acta*, **58**, p5443-5454.

Zheng C.Q., C.C. Allen, R.G. Bautista, 1986, Kinetic study of the oxidation of pyrite in aqueous ferric sulfate, *Ind. Eng. Chem. Process. Des. Dev.*, **23**, p308-317.

ANALYTICAL METHODS

Determination of Ferrous and Total Iron

The following solutions were used in the determinations:

Potassium dichromate solution

About 10 g $K_2Cr_2O_7$ was dried in an oven at about 105 °C for 1-2 hours. About 8.8 g of the dried $K_2Cr_2O_7$ was dissolved in 2 ℓ distilled water, to form a standard solution of concentration about 0.015 M.

Concentration (mol.ℓ^{-1}) = mass in grams/ (294.20 g.mol^{-1} x V)

Spekker acid solution

450 ml concentrated (98 %) sulfuric acid and then 450 ml concentrated (85 %) phosphoric acid were slowly added to 1200 ml distilled water with stirring. The solution was allowed to cool before transferring to a storage bottle.

Ferric acid solution

300 ml spekker acid solution and 600 ml concentrated (32 %) hydrochloric acid were slowly added to 1200 ml distilled water with stirring. The solution was allowed to cool before transferring to a storage bottle.

Stannous chloride solution (5 %)

50 g stannous chloride ($SnCl_2$) was weighed out into a 100 ml beaker. 50 ml concentrated (32 %) hydrochloric acid was added and the solution was heated to about 50 °C and agitated until all the salt had dissolved. After cooling, the solution was diluted to 1 ℓ with distilled water and stored in a glass container with a few granules of tin metal.

Mercuric chloride solution (saturated)

1 ℓ distilled water was added to 50 g mercuric chloride ($HgCl_2$) and agitated for 2 hours. If all the mercuric chloride dissolved, a further small amount was added and the solution was agitated for a further 2 hours.

Barium diphenylamine sulfonate indicator

1.0 g barium diphenylamine sulfonate ($C_{24}H_{20}BaN_2O_6S_2$) was weighed out in a 250 ml beaker. 100 ml concentrated (98 %) sulfuric acid was added and the solution was agitated until the salt had completely dissolved.

Procedures

Sample Preparation

The samples used in the titrations were clear solutions. Generally 5 ml or 10 ml aliquots were suitable, depending on the concentrations of iron present.

Fe(II) titration

The required aliquot was pipetted into a conical flask. Spekker acid was added (10 ml), followed by 3-4 drops of barium diphenyl sulfonate indicator. The sample was titrated with potassium dichromate until the first permanent colour change from orange to purple.

$$[Fe(II)]\ (mol.\ell^{-1}) = [K_2Cr_2O_7] \times V_{titre} \times 55.85 \times 6 / V_{aliquot}$$

Fe(total) titration

The required aliquot of sample was pipetted into a conical flask. Ferric acid was added (30 ml) and the solution was heated to boiling point. Stannous chloride was added dropwise until the yellow colour of the solution disappeared. One extra drop was added and the total amount of stannous chloride added recorded. The solution was cooled to room temperature and mercuric chloride solution (10 ml) was added, forming a silky white precipitate. If no precipitate formed, too little stannous chloride was added, and if the precipitate was heavy and grey, too much stannous chloride was added. In either case the experiment had to be aborted. 4-8 drops of

barium biphenylamine sulfonate indicator were added and the sample was titrated with potassium dichromate until the first permanent colour change from yellow/green to purple.

$$[Fe^{total}]\ (mol.\ell^{-1}) = [K_2Cr_2O_7] \times V_{titre} \times 55.85 \times 6 / V_{aliquot}$$

FERRIC LEACHING OF PYRITE WITH AN ELECTROCHEMICAL REGENERATION OF FERRIC IRON

In an endeavour to leach pyrite at a constant redox potential, a current was used to regenerate ferric iron that was consumed by leaching. A two compartment electrochemical cell with the two compartments separated by an anion exchange membrane (Selemion membrane AMV) was used (See Figure A2.1). Each compartment had a capacity of about 3 litres. The anode and cathode were rectangular blocks of graphite (Ellor grade 18 from Le Carbonne), approximately 15 x 10 x 0.5 cm in dimension. Ferric sulfate leaching medium was used in the anodic compartment, while sulfuric acid (pH 1.5) was used in the cathodic compartment.

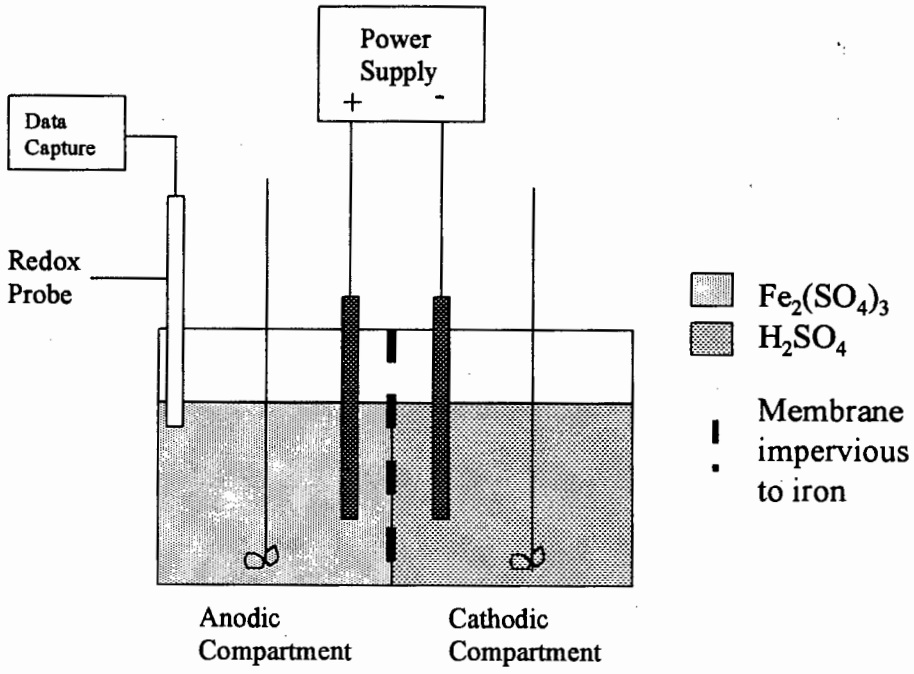

Figure A2.1 Experimental cell

A current was applied to oxidise ferrous iron to ferric iron at the anode, and the membrane prevented the reverse reaction from occurring at the cathode. To compensate for the redox potential decrease resulting from leaching, a variable current is required, because the rate of leaching changes with time and with redox potential. In this work, however, constant currents were used because there was no feedback mechanism to control the current.

In the presence of an oxidising current, the equations derived in Section 3.5 must be modified as follows:

$$\frac{d[Fe^{2+}]}{dt} = -15r_{FeS_2} - \frac{ni}{FV} = r_{Fe^{2+}} - \frac{ni}{FV} \qquad [A2.1]$$

and

$$\frac{d[Fe^{3+}]}{dt} = 14r_{FeS_2} + \frac{ni}{FV} \qquad [A2.2]$$

Hence from the Nernst equation

$$\frac{dE}{dt} = \frac{RT}{nF} \cdot \left(r_{FeS_2} \left(\frac{14}{[Fe^{3+}]} + \frac{15}{[Fe^{2+}]} \right) + \frac{ni}{FV} \left(\frac{1}{[Fe^{3+}]} + \frac{1}{[Fe^{2+}]} \right) \right) \qquad [A2.3]$$

and

$$r_{FeS_2} = \frac{\frac{nF}{RT} \cdot \frac{dE}{dt} - \frac{ni}{FV} \left(\frac{1}{[Fe^{3+}]} + \frac{1}{[Fe^{2+}]} \right)}{\frac{14}{[Fe^{3+}]} + \frac{15}{[Fe^{2+}]}} \quad (\text{in mol.}\ell^{-1}.s^{-1}) \qquad [A2.4]$$

The measured change in potential in the presence of a current can thus be divided into two parts: that corresponding to ferrous oxidation by the current and that corresponding to ferric reduction by leaching.

$$\left(\frac{dE}{dt}\right) = \left(\frac{dE}{dt}\right)_{leach} + \left(\frac{dE}{dt}\right)_{current} \qquad [A2.5]$$

where

$$\left(\frac{dE}{dt}\right)_{leach} = \frac{RT}{nF} \cdot r_{FeS_2}\left(\frac{14}{[Fe^{3+}]} + \frac{15}{[Fe^{2+}]}\right) \qquad [A2.6]$$

and

$$\left(\frac{dE}{dt}\right)_{current} = \frac{RT}{nF} \cdot \frac{ni}{FV}\left(\frac{1}{[Fe^{3+}]} + \frac{1}{[Fe^{2+}]}\right) \qquad [A2.7]$$

Ideally, the rate of dissolution of pyrite can be determined by monitoring the solution redox potential, if the current is accurately known. It is essential to know the current efficiency of the system to be able to calculate what proportion of the applied current is utilised in converting ferrous to ferric iron.

The current efficiency was found to be very low, especially when the iron concentration was low (because of the insufficiency of charge carriers) and when the currents were high (probably due to side reactions occurring). The redox potential also had a large effect on the current efficiency. At high redox potentials, the concentration of ferrous iron is low, so the current efficiency drops accordingly. It is thus important to quote the current efficiency with respect to the iron concentration, current and redox potential. The effect of stirring rate and temperature were not investigated.

There was a lot of variability in calculating the current efficiency, as was noticed by repeating experiments. Because of this, the current efficiency was determined immediately before each leaching test.

When pyrite was added to the anodic compartment, the redox potential immediately dropped, then reached a plateau or a turning point, and started rising again. This initial drop was probably a transient effect, caused by the charging effect expected when a solid is added to a solution of a different potential. The leaching rates were calculated at the plateau or turning point, where the current was assumed to perfectly balance the leach rate ($dE/dt = 0$). In some cases, no plateau or turning point was reached but the change in potential with time was very slow, and the average slope was used to calculate the leaching rate. Ideally both methods should be acceptable, but it would be preferable to be able to quote the leach rates at a point where the applied current exactly balanced the leach rate.

The behaviour of the potential was not reproducible. There appeared to be a transient effect when the ore was added, as has been noticed in the dynamic leach tests discussed in Chapter 4. Also any uncertainties in measurements of the volume, current and current efficiency had a large effect on the determination of the leach rate. As a result, no reliable results were gained from this work.

The membrane was slightly damaged after continuous exposure to the abrasive pyrite. This damage was not visible to the naked eye, but could be seen at 10 x magnification under a light microscope. Damage was only evident on the side of the membrane exposed to ore. It still remained impervious to ferric and ferrous iron so was considered suitable for further use. The membrane also developed a slightly orange colour after being in contact with the ferric solution. It is likely that precipitates had formed in the membrane, and to remove these, the membrane was soaked in dilute HCl and a reducing agent (ascorbic acid) for about 1.5 hours. This cleaning procedure did not seem to have any detrimental affect on the membrane.

In principle, this method of determining the leach rate at a constant redox potential is valid, yet it is prone to experimental difficulties and is strongly dependent on theoretical interpretation.

VARIATION IN TOTAL IRON CONCENTRATION

$$\frac{d[Fe^{tot}]}{dt} = \frac{d[Fe^{2+}]}{dt} + \frac{d[Fe^{3+}]}{dt} = \frac{1}{15}\frac{d[Fe^{2+}]}{dt} = \frac{zF}{RT}\frac{dE}{dt}\frac{-[Fe^{2+}]}{(14\frac{[Fe^{3+}]}{[Fe^{2+}]}+15)} \qquad [A3.1]$$

Since

$$[Fe^{2+}] = \frac{[Fe^{tot}]}{(\frac{[Fe^{3+}]}{[Fe^{2+}]}+1)} \qquad [A3.2]$$

we have

$$\frac{d[Fe^{tot}]}{dt} = \frac{zF}{RT}\frac{dE}{dt}\frac{-[Fe^{tot}]}{(\frac{[Fe^{3+}]}{[Fe^{2+}]}+1)(14\frac{[Fe^{3+}]}{[Fe^{2+}]}+15)} \qquad [A3.3]$$

$$\frac{d}{dt}(\ln[Fe^{tot}]) = \frac{1}{[Fe^{tot}]}\frac{d[Fe^{tot}]}{dt} = \frac{zF}{RT}\frac{dE}{dt}\frac{-1}{(\frac{[Fe^{3+}]}{[Fe^{2+}]}+1)(14\frac{[Fe^{3+}]}{[Fe^{2+}]}+15)} \qquad [A3.4]$$

Hence the following equation can be used iteratively:

$$\ln([Fe^{tot}]) = \{\ln[Fe^{tot}]\}_{t=0} + \frac{d}{dt}(\ln[Fe_{tot}]).\Delta t \qquad [A3.5]$$

It should be noted that the variation of total iron concentration over the course of the experiments was extremely small, of the order of 0.04 %.

CURVE FITTING OF POTENTIAL VERSUS TIME DATA

The raw E versus t data were smoothed by fitting a function of the form $y = A(\ln(t))^B$ to $(E_{initial}/E(t) - 1)$. A typical example is given below.

Figure A4.1 shows the experimental and calculated potential values for a leaching experiment with 0.38 g pyrite added to 50 ml 0.375 M ferric solution. The two curves can hardly be distinguished. The values of A and B were 6.6×10^{-4} and 2.49 respectively, with an objective function of 0.0003 for the 1600 data points.

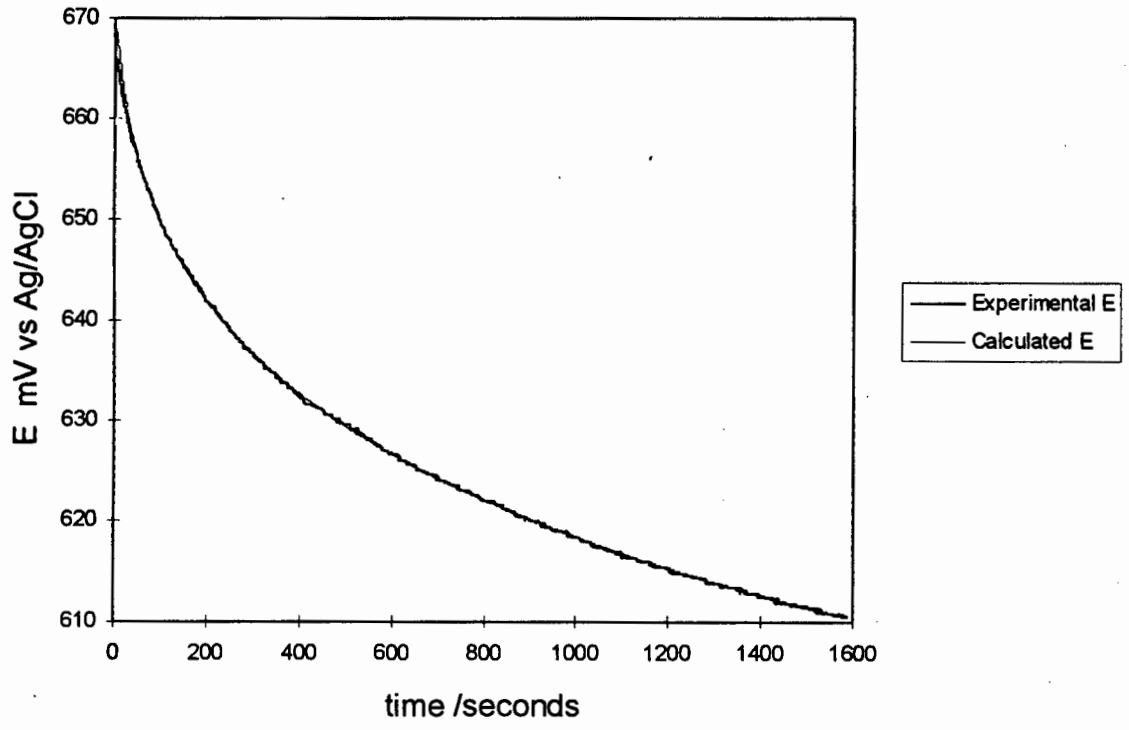

Figure A4.1 Experimental and calculated potential versus time data

CONVERSION BETWEEN RATE BASES

The following equations were used to convert all literature rates to common bases:

$$(molFe^{2+}).\ell^{-1}.s^{-1} = 15(molFeS_2).\ell^{-1}.s^{-1}$$

$$(molFe^{2+}).(molFeS_2)^{-1}.s^{-1} = [15(molFeS_2).\ell^{-1}.s^{-1}] \cdot [\frac{(120\,gFeS_2.mol^{-1})}{(gFeS_2).\ell^{-1}}]$$

$$(molFe^{2+}).(m^2FeS_2)^{-1}.s^{-1} = [15(molFeS_2).\ell^{-1}.s^{-1}] \cdot [\frac{(120\,gFeS_2.mol^{-1})}{(gFeS_2).\ell^{-1}}] \cdot [\frac{1}{(m^2FeS_2).mol^{-1}}]$$

$$(m^2FeS_2).mol^{-1} = [(m^2FeS_2).kg^{-1}] \cdot [0.12kgFeS_2.mol^{-1}]$$

$$= \frac{\pi d^2}{\rho.\pi\frac{d^3}{6}} \cdot [0.12kgFeS_2.mol^{-1}]$$

$$= \frac{6}{\rho d} \cdot [0.12kgFeS_2.mol^{-1}]$$

$$= \frac{6}{5000d} \cdot [0.12kgFeS_2.mol^{-1}]$$

Note: Assumptions

- reaction stoichiometry remained constant as in Equation 3.3
- molar mass of pyrite = 120 $g.mol^{-1}$
- density of pyrite = 5000 $kg.m^{-3}$
- spherical particles were assumed and used to calculate the geometric surface area

DATA FROM McKIBBEN AND BARNES (1986)

Reaction conditions:

temperature 30 °C

pH 1.89

pyrite mass 3 g

slurry volume 800 ml

particle size +125-250 μm

$[Fe]_{total}$ 2 mM

$[Fe^{2+}]$ versus time data were plotted, and fitted with the function

$[Fe^{2+}] = -9x10^{-11}t^2 + 2x10^{-5}t+0.035$.

The rate was found by differentiating this function i.e. $d[Fe^{2+}]/dt = -18x10^{-11}t + 2x10^{-5}$.

$[Fe^{3+}]$ was calculated as the difference between $[Fe]_{total}$ and $[Fe^{2+}]$.

Time s	$[Fe^{2+}]$ mM	$[Fe^{3+}]$ mM	$d[Fe^{2+}]/dt$ $mol.\ell^{-1}.s^{-1}$
0	0	2	2E-08
5610	0.185	1.815	1.9E-08
11220	0.315	1.685	1.8E-08
28020	0.611	1.389	1.5E-08
33660	0.648	1.352	1.39E-08
39240	0.722	1.278	1.29E-08
85260	1.279	0.721	4.65E-09
60840	1.333	0.667	9.05E-09
96420	1.296	0.704	2.64E-09
114420	1.407	0.593	-6E-10
120000	1.519	0.481	-1.6E-09
125580	1.556	0.444	-2.6E-09

DATA FROM BOOGERD *et al.* (1991)

Reaction conditions:

temperature 70 °C

pH 1.5

pyrite mass 0.44 g

slurry volume 50 ml

particle size 10 μm

The variation of ferrous and total iron with time were given. $[Fe^{3+}]$ was calculated as the difference. The rate was calculated as the change in ferrous concentration with time.

Time s	$[Fe^{2+}]$ mM	$[Fe]_{tot}$ mM	$[Fe^{3+}]$ mM	$d[Fe^{2+}]/dt$ $mol.\ell^{-1}.s^{-1}$
0	0	93.3	93.3	
3600	15	93.3	78.3	4.17E-06
7200	30	93.9	63.9	4.17E-06
10800	42.9	94.4	51.5	3.58E-06
14400	49.1	95.1	46	1.72E-06
18000	55.4	96.1	40.7	1.75E-06
21600	58.9	96.7	37.8	9.72E-07
25200	61.2	96.7	35.5	6.39E-07
28800	62.9	96.7	33.8	4.72E-07
32400	65.6	96.7	31.1	7.5E-07